UNIVERSIDAD NACIONAL AUTÓNOMA DE MEXICO

PROGRAMA DE MAESTRÍA Y DOCTORADO EN CIENCIAS MATEMÁTICAS Y DE LA ESPECIALIZACIÓN EN ESTADÍSTICA APLICADA

ANALYSIS OF THE STANDING AND TRAVELING WAVE SOLUTIONS OF THE ONE-DIMENSIONAL M^5 −MODEL FOR THE MESENCHYMAL CELL MOVEMENT

TESIS
QUE PARA OPTAR POR EL GRADO DE:
DOCTOR EN CIENCIAS

PRESENTA:
SALVADOR CRUZ GARCÍA

TUTOR PRINCIPAL
DRA. CATHERINE GARCÍA REIMBERT
INSTITUTO DE INVESTIGACIONES EN MATEMÁTICAS APLICADAS Y EN SISTEMAS

MIEMBROS DEL COMITÉ TUTOR
DR. RAMÓN GABRIEL PLAZA VILLEGAS
INSTITUTO DE INVESTIGACIONES EN MATEMÁTICAS APLICADAS Y EN SISTEMAS

DR. ANTONIO CAPELLA KORT
INSTITUTO DE MATEMÁTICAS

CIUDAD DE MÉXICO, MAYO 2017

RESUMEN

La migración mesenquimática es una estrategia de movimiento celular individual en la cual, para formar rutas de migración, las células liberan enzimas proteolíticas que degradan las fibras de colágeno que conforman la estructura tridimensional de la matriz extracelular. En esta tesis realizamos un estudio de las familias de soluciones de ondas estacionarias y viajeras de la versión unidimensional del modelo M^5, éste fue propuesto por Hillen para describir el movimiento celular.

Resaltamos la relación entre el tamaño de la población celular y el tipo de rastro de fibras reorientadas que las células dejan a su paso. Estudiamos además el comportamiento asintótico de los perfiles de onda estacionarios y viajeros; mediante el uso de series de Taylor demostramos que estos perfiles convergen de manera exponencial a sus estados estacionarios. Por otro lado, hemos construido analíticamente aproximaciones de las soluciones de ondas estacionarias y viajeras; nuestra técnica consiste en obtener mediante el método de polinomios de Lagrange un sistema de ecuaciones aproximadas con solución exacta. Como parte de la investigación, analizamos la estabilidad espectral de los miembros de las familias de ondas estacionarias y viajeras. Nos encontramos con que las ondas estacionarias son espectralmente estables y que el espectro del operador linealizado alrededor de ellas consiste únicamente de espectro esencial. Para demostrar que en el caso estacionario el espectro puntual es el conjunto vacío, usamos estimadores de energía junto con la técnica de Goodman de la variable integrada. Para las ondas viajeras el panorama es diferente, estos perfiles son espectralmente inestables debido a que el espectro esencial alcanza el semiplano derecho cerrado. Con miras a conseguir estabilidad espectral, construimos un espacio de Sobolev pesado donde el espectro esencial es parte del semiplano izquierdo abierto. El problema de la localización del espectro puntual no ha podido ser resuelto hasta el momento.

ABSTRACT

Mesenchymal migration refers to a proteolytic and path generating strategy of individual cell motion across the network of collagen fibres that compose the 3D extracellular matrix. In this thesis we inquire into the families of standing and traveling wave solutions of the one-dimensional version of the M^5-model, which was put forward by Hillen to describe the mesenchymal cell movement.

We highlight the relation between the size of the cell population and the trail of reorganized fibres that cells leave behind their wake. The long-time asymptotic behaviour of the standing and traveling wave profiles is examined; using Taylor expansions we show that each of these profiles converges exponentially to its end states. We have constructed analytic expressions that approximate the standing and traveling wave solutions, our technique consists in getting an exactly solvable approximate system through the use of Lagrange's interpolation method. It is explored the spectral stability of the members of the families of standing and traveling waves. Regarding the standing waves, they are spectrally stable and the spectrum of the linearized operator around the waves consists solely of essential spectrum. To prove that in the standing case the point spectrum is empty we use energy estimates together with the integrated-variable technique of Goodman. The panorama is completely different in the traveling case; the wave profiles are spectrally unstable due to the fact that the essential spectrum reaches the closed right-half complex plane. In our pursuit of spectral stability we have constructed a weighted Sobolev space where the essential spectrum lies inside the open left-half complex plane. The question of where is the point spectrum still remains open.

CONTENTS

INTRODUCCIÓN

Con el propósito de propagarse a otras partes del cuerpo, las células metastásicas se liberan del tumor primario, invaden el tejido circundante y logran intravasarse en los vasos linfáticos y sanguíneos para viajar a través de la vasculatura; eventualmente las células tumorales se extravasan en el parénquima—tejido que conduce la función específica del órgano y que por lo general comprende la mayor parte de éste—de un órgano distante, donde finalmente se establecen y proliferan para formar un tumor secundario [22, 55]. Las células cancerosas muestran dos tipos de estrategias de migración: la colectiva y la individual [14]. La migración colectiva es un fenómeno en el que las células mantienen adhesiones entre ellas, el movimiento es grupal en la forma de hebras, láminas o racimos [18]. En cambio, durante la migración individual no hay interacciones célula-célula, cada célula se mueve sola y hay poca relación entre el patrón de migración de una célula y el de sus vecinas [4]. Este tipo de movimiento a su vez se divide en mesenquimático y ameboide [18]. El movimiento mesenquimático involucra degradación proteolítica y remodelación—creación de rutas de migración—de la matriz extracelular (MEC). A diferencia de las células mesenquiáticas, las células ameboides no intervienen en la remodelación de los componentes de la MEC [37, 18, 57]. La MEC es una malla tridimensional compuesta por un entretejido de fibras formadas por una mezcla de proteínas estructurales [9]. El entramado de la MEC actúa como un andamio que estabiliza la estructura física de los tejidos, y desempeña además un papel activo en la regulación de las funciones celulares tales como la adhesión, proliferación y migración. En particular, en el fenómeno de migración celular, la topografía del sustrato extracelular proporciona orientación por contacto, con la cual las células son impulsadas a migrar en una dirección paralela a la orientación local de las fibras de la matriz [39].

En este trabajo nos centramos en la migración mesenquimática. En [24], Hillen propuso un modelo mesoscópico (a nivel individual) n-dimensional para el movimiento mesenquimático, en el que se incluyen la orientación por contacto y la degradación preoteolítica. Este modelo, al que nos referiremos como el modelo M^5, está basado en el modelo integro-diferencial de transporte, formulado por Othmer *et al.* [40] para describir el proceso de salto de velocidad, que consiste de periodos de recorridos en una cierta dirección interrumpidos por reorientaciones instantáneas. El modelo M^5 es un sistema de dos ecuaciones integro-diferenciales, una de ellas es una ecuación de transporte para el movimiento celular. En la formulación de ésta la dirección de movimiento es dictada por un peso probabilístico, el cual representa a la distribución ángular de las fibras. El cambio de la probabilidad en

el espacio y el tiempo es descrito por una ecuación dinámica. En el modelo, la acción proteolítica sobre la matriz depende de la orientación relativa entre la dirección de la fibra y la dirección de movimiento, y depende también del tipo de tejido, que puede ser no dirigido o dirigido. En el tejido no dirigido las fibras son axialmente simétricas, debido a esto las células no son capaces de distinguir entre los dos sentidos opuestos de una fibra. Los tejidos dirigidos, por el contrario, están formados por fibras asimétricas que poseen su propia polaridad.

En [5], Chauviere *et al.* extendieron el modelo M^5 para incluir quimiotaxis—movimiento hacia o lejos de una sustancia química—y las interacciones célula-célula. En el caso del movimiento ameboide, Chauviere y Preziosi modificaron en [6] la ecuación de transporte para considerar que la frecuencia de las reorientaciones de las células puede depender de factores ambientales tales como la densidad celular y/o la densidad de la MEC. Recientemente, mediante un escalamiento parabólico de la ecuación integral de transporte, Painter y Hillen obtuvieron una ecuación de difusión que modela macroscópicamente la invasión de células de glioma [42]. Esta misma ecuación también ha sido aplicada por Hillen y Painter [26] en los patrones de movimiento de los lobos. Engwer *et al.* [10] hicieron modificaciones al modelo de Painter y Hillen para considerar de manera explícita los mecanismos de adhesión entre las células de gliomas y los tractos de materia blanca cerebral.

Para entender qué papeles desempeñan la orientación por contacto y la remodelación de la MEC en la organización espacial de las células, Painter [41] hizo cambios a la versión del modelo M^5 para tejidos dirigidos. En su versión, la formulación del modelo depende de la dinámica de la matriz, en la que se involucran la ruptura de la MEC por degradación proteolítica focalizada, y la producción y montaje de nuevos componentes de la matriz. Painter resolvió el modelo de manera numérica en un dominio rectangular, y encontró que, dentro de un arreglo inicial de fibras orientadas aleatoriamente, la acción conjunta de orientación por contacto y remodelación de la MEC puede generar patrones estacionarios estables en forma de red. Esta forma de red se debe a la interconexión de cadenas celulares—células formadas en fila india—densas, las cuales son mantenidas por caminos de fibras alineadas predominantemente con la dirección de migración. Dichos caminos están rodeados por zonas de fibras aleatoriamente orientadas donde la densidad de células es menor.

Motivados por los resultados numéricos de Painter, Hillen *et al.* [25] investigaron los estados estacionarios del modelo M^5 para el caso del tejido no dirigido. Interesados en obtener soluciones con validez biológica, los autores construyeron un espacio adecuado de soluciones que admitiera funciones medibles. En $\mathbb{R}^n$, Hillen *et al.* descubrieron que una distribución radial uniforme de células y fibras (tejido homogéneo) da forma a un estado estacionario del sistema. Para diseñar tejidos más complejos, con caminos y con campos de fibras dispuestas en paralelo, Hillen y colaboradores hicieron uso de la función delta de Dirac para representar una masa de fibras alineadas en una sola dirección. Con el propósito de poder considerar distribuciones δ para las fibras, y lograr así construir estados estacionarios tipo red, Hillen *et al.* [25] introdujeron los conceptos de estado estacionario débil y de estado estacionario puntual. Con el primer concepto consiguen categorizar como estados estacionarios a los arreglos de fibras colocadas completamente en paralelo (tejidos estrictamente alineados). El segundo concepto les permitió incluir, en $\mathbb{R}^2$, estados estacionarios tipo parches y estados estacionarios del tipo red. El primer tipo consiste

de tejidos homogéneos montados sobre conjuntos disjuntos; los conjuntos están divididos por curvas de longitud finita que pueden ser cerradas pero sin intersecciones entre ellas; sobre éstas la orientación de las células y las fibras está determinada en cada punto por la dirección del vector tangente. Es segundo tipo de estado estacionario es similar, pero difiere en que las intersecciones son permitidas.

Con la idea de idetificar los mecanismos de migración que podrían llevar a la agregación celular en la migración mesenquimática en dimensiones mayores, Wang *et al.* [56] estudiaron en la versión unidimensional del modelo M^5, el cual corresponde al caso en el que las células se mueven en un medio de tejidos estrictamente alineados. Abordando el caso unidimensional se pueden hacer descubrimientos importantes. Por ejemplo, Doyle *et al.* [8] descubrieron que la topografía unidimensional de la MEC induce una rápida diseminación de las células y una migración uniaxial similar a la que ocurre en una MEC tridimensional orientada. En [56], Wang *et al.* encontraron que la agregación celular es posible en tejidos dirigidos pero no lo es en los tejidos no dirigidos, los autores demostraron que para los tejidos dirigidos existen familias de ondas estacionarias y viajeras. Las familias están conformadas por pulsos para las células y frentes decrecientes para la matriz. Estas familias están indizadas por un continuo de velocidades de onda, y dentro de cada familia sus miembros tienen diferentes amplitudes. Nuestro estudio parte de estos resultados.

En esta tesis, después de exponer detalladamente en el Capítulo 1 los antecedentes biológicos y el modelo matemático que motivó nuestro estudio, presentaremos en el Capítulo 2 los resultados obtenidos por Wang *et al.* [56] sobre la existencia de las soluciones de ondas estacionarias y viajeras de la versión unidimensional del modelo M^5. En el capítulo profundizamos además en la naturaleza de las familias de los perfiles de onda; en particular, nos encontramos con que los pulsos más altos (los cuales tienen una mayor densidad celular) viajan a menor velocidad que los pulsos de menor amplitud. Ampliamos los resultados de Wang *et al.* [56] con respecto a la relación entre los dos extremos de los frentes de onda. Concluimos el capítulo demostrando que los perfiles de onda tienden de manera exponencial a sus estados estacionarios.

En el Capítulo 3 obtenemos de manera analítica soluciones aproximadas de las ondas estacionarias y viajeras del modelo M^5 unidimensional. Tomamos ventaja del hecho de contar con una expresión explícita de la órbita heteroclínica que da origen a los dos perfiles de onda. Usamos dicha expresión para desacoplar la ecuación para el frente de onda, sin embargo, ésta no puede ser resuelta analíticamente debido a la presencia de una no linealidad logarítmica. Interpolando dicha no linealidad mediante el método de Lagrange obtenemos una ecuación aproximada con solución exacta. Nuestra idea viene del trabajo de Petrovskii *et al.* [47] en la ecuación unidimensional de Fisher-Kolmogoroff, quienes usaron una técnica basada en aproximaciones lineales a trozos para conseguir de manera aproximada una solución continua de frente de onda decreciente.

Debido a que estamos interesados en la naturaleza de los perfiles de onda, es de gran interés determinar la estabilidad espectral de los perfiles de onda estacionarios y viajeros. La estabilidad espectral se refiere a que el conjunto $\lambda \quad \mathbb{C} \quad 0 \quad \mathfrak{Re}\lambda \geq 0$ no contiene parte alguna del espectro del operador linealizado alrededor de estos perfiles. En el Capítulo 4 formulamos el problema espectral para las ondas estacionarias y damos las definiciones de conjunto resolvente, espectro y estabilidad espectral. El espectro se define como la unión de dos conjuntos disjuntos: el espectro puntual y el espectro esencial. En este

capítulo demostramos que todos los miembros de la familia de ondas estacionarias son espectralmente estables y que, de hecho, el espectro es puramente esencial. Encontramos además que el eigenvalor cero tiene asociado un eigenespacio de dimensión infinita, lo que hace que pertenezca al espectro esencial y no al espectro puntual. En lo que respecta a cómo se determinó el espectro puntual, resultó de gran ayuda excluir el eigenvalor cero, debido a que esto nos permitió llevar el problema espectral original a un problema equivalente escalar de eigenvalores cuadráticos. La formulación escalar nos permitió usar la técnica de Goodman [21] de la *variable integrada* para establecer, mediante estimadores de energía, que el espectro puntual es el conjunto vacío. El espectro esencial en el caso viajero es estudiado en el Capítulo 5. Hemos hallado que los miembros de todas las familias de ondas viajeras son espectralmente inestables, lo que se debe a que parte del espectro esencial toca al eje imaginario. Para recorrer el espectro esencial hacia el semiplano izquierdo abierto hemos construido un espacio de Sobolev pesado-exponencialmente. En dicho espacio el cero es un eigenvalor simple que pertenece al espectro puntual. La estabilidad espectral de las ondas viajeras aún no ha podido ser determinada, ya que la ubicación del espectro puntual supone un problema que no ha podido ser resuelto hasta el día de hoy. Por último, en el Capítulo 6 presentamos una discusión general de los resultados presentados en esta tesis y las perspectivas de investigación futuras.

INTRODUCTION

In order to spread to other parts of the body, metastatic tumor cells shed from the primary solid tumor, invade the surronding tissue and intravasate into lymphatic and blood vessels to transit through the vasculature, eventually tumor cells extravasate into the parenchyma—the tissue which conducts the specific function of the organ and which usually comprises the bulk of the organ—of a distant organ and proliferate to form a secondary tumor [22, 55]. Cancer cells exhibit two different strategies of migration, they move either collectivelly or individually [14]. Collective migration occurs when cells retain cell-cell junctions; in such strategy groups of cells migrate as strands, sheets, or clusters [18]. On the contrary, during individual migration there is an absence of cell-cell interactions, every single cell makes the journey alone and the migration pattern between a cell and its neighbors is low correlated [4]. Additionally, individual cell movement can be broken down into mesenchymal and amoeboid [18]. Mesenchymal motion involves the protease-mediated degradation and remodeling—creation of migration tracks—of the extracellular matrix (ECM). In contrast to mesenchymal cells, amoeboid cells do not cause remodeling of ECM components [37, 18, 57]. The ECM is a 3D network constructed with interwoven fibres composed of a mixture of structural proteins [9]. The architecture of ECM provides a scaffolding that stabilizes the physical structure of tissues, and it also plays an important role in regulating cellular functions such as cell adhesion, proliferation and migration. In particular, in the cell migration phenomenon the topography of the extracellular substratum provides contact guidance, wherein cells are induced to migrate parallel to the local orientation of the matrix fibres [39].

In this work, the focus is on mesenchymal migration. In [24], Hillen proposed an n-dimensional mesoscopic (individual level) model, to which we refer hereafter as the M^5-model, for mesenchymal motion which includes contact guidance and proteolytic degradation. The model is based on the integral transport model formulated by Othmer *et al.* [40] to describe the velocity-jump process, where periods of runs in a given direction are interrupted by instants of reorientation. The M^5-model is a system of two coupled integro-differential equations, one is an integral transport equation for the cell motion in which the direction of movement is fixed by a probability weight that models the local angular distribution of matrix fibres. The change for the space-time-varying probability is described by an evolution equation. In the model the proteolytic action on the matrix is dependent on the relative orientation between the fibre direction and the movement direction, and on the type of tissue which can be either undirected or directed. In undirected tissues

the fibres are axially symmetric, so that cells are unable to distinguish between the two opposite fibre directions. Conversely, directed tissues are composed of asymmetric fibres that have ends possessing their own polarity.

In [5], Chauviere *et al.* further developed the M^5-model to include chemotaxis—movement either toward or away from a chemical stimulus—and cell-cell interactions. In the case of amoeboid movement, Chauviere and Preziosi modified in [6] the transport model to account that the frequency of turning of cells may depend on environmental factors such as the cell density and/or the ECM density. More recently, Painter and Hillen [42] applied a parabolic scaling to the integral transport equation in order to obtain a diffusion equation that models the macroscopic process of glioma invasion. This last equation has also been applied by Hillen and Painter [26] in the movement patterns of wolves. Engwer *et al.* [10] extended the model provided by Painter and Hillen to explicitly consider adhesion mechanisms between glioma cells and the myelinated fiber tracts of white matter ECM.

To understand the role of contact guidance and ECM remodeling on the spatial organization of the cells, Painter performed in [41] adaptations of the M^5-model for undirected tissues. The model is formulated for different matrix dynamics which involves matrix degradation due to focussed proteolysis and the production and assembly of new matrix components. Painter solved numerically the model in 2D rectangular domains, he found that for an initially random orientation of matrix fibres, the combination of contact guidance and ECM remodeling can generate stable steady network patterns. These networks are structured by interlocked dense cell-chains—cells following each other in Indian file—sustained by pathways of fibres predominantly aligned along the direction of migration, which are enclosed by zones with fibres randomly oriented where the density of cells is lower.

Inspired by Painter's numerical results, Hillen *et al.* [25] investigated the steady states of the M^5-model for the particular case of undirected tissue. To obtain biologically meaningful solutions the authors constructed a suitable solution framework of measure-valued functions. For $\mathbb{R}^n$, it was found by Hillen *et al.* that cells uniformly distributed in orientation and density borne up by fibres uniformly radially oriented (homogeneous tissue) compose a steady state of the system. To design more complex tissues with tracks and fields of parallel-oriented fibres, Hillen and coworkers made use of the Dirac delta function to represent a mass of fibres concentrated entirely in a single direction. In order to allow for δ-distributions for the fibres and then manage to build network type steady states, Hillen *et al.* introduced the concepts of weak steady state and pointwise steady state. With the first concept, arrangements of cells and fibres aligned in a totally parallel fashion (strictly aligned tissues) are distinguished as steady states of the system. The second concept allows to include, in $\mathbb{R}^2$, patchy steady states and steady states of network type. The former consists of homogeneous tissue disposed over disjoint open sets, which are divided by curves of finite length possibly closed but without intersections between them, the orientation of cells and fibres along the curves is fully determined by the direction of the tangent vector at each point. The latter is similar, differing in that intersections are admissible.

With the aim of identifying migratory mechanisms that could lead to cellular aggregation in the high dimensional mesenchymal migration, Wang *et al.* [56] studied the one-dimensional version of the M^5-model, which corresponds to the case where cells move inside an environment of strictly aligned tissues. Important insights can be gained through

the one-dimensional approach either at the theoretical or experimental levels; for example, Doyle *et al.* [8] discovered that the 1D ECM topography induces a rapid cell spreading and uniaxial migration similar to what occurs in an oriented 3D ECM. In [56], Wang *et al.* found that celluar aggregation is possible for directed tissue but not for the undirected one; the authors proved that, for directed tissue, there exist families of standing and traveling wave solutions. The families are composed of pulses for the cells and decreasing fronts for the matrix. These families are indexed by a continuum of wave speeds, and inside each family their members have different amplitudes among them. Our study depart from these results.

In this thesis, after presenting in detail in Chapter 1 the biological background and the mathematical model that motivated our study, we recall in Chapter 2 the results obtained by Wang *et al.* [56] on the existence of standing and traveling wave solutions to the one-dimensional version of the M^5-model. Besides, in the chapter, we go deeper into the nature of the families of wave profiles. We have discovered that the higher amplitude pulses (which have a greater cell density) travel slower than the shorter ones. We extend the results of Wang *et al.* [56] on the relation between the two ends of the wave fronts. We finish the chapter by showing that the wave profiles tend exponentially to their end states.

In Chapter 3 we find approximate analytical standing and traveling wave solutions to the one-dimensional M^5-model. To do so, we took advantage of the fact that we have an explicit expression of the heteroclinic that gives rise to both wave profiles. We used that expression to decouple the equation of the wave front, which cannot be solved analytically due to the presence of a logarithmic nonlinearity. Using Lagrange's method we interpolate that nonlinerity, obtaining in this way an exactly solvable approximate equation. Our inspiration comes from the work of Petrovskii *et al.* [47] on the one-dimensional Fisher-Kolmogoroff equation, in which the authors used a technique based on a piecewise-linear approximation in order to provide an approximate continuous decreasing wave front solution.

Since the nature of the wave profiles is our main concern, it is of great interest determining the spectral stability of the standing and traveling wave profiles. By spectral stability we mean the requirement that the set $\lambda \in \mathbb{C} \setminus 0 \quad \mathfrak{Re}\lambda \geq 0$ contains no part of the spectrum of the linearized operator around the standing- or traveling-wave profiles. In Chapter 4 we formulate the spectral problem for the standing waves and give the definitions of resolvent set, spectrum and spectral stability. The spectrum is defined as the union of two disjoint sets: the point spectrum and the essential spectrum. In the chapter we show that all the members of the family of standing waves are spectrally stable, and that indeed the spectrum is purely essential. We find that the eigenvalue zero is associated to an infinite dimensional eigenspace, which makes it belong to the essential spectrum and not to the point spectrum. In regard to determination of the point spectrum, it was helpful to exclude the zero eigenvalue since this allowed us to bring the original spectral problem into an equivalent scalar quadratic eigenvalue problem. The scalar formulation has enabled us to use Goodman's *integrated variable* technique [21] to establish, via energy methods, that the point spectrum is empty. The essential spectrum for the traveling case is studied in Chapter 5. We found out that the members of all the families of traveling waves are spectrally unstable, this is because part of the essential spectrum reaches the imaginary axis. To move the essential spectrum to the open left-half complex plane we

have constructed an appropriate exponentially-weighted Sobolev space. In such space, zero is a simple eigenvalue that belongs to the point spectrum. The question about the spectral stability of the traveling waves remains open since the issue of locating the point spectrum entails a problem that has not been overcome yet. A general discussion of both the results of this thesis and the perspectives of future work is left to Chapter 6.

CHAPTER

ONE

THE M^5-MODEL FOR MESENCHYMAL MIGRATION INSIDE DIRECTED TISSUES

1.1

Biological Background

Tumor invasion and metastasis constitute one of the so-called "hallmarks of cancer". To metastasize, neoplastic cells detach from the primary tumor, invade the host stroma, then penetrate into the bloodstream or the lymphatic circulation (intravasation). If cancer cells survive to the hostile environment that represents the circulatory system (due to the impossibility to absorb nutrients, immune defenses and turbulent forces of movement), they leave the vascular or lymphatic channels (extravasation) and form a secondary tumor elsewhere in the body (colonization) [12, 22, 55].

To reach lymph or blood vessels, tumor cells move through the extracellular matrix (ECM) [30]. The ECM is a 3D fibre network composed primarily of collagen, laminin, fibronectin and proteoglycans [9]. Collagen fibrils (about 20–200 nm in diameter), which reach lengths of the order of several hundred of micrometers, often aggregate into larger cablelike bundles to form microscale collagen fibers [34]. Besides serving as a physical support to the tissue, the fibrous architecture of the ECM provides the required scaffold to support cell adhesion, proliferation, differentiation and migration [23, 35]. ECM acts as a highway system along which cells move. During cell migration, directional information can be provided by the orientation of the matrix fibres, in the process known as *contact guidance* the matrix facilitates movement in either direction parallel to the fibres [39]. Figure 1.1 shows a schematic representation of the extracellular matrix and the movement of cells inside thereof.

To perform migration, a cell requires to modify the morphology and stiffness of its body to interact dynamically with the structure of the host tissue [18]. Cell migration in normal and cancer cells involves a series of continuous cycles of cell protrusion-contraction together with cell adhesion to and deadhesion from the ECM substrate [17, 18]. Traction forces generated by contractile cell-matrix interactions result in a forward gliding of the cell body

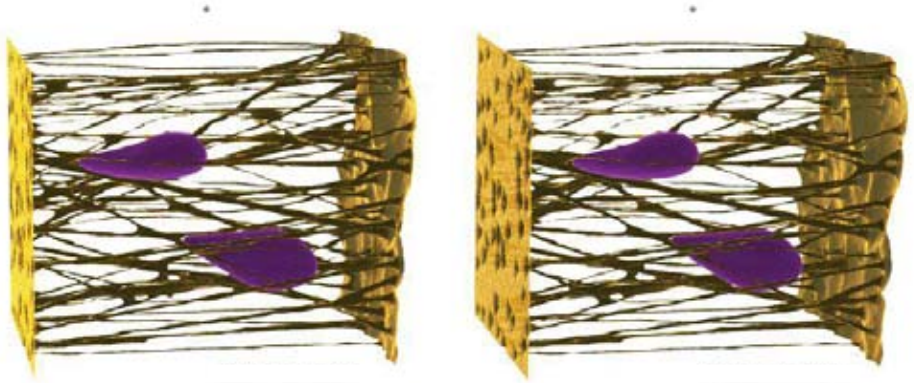

Figure 1.1: Cross-view illustration of the extracellular matrix and cell migration. Illustration by Ramiro Chávez Tovar.

and its rear end [18]. According to Friedl *et al.* [17, 18], migration of most cells consists of a cyclic five-step process. First, at the leading edge of the moving cells, pseudopods are formed by intracellular polymerization of actin filaments (step 1). Then, these protrusions come into contact with ECM ligands, forming focal contacts through the clustering of adhesion proteins (step 2). To overcome the physical barrier that the components of the ECM represent cells locally degrade the ECM substrate, via the activation of cell surface proteases (proteolytic/degrading enzymes like MT1-MMP and uPA/uPAR), to create the space necessary for migration (step 3). Actomyosin contraction (step 4), driven by the binding of actin filaments to myosin II, results in the disassembly of focal adhesions in the back of the cells (step 5). While weakening of adhesion strength occurs at the trailing edge, substrate binding at the leading edge remains and elongation continues further.

A number of *in vitro* and *in vivo* studies suggest that cells move inside the surrounding tissue by two different migration modes [18]: collective and individual. In the former, cells move as solid strands, sheets or clusters, which are maintained by cell-to-cell adhesions. Collective migration represents the predominant mechanism of invasion and metastasis in lobular breast cancer, epithelial prostate cancer and large-cell lung cancer [17, 18]. It also plays an important role in normal physiological functions, among them tissue repair and embryological development [16]. Individual migration refers to the dissemination of single cells once homophilic adhesions to neighboring cells have been broken [15, 18], it takes place in the spreading of leukaemias, lymphomas and sarcomas [18].

Individual cell migration, in turn, exhibits two different phenotypes of movement: *mesenchymal* and *amoeboid*. The key difference between the two strategies of migration resides in the mechanisms employed to cross the ECM barrier. In mesenchymal migration the action of proteases is present, they execute degradation and remodeling of the local extracellular environment, creating tube-like matrix defects along the path of migration [18, 57]. Amoeboid migration, on the other hand, does not require proteolytic activation, instead, cells squeez through narrow gaps in the ECM, suffering frequent modifications in their shape without altering the ECM structure. The migration velocity represents another difference in the modes of cell migration: mesenchymal cells are characterized by developing strong and lasting focal contacts with the extracellular substratum, and these

attributes make them move slowly, with velocities varying from 0.1 to 2 μm/min. In contrast, amoeboid cells are faster: achieving velocities up to 20 μm/min, they move inside the tissue forming brief and weak focal adhesions with matrix fibres [37, 18]. In this work we focus our study on mesenchymal migration.

1.2

The M^5-Model

The main purpose of the current chapter is to introduce the transport model developed by T. Hillen [24] for the movement of mesenchymal cells inside tissue. The model formulation encompasses the cell motion within *undirected tissues* and inside *directed tissues*. In undirected tissues the fibres are symmetric, so that the cells are unable to distinguish between two opposite directions of migration. In directed tissues the fibres are asymmetric and the two ends have a specific polarity (up/down, forward/backward). This is the one we are interested in here.

It is assumed that the motion of each cell is governed by the velocity-jump process, in which periods of straight motion called runs, alternate at discrete times with an instantaneous reorientation tumbling. It is also assumed that the preferred directions of movement are determined by the angular distribution of the matrix fibres; this is the previously mentioned contact guidance. In addition, the influence of cell-to-cell interactions (among them, adhesion and contact inhibition) is neglected, which means that the cell movement is dominated by cell-ECM interactions. Another assumption is that during migration cells neither proliferate nor die, that is, cell density is conserved.

The transport model proposed by Hillen [24], hereafter referred to as the M^5-Model, for mesenchymal cell movement describing a velocity-jump processes inside *directed* tissues reads

$$\begin{aligned} p_t(x,t,v) + v \cdot \quad p(x,t,v) &= -\mu p(x,t,v) + \mu \frac{q(x,t,\hat{v})}{\omega}\rho(x,t), \\ q_t(x,t,\theta) &= \kappa\left(\Pi_d(x,t,\theta) - A_d(x,t)\right)\rho(x,t)q(x,t,\theta). \end{aligned} \tag{1.1}$$

The function $p(x,t,v)$ denotes the density of cells at location x $\mathbb{R}^n$, at time $t \geq 0$, moving with velocity v V. The velocity space $V \subseteq \mathbb{R}^n$ is radially symmetric and is given by $V = [s_1, s_2] \times \mathbb{S}^{n-1}$, where $0 < s_1 \leq s_2 <$ is the range of all possible speeds and $\mathbb{S}^{n-1}$ is the unit sphere in $\mathbb{R}^n$. The macroscopic cell density denoted by $\rho(x,t)$ is the total amount of cells at x and is calculated by

$$\rho(x,t) = \int_V p(x,t,v)\, dv.$$

The transport term $v \cdot \quad p$ represents the fact that every single cell moves with its own velocity. The terms on the right-hand side of the first equation describe the reorientation of the cells: cells turn away from velocity v with a turning rate $\mu > 0$ (1/mean run-time)

and choose velocity v with a probability $q(x,t,\hat{v})/\omega$. Here we assume that μ is a constant, but in principle it may depend on environmental factors like the number of cells and/or the ECM density [6]. The probability density $q(x,t,\theta)$ describes the fibres at location $x \quad \mathbb{R}^n$ and at time $t \geq 0$ with orientation $\theta \quad \mathbb{S}^{n-1}$, and satisfies

$$\int_{\mathbb{S}^{n-1}} q(x,t,\theta)\, d\theta = 1. \tag{1.2}$$

We write $\hat{v}$ to denote the unit vector $\hat{v} = v/\ \ v\ \ $ in direction of v, and ω denotes the weight parameter defined by

$$\omega = \begin{cases} \frac{s_2^n - s_1^n}{n}, & \text{for } s_1 < s_2, \\ s^{n-1}, & \text{for } s_1 = s_2 = s. \end{cases}$$

Hence, cells select the velocity $v \quad V$ with a probability $q(x,t,\hat{v})/\omega$, this reflects the effect of contact guidance as a driver of cell migration. The quotient q/ω defines a probability density in V and satisfies

$$\int_V \frac{q(x,t,\hat{v})}{\omega}\, dv = 1.$$

The constant $\kappa > 0$ denotes the rate of matrix degradation, which represents the proteolytic action per cell on the ECM. $\Pi_d(x,t,\theta)$ denotes the *mean projection* of the direction of cell movement along a fibre with orientation θ, it is computed by

$$\Pi_d(x,t,\theta) = \frac{1}{\rho(x,t)} \int_V \theta \cdot \hat{v}\, p(x,t,v)\, dv.$$

This is a measure of the encounter angle between the migrating cell population and fibres with a given orientation θ. In other words, it gives the level of alignment of the cells with such fibres. The major fibre cleavage occurs when cells move in a direction $\hat{v}$ opposite to that of the fibres ($\theta \cdot \hat{v} = -1$), which is when the movement turns out to be impossible without destroying the fibres. Then, the mean projection is $\Pi_d(x,t,\theta) = -1$ when the entire population displaces in counter direction of θ. Fibre degradation is also expected when cells and matrix fibres meet at a right angle ($\theta \cdot \hat{v} = 0$); the value $\Pi_d(x,t,\theta) = 0$ corresponds to the situation when every cell has a direction of propagation orthogonal to θ. In contrast, fibres oriented parallel to the movement direction ($\theta \cdot \hat{v} = 1$) are left intact, as if all moving cells are aligned with θ then we have that $\Pi_d(x,t,\theta) = 1$.

The *relative alignment* is the mean value of the mean projections over all fibre directions, it measures the local aligment of cells and fibres. It is given by

$$A_d(x,t) = \int_{\mathbb{S}^{n-1}} \Pi_d(x,t,\theta) q(x,t,\theta)\, d\theta.$$

1.2.1

The one-dimensional M^5-model

In this work we are interested in the one-dimensional version of the transport model for mesenchymal cell movement inside a directed tissue, which describes the case where mes-

enchymal cell population moves within a directed tissue made up of *highly aligned* fibres. The one-dimensional model may seem somewhat unrealistic, but indeed it is not. Using microphotopatterned ECM protein lines, Doyle and colleagues found in their research that the 1D ECM topography closely mimics rapid cell spreading and uniaxial migration triggered by oriented 3D ECM [8].

In a wide range of tissues of the human body, from myocardial to connective tissues, tissue function is dictated by the cell and ECM organization [59]. In a recent study Xing *et al.* used synthetic nanogratings to produce highly aligned nanofibrous natural ECM scaffold. Their results revealed that such aligned scaffold can effectively support human mesenchymal stem cells proliferation and has a superior inflammatory response in comparison with its unaligned counterpart [59].

Human tissues composed of highly ordered arrays of matrix fibres is a significant part of white matter tracts such as the corpus callosum of the human brain [2]. Using aligned electrospun nanofibers, which mimic the white matter morphology, Johnson *et al.* [32] provide evidence that malignant gliomas travel faster in aligned nanofibers when compared to randomly organized nanofibers. On aligned fibers the effective velocities are $4.2 \pm 0.39\,\mu$m/h while on random fibers are $0.8 \pm 0.08\,\mu$m/h, values which closely match those from experimental observations *in vivo*.

Below, we repeat Hillen's derivation of the one-dimensional version the M^5-model (see [24]). It is assumed that the cell population moves with a fixed speed $v = s$; since in one dimension cells can only move towards the right or the left, we have that $\mathbb{S}^0 = \{-1, +1\}$, thus $\theta = \pm 1$, $V = \{s\} \times \mathbb{S}^0$ and $\hat{v} = \pm 1$.

We introduce the notation:

$$p^{\pm}(x,t) = p(x,t,\pm s) \quad \text{and} \quad q^{\pm}(x,t) = q(x,t,\pm 1).$$

Condition (1.2), in this case, becomes

$$q^+(x,t) + q^-(x,t) = 1.$$

The mean projection on both directions, $\theta = \pm 1$, is calculated by the formula

$$\Pi_d(x,t,\theta) = \frac{1}{p^+ + p^-}\left(\theta(+1)p^+ + \theta(-1)p^-\right).$$

Defining

$$\Pi_d^{\pm} := \Pi_d(x,t,\pm 1) = \pm\frac{p^+ - p^-}{p^+ + p^-},$$

the relative alignment comes from

$$A_d(x,t) = \Pi_d^+ q^+ + \Pi_d^- q^- = \frac{p^+ - p^-}{p^+ + p^-}\left(q^+ - q^-\right).$$

Then, according with the equation for $q(x,t,\theta)$ in (1.1) we arrive at

$$q_t^+ = \kappa\left(p^+ - p^-\right)\left(q^- - q^+ + 1\right)q^+$$

and

$$q_t^- = \kappa\left(p^+ - p^-\right)\left(q^- - q^+ - 1\right)q^-.$$

Therefore the one-dimensional M^5-model reads:

$$\begin{aligned} p_t^+ + sp_x^+ &= -\mu p^+ + \mu q^+ \left(p^+ + p^-\right), \\ p_t^- - sp_x^- &= -\mu p^- + \mu q^- \left(p^+ + p^-\right), \\ q_t^+ &= \kappa \left(p^+ - p^-\right) \left(q^- - q^+ + 1\right) q^+, \\ q_t^- &= \kappa \left(p^+ - p^-\right) \left(q^- - q^+ - 1\right) q^-. \end{aligned} \tag{1.3}$$

In [56], Wang *et al.* proved that $q^+ + q^- = 1$ is an invariant manifold, this finding allows to convert system (1.3) into a system of equations for the total cell population $p = p^+ + p^-$, the population flux $j = s(p^+ - p^-)$ and the probability of moving to the right q^+. The equivalent system writes as

$$\begin{aligned} p_t + j_x &= 0, \\ j_t + s^2 p_x &= -\mu j + \mu s \left(2q^+ - 1\right) p, \\ q_t^+ &= \frac{2\kappa}{s} j q^+ \left(1 - q^+\right). \end{aligned} \tag{1.4}$$

In order to see the kind of movement patterns emerge during the invasion of the tissue by the cells, Wang *et al.* [56] sought traveling wave solutions for system (1.4). The authors showed the existence of standing and traveling pulse solutions for the population of invasive cells and traveling front waves for the completely oriented fibres. Henceforth, our task will be to study the structural nature and stability properties of these solutions.

CHAPTER
TWO

EXISTENCE AND NATURE OF M^5-STANDING AND TRAVELING WAVES

2.1

The Existence

We begin the chapter by exposing how the system of traveling wave equations is derived, and by summing up the results of existence of standing and traveling wave solutions reported by Wang *et al.* in [56].

Making use of the traveling wave *ansatz*,

$$p(x,t) = \bar{p}(z), \quad j(x,t) = \bar{j}(z), \quad q^+(x,t) = \bar{q}^+(z), \quad z = x - ct,$$

with wave speed $0 \leq c \leq s$, system (1.4) turns into the system of ordinary differential equations:

$$\begin{aligned} -c\bar{p}_z + \bar{j}_z &= 0, \\ -c\bar{j}_z + s^2\bar{p}_z &= -\mu\bar{j} + \mu s\left(2\bar{q}^+ - 1\right)\bar{p}, \\ -c\bar{q}^+_z &= \frac{2\kappa}{s}\bar{j}\bar{q}^+\left(1 - \bar{q}^+\right). \end{aligned} \tag{2.1}$$

The solutions must satisfy the boundary conditions

$$\begin{aligned} &\lim_{z \to \pm} \ \bar{p}(z) = \lim_{z \to \pm} \ \bar{j}(z) = 0, \\ &\lim_{z \to +} \ \bar{q}^+(z) = q_r^+, \\ &\lim_{z \to -} \ \bar{q}^+(z) = q_l^+ \text{ with } 0 \leq q_r^+ < q_l^+ \leq 1. \end{aligned} \tag{2.2}$$

As suggested by the boundary conditions, the solutions that are of interest are two traveling pulses that approach the origin as $z \quad \pm \quad$, and a traveling wave front joining up q_l^+ and q_r^+.

The difference between the magnitudes of the boundary conditions for solution $\bar{q}^+(z)$ represents that the amount of right-oriented fibres changes as cells move along ECM fibres, which is due to the ability of cells to reorient collagen fibres. The pulses mean that the reoriented ECM structure, in turn, directs cells to form cellular aggregates with density $\bar{p}(z)$.

The interesting thing about this kind of solutions is that they can give us an idea of the potential effect of unidirectional scaffolds on the migratory behavior of cells, which is relevant because of its applications in biomedicine. For example, Gallego-Perez *et al.* [19] studied directional tumor cell migration guided by a 1D line-patterned microfabricated platform. During the migration assay, time-lapse microscopy was used to track migratory behaviors of glioblastoma multiforme (GBM), and adenocarcinoma of the lung and colon. The results showed that all the tumor cells exhibited persistently unidirectional motility, with percentages of unidirectionally of $84.0 \pm 3.5\%$, $58.3 \pm 6.8\%$ and $69.4 \pm 5.4\%$ for the GBM, lung, and colon tumor cells, respectively. Jain *et al.* [31] have designed a promising technology for the treatment of GBM that exploits its migratory and invasive ability. The authors fabricated a tumor guide consisting of aligned PCL nanofibres that provide topographical cues that mimic blood vessels and white matter tracts. In their study, the PLC guidance conduit was implanted near U87MG-eGFP human glioblastoma cells to encourage unidirectional movement towards an extracortical sink containing an apoptosis-inducing hydrogel. Jain *et al.* observed that the tumor volume in the brain, outside the aligned fiber conduit, is significantly smaller in comparison with no implant. Current therapies include surgical removal, radiotherapy and chemotherapy, however, in some cases, the tumor may be inoperable because of the size or location. In some other cases, because hypoxic tumor cells are resistant to radiation and to anticancer drugs, radiotherapy and chemotherapy are ineffective to eliminate tumor cells. This technology brings new options for brain cancer treatments, in which, cancer cells would be completely removed by directing inaccessible tumors to the surface of the brain to be surgically removed or by directing cells to an apoptotic sink.

From the integration of the first equation in (2.1) and the boundary conditions, it is obtained the invariant of motion

$$\bar{j} = c\bar{p}. \tag{2.3}$$

Substituting (2.3) into the last two equations of (2.1) produces the system

$$\begin{aligned} \left(c^2 - s^2\right)\bar{p}_z &= \mu\bar{p}\left[c - s(2\bar{q}^+ - 1)\right], \\ \bar{q}_z^+ &= -\frac{2\kappa}{s}\bar{p}\left(1 - \bar{q}^+\right)\bar{q}^+. \end{aligned} \tag{2.4}$$

As noted by Wang *et al.* [56], when $c = s$ the equation for $\bar{p}$ becomes singular, then it happens that $\bar{q}^+ = 1$ is a homogeneous steady solution, which means that the whole cell population spreads to the right all the time. This solution, however, does not fit the boundary conditions of the problem, therefore the case $c = s$ is neglected. Thus, (2.4) is written in the form

$$\begin{aligned} \bar{p}_z &= \frac{\mu}{c^2 - s^2}\bar{p}\left[c - s\left(2\bar{q}^+ - 1\right)\right], \\ \bar{q}_z^+ &= -\frac{2\kappa}{s}\bar{p}\left(1 - \bar{q}^+\right)\bar{q}^+. \end{aligned} \tag{2.5}$$

The system is characterized by having a continuum of steady states:

$$\left\{(\bar{p}, \bar{q}^+) \;\; \bar{p} = 0,\, \bar{q}^+ = \theta \text{ with } 0 \leq \theta \leq 1\right\}.$$

Here θ does not denote fibres orientation as in Section 1.2; just for keeping the notation of the authors in [56], hereinafter θ is a continuum probability parameter representing the probability that cells move to the right.

It was shown by Wang *et al.* [56] that for every value of c on the interval $0 \leq c < s$, there is a critical value $\theta^* = \frac{c+s}{2s}$ such that the steady state $(0, \theta)$ is stable for all $0 < \theta < \theta^*$, and unstable for all $\theta^* < \theta < 1$. More precisely, the authors proved the following.

Lemma 2.1. [56] *Assume $0 \leq c < s$. Let $(\bar{p}, \bar{q}^+)$ be a solution of (2.5) subject to initial conditions $\bar{p}_I > 0$ and $0 < \bar{q}_I^+ < 1$. Then the ω-limit set of solutions to system (2.5) is contained in the following set:*

$$\mathbb{N} = \left\{(\bar{p}, \bar{q}^+) \;\; \bar{p} = 0,\; 0 < \bar{q}^+ < \theta^*\right\},$$

and the α-limit set is contained in the set

$$\mathbb{G} = \left\{(\bar{p}, \bar{q}^+) \;\; \bar{p} = 0,\; \theta^* < \bar{q}^+ < 1\right\},$$

where θ^* is a constant between 0 and 1 determined by $\theta^* = \frac{c+s}{2s}$.

In view of the foregoing, a traveling (or a standing) wave solution is determined by a heteroclinic orbit departing from a left steady state $(0, q_l^+)$, with $\theta^* < q_l^+ < 1$, and asymptotically arriving at some right steady state $(0, q_r^+)$, with $0 < q_r^+ < \theta^*$. In regard to $\bar{q}^+ = 0$ and $\bar{q}^+ = 1$, by solving (2.5) it is seen that if $\bar{q}^+ = 0$ then $\bar{p} \quad + \quad$ as $z \quad - \quad$, and that when $\bar{q}^+ = 1$, $\bar{p} \quad + \quad$ as $z \quad + \quad$. This implies that neither a heteroclinic connection to $(0, 0)$, nor a heteroclinic connection from $(0, 1)$, have the chance to exist.

The results on existence of standing and traveling wave solutions obtained by Wang *et al.* [56] are stated as follows:

Theorem 2.2. [56] *Let us consider the system (2.5) given traveling speed c with $0 \leq c < s$ and $\theta^* = \frac{c+s}{2s}$. Then for any equilibrium $(0, c_1)$ with $\theta^* < c_1 < 1$ there exists another equilibrium $(0, c_2)$ with $0 < c_2 < \theta^*$ such that there is a bounded, nonnegative, heteroclinic orbit connecting $(0, c_1)$ to $(0, c_2)$. That is, there exists a traveling solution $(\bar{p}, \bar{q}^+)$ of the system (2.5) connecting two equilibria. Particularly, the system (2.5) admits a standing wave for $c = 0$.*

According to Theorem 2.2 we have for the boundary conditions (2.2) that $0 < q_r^+ < \theta^*$ and $\theta^* < q_l^+ < 1$. Moreover, we have that every left steady state $(0, q_l^+)$ connects with some right steady state $(0, q_r^+)$. Indeed, in [56] Wang *et al.* derived a relation between the left end state q_l^+ and the right end state q_r^+ by proving the following

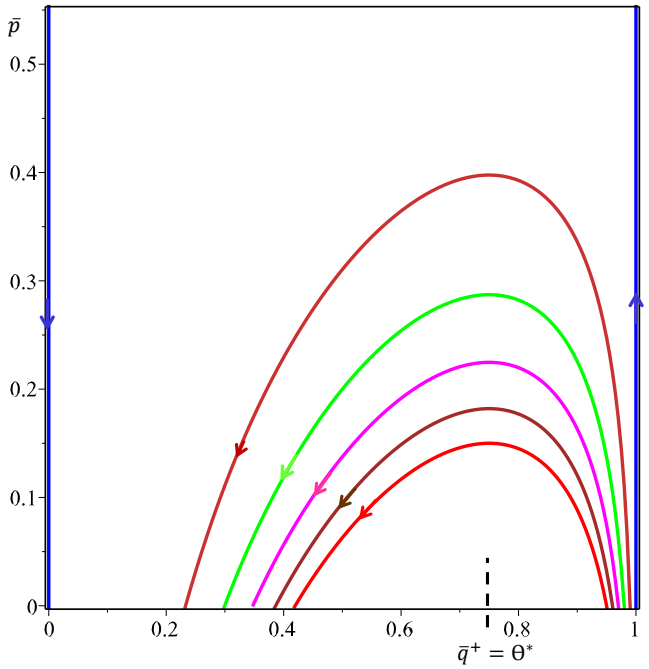

Figure 2.1: Family of heteroclinic orbits corresponding to a fixed wave speed c. Arrows indicate the direction of the trajectories. The wave speed is $c = 0.25\,\mu$m/min and we have taken $s = 0.5\,\mu$m/min, $\mu = 0.05$/min and $\kappa = 0.1$. Parameter values were obtained from [41].

Lemma 2.3. [56] *Given a speed c satisfying $0 \leq c < s$, the left and right equilibria $(0, q_l^+)$ and $(0, q_r^+)$ are related as*

$$\left(\frac{1-q_r^+}{1-q_l^+}\right)^{s-c} = \left(\frac{q_l^+}{q_r^+}\right)^{s+c}, \qquad 0 \leq c < s. \tag{2.6}$$

Theorem 2.2 tell us that for every c fixed, system (2.5) admits a family of traveling wave pairs $(\bar{p}, \bar{q}^+)$, in which $\bar{p}$ is a pulse for the total cell population and $\bar{q}^+$ is a probabilty density front. Each one of these families corresponds to a family of heteroclinic orbits like the one portrayed in Figure 2.1. The families are different from one another; due to relation (2.6) every couple of orbits that share the same left equilibrium point $(0, q_l^+)$, but are indexed by different wave speeds, do not have the same right equilibrium point. In terms of the wave fronts this means that two wave fronts starting at the same left end q_l^+, propagating with different speeds, will converge to different right ends. This issue will be discussed in greater depth in the following section.

Another remarkable feature of the solutions is that all members of the families of traveling waves are invariant under the translation $x \quad x + a$, with $a \quad \mathbb{R}$, which is grounded in the fact that system (2.5) is autonomous.

2.2

The Nature of the M^5-Traveling Waves

The aforementioned heteroclinic orbits were computed explicitly by Wang *et al.* [56], which are given by the formula

$$\bar{p}(\bar{q}^+) = \frac{\mu s}{2\kappa} \ln \left(\frac{1-\bar{q}^+}{1-q_l^+} \right)^{\frac{1}{c+s}} \left(\frac{\bar{q}^+}{q_l^+} \right)^{\frac{1}{s-c}} . \tag{2.7}$$

From this expression it is manifest that the heteroclinic trajectory is a function of c and the left end state q_l^+. Wang *et al.* found that for fixed values of c and q_l^+, $\bar{p}(\bar{q}^+)$ reaches its maximum value when $\bar{q}^+ = \theta^*$, which is

$$\bar{p}_{\max} = \frac{\mu s}{2\kappa} \ln \left(\frac{1-\theta^*}{1-q_l^+} \right)^{\frac{1}{c+s}} \left(\frac{\theta^*}{q_l^+} \right)^{\frac{1}{s-c}} , \qquad \theta^* = \frac{c+s}{2s}. \tag{2.8}$$

For the traveling wave pair $(\bar{p}, \bar{q}^+)$ this means that the pulse $\bar{p}$ attains its maximum value at the point where the wave front $\bar{q}^+$ takes the value θ^*. In addition, Wang *et al.* stand out that *within* a family of traveling wave pairs propagating with speed c, the amplitude $\bar{p}_{\max}$ of the family of pulses is an increasing function with respect to q_l^+ (see Figure 2.2 (a)). Concerning the fronts within a familiy of traveling waves, we estabish below the relationship between their amplitude $q_l^+ - q_r^+$ and the left end q_l^+. Going a little further, we characterize the dependence of $\bar{p}_{\max}$ and the amplitude of $\bar{q}^+$ on the wave speed c, that is to say, we characterize their behaviour *among* families with distinct wave speeds.

2.2.1

Within a family

As with pulses, the change in the amplitude of wave fronts spreading with the same speed is correlated with the left end q_l^+. In Figure 2.2 (b), for wave fronts with a fixed wave speed, we notice that the amplitude grows as q_l^+ moves up away from θ^* since q_r^+ in turn goes down to zero. More concretely, we have the following result.

Proposition 2.4. *Let c be a given wave speed. Then the right end q_r^+ is a decreasing function of the left end.*

Proof. We use (2.6) to obtain

$$\frac{\partial q_r^+}{\partial q_l^+} = \frac{\left[2sq_l^+ - (s+c)\right] q_r^+ \left(1-q_r^+\right)}{\left[2sq_r^+ - (s+c)\right] q_l^+ \left(1-q_l^+\right)}.$$

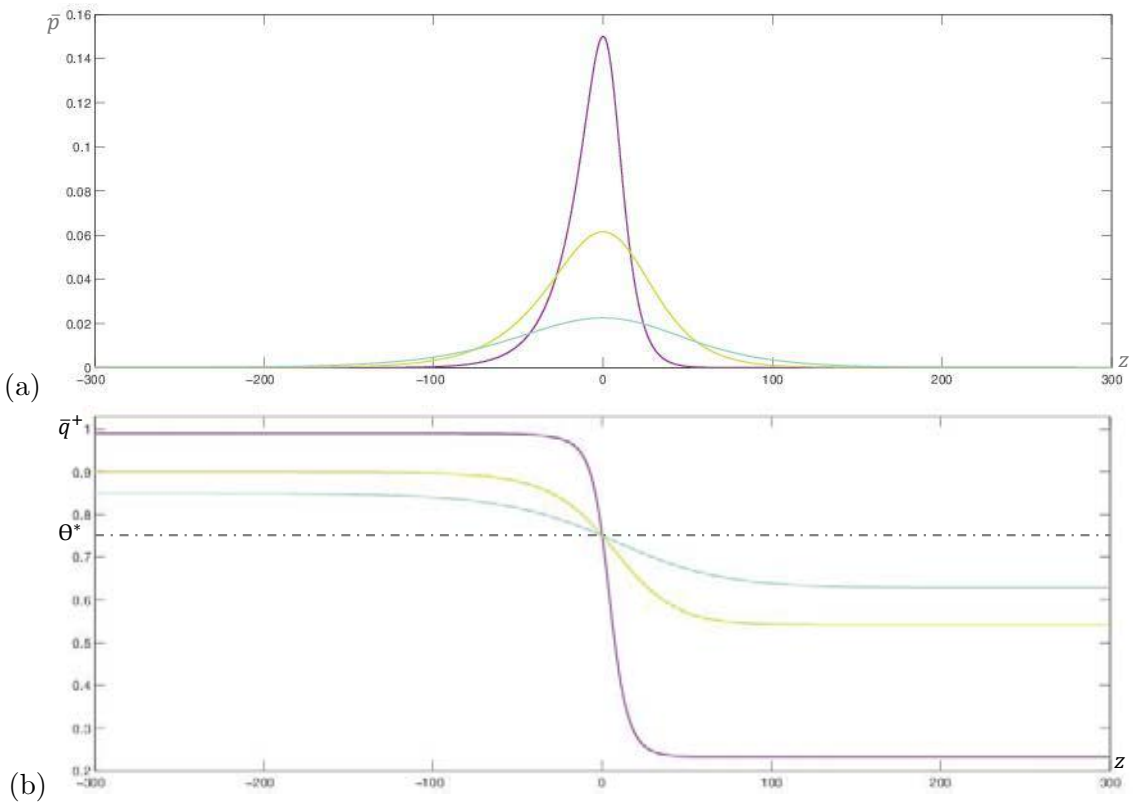

Figure 2.2: Illustration of a family of traveling waves of fixed wave speed in which the members are parametrized by the left end q_l^+. Parameters are $s = 0.5\,\mu$m/min, $c = 0.25\,\mu$m/min, $\mu = 0.05$/min and $\kappa = 0.1$. (a) $\bar{p}_{\max}$ increases as q_l^+ increases; the shortest pulse is produced by $q_l^+ = 0.85$, the middle one by $q_l^+ = 9$ and the tallest one by $q_l^+ = 0.99$. (b) q_r^+ decreases with respect to q_l^+; $q_l^+ = 0.85$ bears the biggest right end, $q_r^+ \approx 0.6279$, $q_l^+ = 0.9$ bears the middle one, $q_r^+ \approx 0.5419$, and $q_l^+ = 0.99$ the smallest one, $q_r^+ \approx 0.2330$.

By Theorem 2.2, $2sq_l^+ - (s+c) > 0$ and $2sq_r^+ - (s+c) < 0$, hence, since $0 < q_r^+, q_l^+ < 1$, we conclude that $\partial q_r^+ / \partial q_l^+ < 0$. □

Proposition 2.4 and the positive relation between $\bar{p}_{\max}$ and q_l^+ gives us good grounds for saying that, according to the M^5-model, cells form big assemblies when they face zones containing in great abundance fibres pointing in a direction opposite to that of motion, and that such assemblies leave in their wake a track of fibres aligned predominantly in the direction of propagation. For our population of cell moving to the right, this translates to q_r^+ almost zero and q_l^+ close to 1.

On the other hand, small cellular aggregates are expected in regions where matrix fibres are more or less aligned with the direction of motion, in this case matrix suffers minor changes after passage of such aggregates. The present situation corresponds to q_r^+ nearby θ^* and both $q_l^+ - q_r^+$ and $\bar{p}_{\max}$ small.

On these facts, there is enough evidence to conclude that the larger is the pulse the wider is the wave front.

2.2.2

Among families

In the current work we have discovered that among cellular aggregates that leave behind almost the same orientation distribution of fibres, those of larger amplitude propagate slower than the ones of lower amplitude (see Proposition 2.5 below). Based on this result, it becomes evident that the M^5-model suggests that dense cellular aggregates spread through the host tissue at speeds below those at which less dense cellular accumulations propagate.

In terms of pulses and wave fronts, cellular aggregates that generate similar trails of realigned matrix are traveling pulses that are associated to wave fronts with the same left end q_l^+. Then we have obtained the following:

Proposition 2.5. *Let q_l^+ be a given left state. Then the maximum value $\bar{p}_{\max}$ is a decreasing function of the wave speed.*

Proof. Taking a derivative in the parameter c in (2.8), we get

$$\frac{\partial \bar{p}_{\max}}{\partial c} = \frac{\mu s}{2\kappa}\left(\frac{1}{(c+s)^2}\left[\ln(1-q_l^+) - \ln(1-\theta^*)\right] + \frac{1}{(s-c)^2}\left[\ln(\theta^*) - \ln(q_l^+)\right]\right).$$

Since $q_l^+ > \theta^*$, we have that $\ln(1-q_l^+) < \ln(1-\theta^*)$ and $\ln(\theta^*) < \ln(q_l^+)$ for all $c \quad [0, s)$, and therefore $\partial \bar{p}_{\max}/\partial c < 0$. □

To illustrate Proposition 2.5, in Figure 2.3 (a) depicts traveling pulse solutions generated by the same boundary condition q_l^+ and different speeds. The smallest value assigned to c in system (2.5) gave rise to the tallest pulse.

As we have seen before, small pulses and flat wave fronts ($q_l^+ - q_r^+$ small) coexist, thus for the present case where q_l^+ is fixed and $\bar{p}_{\max}$ reduces as the pulse $\bar{p}$ goes faster, q_r^+ needs to increase to reduce the size of the difference $q_l^+ - q_r^+$. The following result relates q_r^+ with the wave speed.

Proposition 2.6. *Fix q_l^+. Then the right end q_r^+ is an increasing function of the wave speed.*

Proof. We differentiate implicitly relation (2.6) with respect to c to get the partial derivative of q_r^+ with respect to c. Thus

$$\frac{\partial q_r^+}{\partial c} = -\frac{q_r^+(1-q_r^+)\ln\left[(1-q_r^+)\,q_l^+ / \left(1-q_l^+\right)q_r^+\right]}{2sq_r^+ - (s+c)};$$

Given that $0 < q_r^+ < q_l^+ < 1$, it is not hard to check that $(1-q_r^+)\,q_l^+ / \left(1-q_l^+\right)q_r^+ > 1$; therefore $\partial q_r^+/\partial c > 0$ because $\theta^* > q_r^+$. □

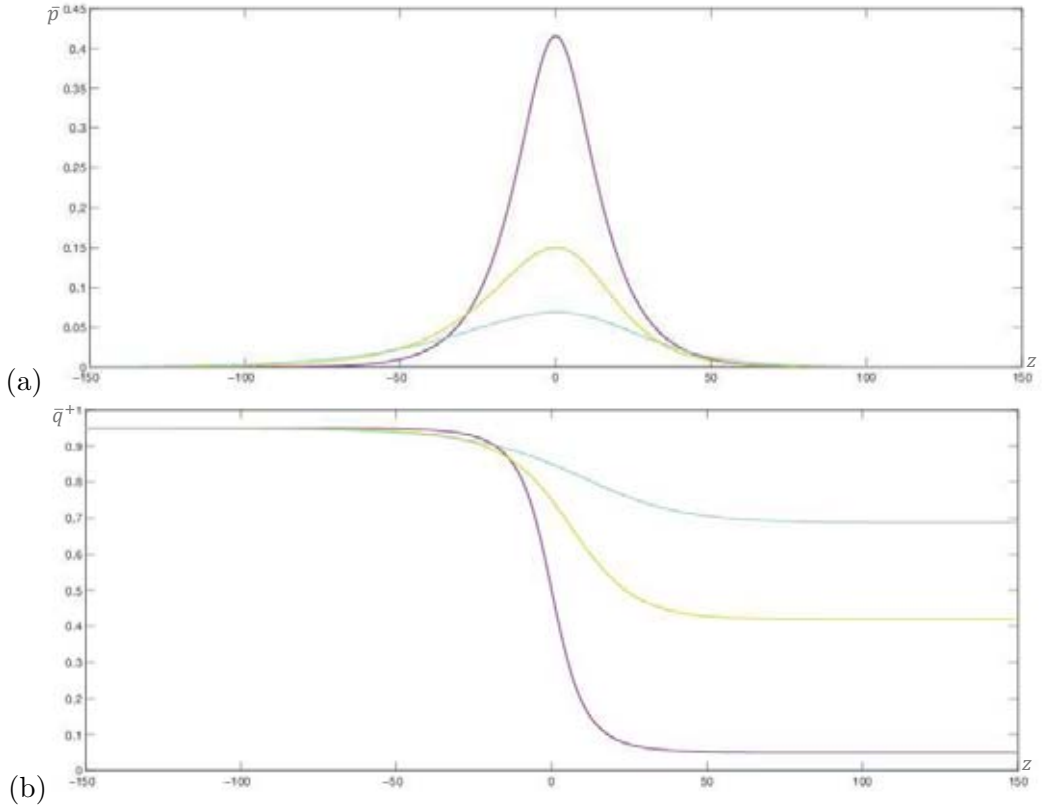

Figure 2.3: Members of three families of traveling waves moving with different speeds; one member per family, all of them are indexed by the same left end q_l^+. Parameters are set as $s = 0.5\,\mu$m/min, $\mu = 0.05$/min, $\kappa = 0.1$ and $q_l^+ = 0.95$. (a) $\bar{p}_{\max}$ decreases as c increases; the tallest pulse corresponds to $c = 0\,\mu$m/min, the middle one to $c = 0.25\,\mu$m/min and the shortest one to $c = 0.35\,\mu$m/min. (b) q_r^+ increases with respect to c; $c = 0$ carries to the smallest right end, $q_r^+ \approx 0.05$, $c = 0.25$ carries to the middle one, $q_r^+ \approx 0.4195$, and $c = 0.35$ to the biggest one, $q_r^+ \approx 0.6875$.

Plots in Figure 2.3 (b) correspond to wave fronts having the same left end q_l^+ and different speeds; we observe that the faster is the front, narrower is the amplitude. We also observe in Figure 2.3 that flat wave fronts are associated to short pulses.

2.3

Exponential Convergence

In this section we analyze the asymptotic behaviour of the traveling waves as $z \quad \pm \quad$. We deduce that for each c in the interval $0 \leq c < s$ the pulses and fronts tend exponentially toward their limits.

Lemma 2.7. *Traveling wave solutions $\bar{p}$ and $\bar{q}^+$ satisfy*

$$\begin{aligned}
\left|d^i/dz^i\left(\bar{q}^+(z)-q_r^+\right)\right| &\leq C\exp\left(-\frac{(c+s-2sq_r^+)\mu}{s^2-c^2}z\right), \quad as \quad z \quad + \quad , \\
\left|d^i/dz^i\left(\bar{q}^+(z)-q_l^+\right)\right| &\leq C\exp\left(-\frac{(c+s-2sq_l^+)\mu}{s^2-c^2}z\right), \quad as \quad z \quad - \quad , \\
\left|d^i/dz^i\left(\bar{p}(z)\right)\right| &\leq C\exp\left(-\frac{(c+s-2sq_r^+)\mu}{s^2-c^2}z\right), \quad as \quad z \quad + \quad , \\
\left|d^i/dz^i\left(\bar{p}(z)\right)\right| &\leq C\exp\left(-\frac{(c+s-2sq_l^+)\mu}{s^2-c^2}z\right), \quad as \quad z \quad - \quad ,
\end{aligned} \tag{2.9}$$

for $i=0,1$, and some uniform $C>0$.

Proof. We begin by obtaining an uncoupled differential equation for $\bar{q}^+$. Upon substituting formula (2.7) into the equation for $\bar{q}^+$ in (2.5) we arrive at

$$\bar{q}_z^+ = -\mu \ln \left(\frac{1-\bar{q}^+}{1-q_l^+}\right)^{\frac{1}{c+s}} \left(\frac{\bar{q}^+}{q_l^+}\right)^{\frac{1}{s-c}} \left(1-\bar{q}^+\right)\bar{q}^+. \tag{2.10}$$

Computing the Taylor series of the right-hand side of this equation we find that, as z $+$.

$$\bar{q}_z^+ = -\frac{(c+s-2sq_r^+)\mu}{s^2-c^2}(\bar{q}^+-q_r^+) + \mathcal{O}\left((\bar{q}^+-q_r^+)^2\right), \tag{2.11}$$

and, that

$$\bar{q}_z^+ = -\frac{(c+s-2sq_l^+)\mu}{s^2-c^2}(\bar{q}^+-q_l^+) + \mathcal{O}\left((\bar{q}^+-q_l^+)^2\right), \tag{2.12}$$

as z $-$. Hence, from (2.11) we obtain

$$\left|\bar{q}^+(z)-q_r^+\right| \sim C_1\exp\left(-\frac{(c+s-2sq_r^+)\mu}{s^2-c^2}z\right), \tag{2.13}$$

as z $+$, for some constant $C_1>0$. In addition, upon substituting (2.13) into (2.11), we get that

$$\left|d/dz\left(\bar{q}^+(z)-q_r^+\right)\right| \sim \frac{(c+s-2sq_r^+)\mu}{s^2-c^2}C_1\exp\left(-\frac{(c+s-2sq_r^+)\mu}{s^2-c^2}z\right),$$

as z $+$.

Likewise, from (2.12) we have that

$$\left|\bar{q}^+(z)-q_l^+\right| \sim C_2\exp\left(-\frac{(c+s-2sq_l^+)\mu}{s^2-c^2}z\right), \tag{2.14}$$

as z $-$, for some constant $C_2>0$. In view of this, we use (2.12) and (2.14) to get

$$\left|d/dz\left(\bar{q}^+(z)-q_l^+\right)\right| \sim -\frac{(c+s-2sq_l^+)\mu}{s^2-c^2}C_2\exp\left(-\frac{(c+s-2sq_l^+)\mu}{s^2-c^2}z\right),$$

as $z \quad - \quad$.

Proceeding analogously as before, it results from equation (2.7) that

$$\bar{p}(\bar{q}^+) = \frac{\mu s(c+s-2sq_r^+)}{2\kappa q_r^+(1-q_r^+)(s^2-c^2)}(\bar{q}^+ - q_r^+) + \mathcal{O}\left((\bar{q}^+ - q_r^+)^2\right), \tag{2.15}$$

as $z \quad + \quad$, and also that

$$\bar{p}(\bar{q}^+) = \frac{\mu s(c+s-2sq_l^+)}{2\kappa q_l^+(1-q_l^+)(s^2-c^2)}(\bar{q}^+ - q_l^+) + \mathcal{O}\left((\bar{q}^+ - q_l^+)^2\right), \tag{2.16}$$

as $z \quad - \quad$.

We substitute (2.13) into the absolute value of (2.15) to obtain

$$\bar{p}(z) \ \sim \frac{\mu s(c+s-2sq_r^+)}{2\kappa q_r^+(1-q_r^+)(s^2-c^2)} C_1 \exp\left(-\frac{(c+s-2sq_r^+)\mu}{s^2-c^2} z\right), \tag{2.17}$$

as $z \quad + \quad$. Similarly, from (2.14) and (2.16) we can deduce that, as $z \quad - \quad$,

$$\bar{p}(z) \ \sim -\frac{\mu s(c+s-2sq_l^+)}{2\kappa q_l^+(1-q_l^+)(s^2-c^2)} C_2 \exp\left(-\frac{(c+s-2sq_l^+)\mu}{s^2-c^2} z\right). \tag{2.18}$$

Write now the equation for $\bar{p}$ in (2.5) as

$$\bar{p}_z = \frac{\mu}{c^2-s^2}\bar{p}[c+s-2sq_r^+ - 2s(q^+ - q_r^+)]. \tag{2.19}$$

Upon substituting (2.13) and (2.17) into (2.19) we find that $\bar{p}_z$ satisfies

$$d\bar{p}/dz \ \sim \frac{\mu^2 s(c+s-2sq_r^+)^2}{2\kappa q_r^+(1-q_r^+)(s^2-c^2)^2} C_1 \exp\left(-\frac{(c+s-2sq_r^+)\mu}{s^2-c^2} z\right),$$

as $z \quad + \quad$.

In a similar manner, (2.14) and (2.18) lead to

$$d\bar{p}/dz \ \sim \frac{\mu^2 s(c+s-2sq_l^+)^2}{2\kappa q_l^+(1-q_l^+)(s^2-c^2)^2} C_2 \exp\left(-\frac{(c+s-2sq_l^+)\mu}{s^2-c^2} z\right),$$

as $z \quad - \quad$.

Finally, we let C be the upper bound of all constant terms that multiply the exponential functions. □

CHAPTER
THREE

APPROXIMATE TRAVELING WAVE SOLUTIONS AND EXACT STANDING WAVE SOLUTIONS

3.1

The Approximation

With the aim of approximating the traveling wave front solution of the one-dimensional Fisher-Kolmogoroff equation, Petrovskii *et al.* use in [47] a piecewise linear function to approximate the nonlinear term that describes the logistic population growth. As a result, upon substituting the traveling wave ansatz, they obtain two exactly solvable linear ODEs instead of one nonlinear ODE. For a population density in the interval $[0, 1]$, one of the equations is for the dynamics of the population with density in the interval $\left[\frac{1}{2}, 1\right]$ over the left-half of the traveling axis; the other one is defined in the complement of the traveling axis for the dynamics of the population with density between 0 and $\frac{1}{2}$. Under appropriate boundary conditions Petrovskii *et al.* match the solutions of the two ODEs, obtaining in this way an approximate continuous decreasing wave front that connects 1 to 0.

With a different approach, for a one-dimensional Fisher equation with degenerate diffusion, Sánchez-Garduño and Maini obtained in [51] an approximation to its sharp front solution. The sharp corresponds to a saddle-saddle heteroclinic trajectory connecting the stationary points $(1, 0)$ and $(0, 0)$ of the system of first-order ODEs that arise from putting the degenerate Fisher equation into a traveling coordinate system. The authors use a perturbation method to obtain an analytic approximation of the heteroclinic trajectory, through which they decouple the equation for the sharp in the system of ODEs. Then the approximate sharp front arises from solving that equation.

Inspired by the ideas developed in [47] and [51], in this chapter we obtain exactly solvable approximate equations for system (2.5), intended to obtain analytic approximations to the pulse and wave front solutions.

Our analysis departs from the uncoupled differential equation for $\bar{q}^+$ gotten in the proof of Lemma 2.7 (see Eq. (2.10)). In this chapter, for ease of notation, we drop the superscripts on $\bar{p}$ and $\bar{q}^+$, then equation (2.10) reads

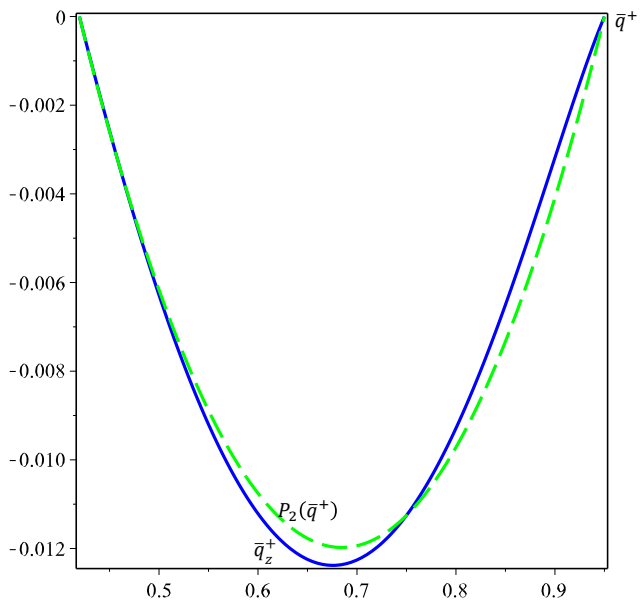

Figure 3.1: q_z^+ (*solid line*) is approximated by quadratic polynomial $P_2(q^+)$ (*dashed line*). Parameters values are set at $s = 0.5\,\mu$m/min, $c = 0.25\,\mu$m/min, $\mu = 0.05$/min and $q_l^+ = 0.95$.

$$q_z^+ = -\mu \ln \left(\frac{1-q^+}{1-q_l^+}\right)^{\frac{1}{c+s}} \left(\frac{q^+}{q_l^+}\right)^{\frac{1}{s-c}} \left(1-q^+\right) q^+. \tag{3.1}$$

As required, q_l^+ and q_r^+ are steady states of equation (3.1). Clearly, function on the right-hand side in (3.1) is 0 at q_l^+. On the other hand, due to relation (2.6), the argument of the logarithmic term is equal to 1 at q_r^+, implying that q_z^+ is zero as promised. In Figure 3.1 we show the graphic of q_z^+, as a function of q^+, for specific values of the parameters. In view that the plot resembles a parabola we approximate the right-hand side in (3.1) by a quadratic function (see Figure 3.1), for this purpose we use the Lagrange polynomial method.

In order to construct the interpolating polynomial we choose three values of q^+: q_r^+, θ^* and q_l^+. We have taken q_r^+ and q_l^+ to ensure that they remain as steady states, and we take $q^+ = \theta^*$ for the sole reason that we know that it lies between q_r^+ and q_l^+.

Since (3.1) vanishes at q_r^+ and q_l^+, it is not hard to see that the Lagrange polynomial that interpolates q_z^+ (as a function of q^+) is

$$P_2(q^+) = \beta_0 (q^+ - q_r^+)(q^+ - q_l^+),$$

where

$$\beta_0 = -\mu \ln \left(\frac{1-\theta^*}{1-q_l^+}\right)^{\frac{1}{c+s}} \left(\frac{\theta^*}{q_l^+}\right)^{\frac{1}{s-c}} \frac{(1-\theta^*)\theta^*}{(\theta^* - q_r^+)(\theta^* - q_l^+)}.$$

In this manner, the approximate equation for q^+ takes the form

$$\frac{d}{dz} q_{\text{app}}^+ = -\beta_0 (q_{\text{app}}^+ - q_r^+)(q_l^+ - q_{\text{app}}^+). \tag{3.2}$$

We consider the initial condition $q^+_{\rm app}(0) = \theta^*$, the initial point is arbitrary because of the translational invariance of (3.2).

The problem can be solved by separation of variables, thus

$$\frac{dq^+_{\rm app}}{(q^+_{\rm app} - q^+_r)(q^+_l - q^+_{\rm app})} = -\beta_0 \left(z - z_0\right), \tag{3.3}$$

where z_0 is the integration constant.

Computing the integral in the left-hand side of (3.3), yields

$$\frac{1}{q^+_l - q^+_r} \ln \quad \frac{q^+_{\rm app} - q^+_r}{q^+_l - q^+_{\rm app}} \quad = -\beta_0 \left(z - z_0\right).$$

The approximate wave front takes the following form:

$$q^+_{\rm app}(z) = \frac{\gamma q^+_r e^{\beta z} + q^+_l}{\gamma e^{\beta z} + 1}, \tag{3.4}$$

where

$$\beta = (q^+_l - q^+_r)\beta_0 \quad \text{and} \quad \gamma = \frac{q^+_l - \theta^*}{\theta^* - q^+_r}.$$

We now substitute (3.4) into the equation for p in (2.5) in order to obtain the equation for the approximate pulse. Therefore we have to solve

$$\frac{d}{dz} p_{\rm app} = \frac{\mu}{c^2 - s^2} p_{\rm app} \quad c + s - 2s \quad \frac{\gamma q^+_r e^{\beta z} + q^+_l}{\gamma e^{\beta z} + 1} \qquad . \tag{3.5}$$

According to the analysis performed in Chapter 2, the pulse p takes the value $p_{\max}$ in the same point where q^+ passes through θ^*, thus the initial condition for (3.5) is $p_{\rm app}(0) = p_{\max}$.

Separating variables and then integrating from 0 up to z gives

$$\begin{aligned} \ln p_{\rm app}(z) - \ln p_{\max} &= \frac{\mu}{c^2 - s^2} \quad (c+s)z - 2s \quad \int_0^z \frac{\gamma q^+_r e^{\beta\tau} + q^+_l}{\gamma e^{\beta\tau} + 1}\, d\tau \\ &= \frac{\mu}{c^2 - s^2} \quad (c+s)z + \ln \left(\frac{\gamma + 1}{\gamma e^{\beta z} + 1} \right)^{\frac{2s}{\beta} q^+_r} - 2s q^+_l \quad \int_0^z \frac{d\tau}{\gamma e^{\beta\tau} + 1} \quad . \end{aligned} \tag{3.6}$$

We calculate the remaining integral by setting

$$\tau = \frac{1}{\beta} \ln y, \quad d\tau = \frac{dy}{\beta y}.$$

Making this, we have

$$\int_0^z \frac{d\tau}{\gamma e^{\beta\tau} + 1} = \frac{1}{\beta} \quad \int_1^{e^{\beta z}} \frac{dy}{y(\gamma y + 1)} = z + \ln \left(\frac{\gamma + 1}{\gamma e^{\beta z} + 1} \right)^{\frac{1}{\beta}}. \tag{3.7}$$

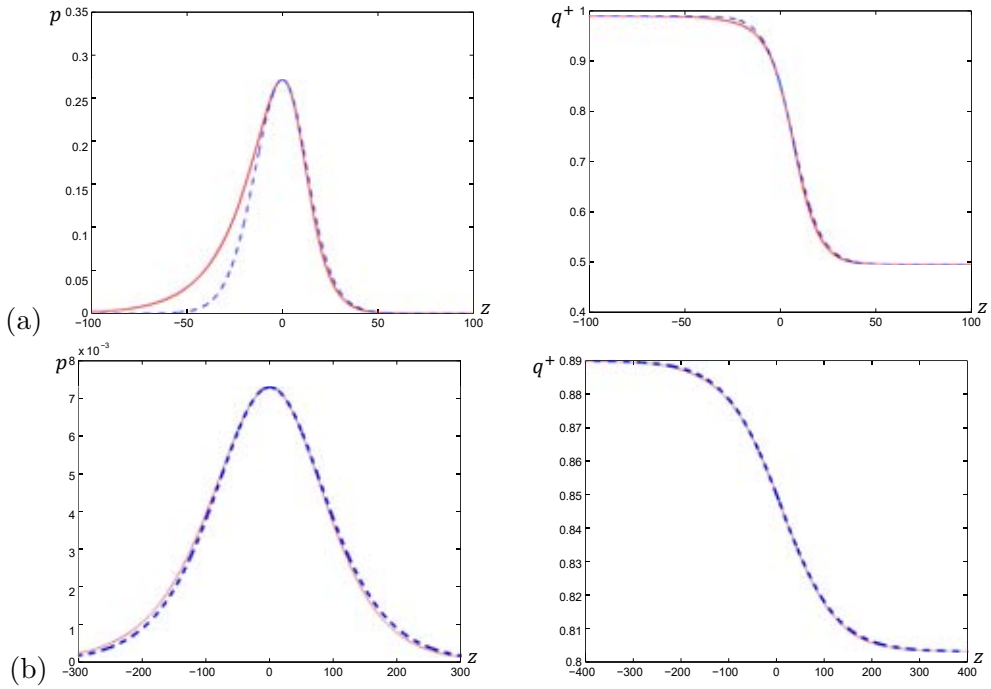

Figure 3.2: Comparison of the approximate solutions (*dashed lines*) with the numerically computed traveling wave solutions (*solid lines*) obtained for the parameters $s = 0.5\,\mu$m/min, $c = 0.35\,\mu$m/min, $\mu = 0.05$/min, $\kappa = 0.1$, (a) $q_l^+ = 0.99$ and (b) $q_l^+ = 0.89$.

Substituting (3.7) into (3.6), we get

$$\ln p_{\rm app}(z) - \ln p_{\max} = \frac{\mu}{c^2 - s^2} \quad (c + s - 2sq_l^+)z + \ln\left(\frac{\gamma+1}{\gamma e^{\beta z}+1}\right)^{\frac{2s}{\beta}q_r^+} + \ln\left(\frac{\gamma+1}{\gamma e^{\beta z}+1}\right)^{-\frac{2s}{\beta}q_l^+}$$

$$= \frac{\mu}{c^2 - s^2} \quad (c + s - 2sq_l^+)z + \ln\left(\frac{\gamma+1}{\gamma e^{\beta z}+1}\right)^{\frac{2s}{\beta}(q_r^+ - q_l^+)} .$$

Therefore $p_{\rm app}$ is given by

$$p_{\rm app}(z) = p_{\max}\left(\frac{\gamma+1}{\gamma e^{\beta z}+1}\right)^{\frac{2\mu s}{\beta(s^2-c^2)}(q_l^+ - q_r^+)} \exp\left(-\frac{(c + s - 2sq_l^+)\mu}{s^2 - c^2}z\right). \tag{3.8}$$

In Figures 3.2 and 3.3 we compare the approximate solutions (3.8) and (3.4) with the numerical solutions of (2.5). Upon using Maple, parameter q_r^+ was computed from equation (2.6) for each given value of q_l^+. It is observed that the agreement between the analytic approximate solutions and the numerically computed solutions is not quite good enough for the pulses featuring large amplitudes. The difference between the analytic and approximate wave fronts of large amplitud seems not to be significant, since (3.4) preserves the form and the steepness of the fronts. With regard to pulses of small amplitude, (3.8) fits very well with the numerical solution. Since the length of the pulses and the amplitude of the fronts change with respect to q_l^+, from these observations it may be concluded that the smaller is q_l^+ the better are the approximations.

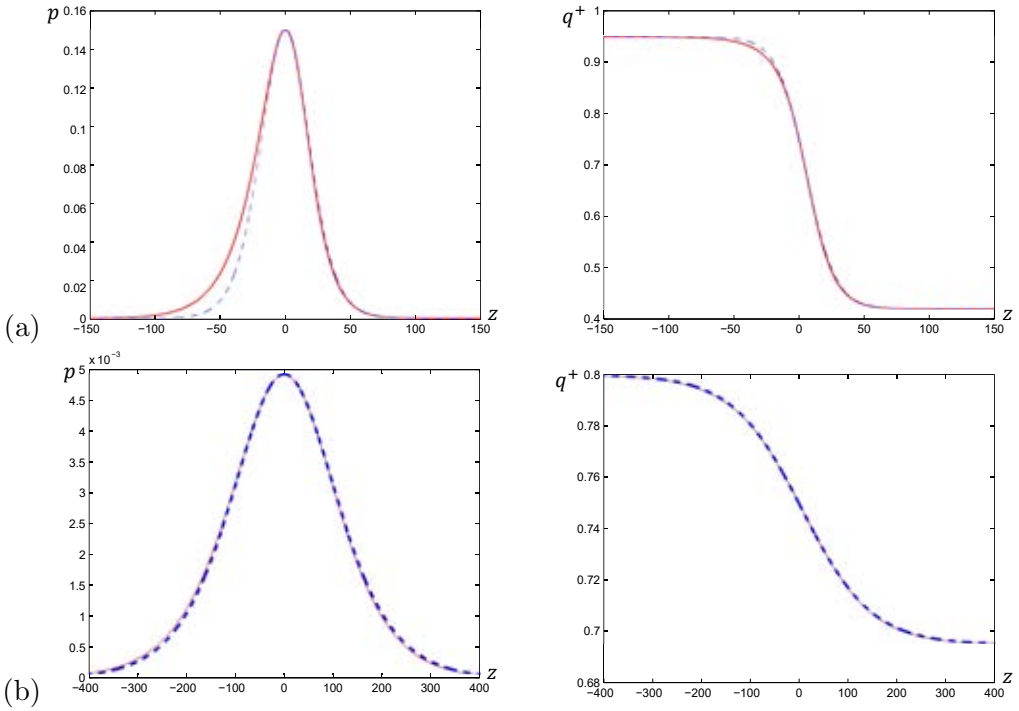

Figure 3.3: Comparison of the approximate solutions (*dashed lines*) with the numerically computed traveling wave solutions (*solid lines*) obtained for the parameters $s = 0.5\,\mu$m/min, $c = 0.25\,\mu$m/min, $\mu = 0.05$/min, $\kappa = 0.1$, (a) $q_l^+ = 0.95$ and (b) $q_l^+ = 0.80$.

3.2

The Approximate-but-Exact Stationary Wave Profiles

In the standing case $c = 0$, in which case $z = x$, the approximate solutions (3.8) and (3.4) of system (2.5) are indeed *exact stationary* wave solutions of system (1.4). The reason is that in the stationary version of system (1.4) one of the equations is $j_x = 0$, which by the boundary conditions (2.2) implies that j is indentically zero. Then, as a consequence, any function q^+ solves the third stationary equation in (1.4). Thus the stationary problem reduces to solving the scalar equation

$$p_x = \frac{\mu}{s}\left(2q^+ - 1\right)p, \tag{3.9}$$

with $p(\pm\quad) = 0$, for any given function q^+ satisfying (2.2). But this problem has already been solved, since $q^+_{\rm app}$ satisfies (2.2) and $p_{\rm app}$ solves (3.9) under the prescribed boundary conditions.

In the present case, where $c = 0$, for a wave front of amplitude $\varepsilon = q_l^+ - q_r^+$, $0 < \varepsilon < 1$, one can find that

$$q_l^+ = \frac{1}{2}(1+\varepsilon) \quad \text{and} \quad q_r^+ = \frac{1}{2}(1-\varepsilon). \tag{3.10}$$

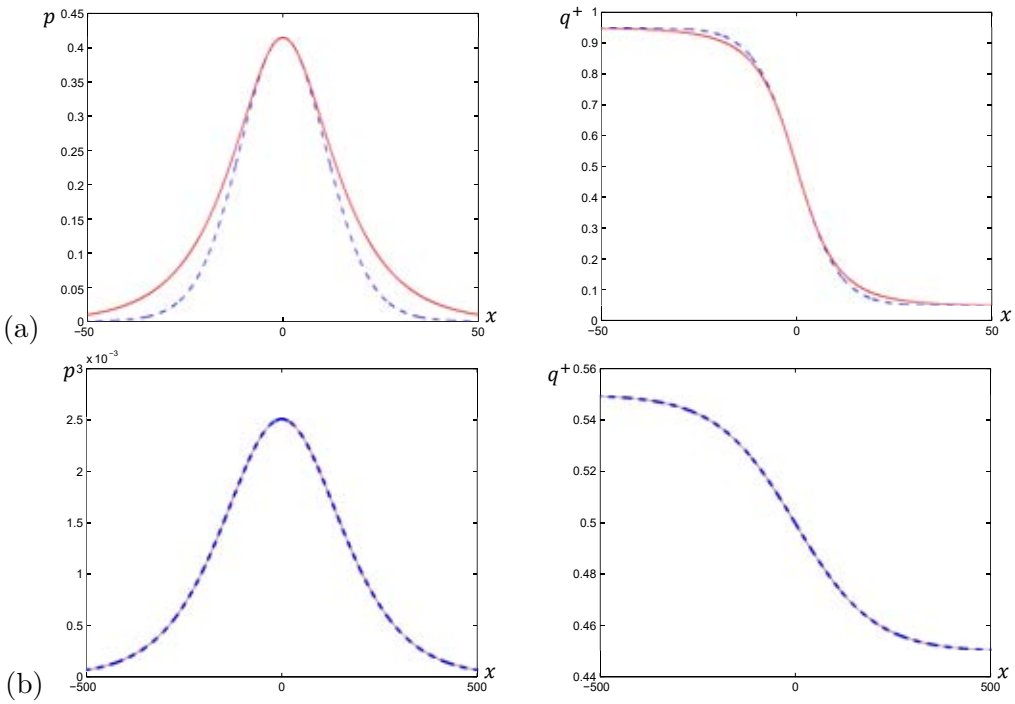

Figure 3.4: Comparison of the approximate solutions (*dashed lines*) with the numerically computed traveling wave solutions (*solid lines*) obtained for the parameters $s = 0.5\,\mu$m/min, $c = 0\,\mu$m/min, $\mu = 0.05$/min, $\kappa = 0.1$, (a) $q_l^+ = 0.95$ and (b) $q_l^+ = 0.55$.

Thanks to this result, (3.8) and (3.4) can be written as

$$p_0(x) = \frac{\beta s \varepsilon}{2\kappa}\left(\operatorname{sech}\left(\frac{\beta x}{2}\right)\right)^{\frac{2\mu\varepsilon}{\beta s}} \quad \text{and} \quad q_0^+(x) = \frac{1}{2} - \frac{\varepsilon}{2}\tanh\left(\frac{\beta x}{2}\right),$$

respectively; with

$$\beta = \frac{\mu}{s\varepsilon}\ln\left(\frac{1}{1-\varepsilon^2}\right).$$

The form that take the standing solutions (3.2) may look more familiar; $p_0(x)$ resembles the solitary wave solution of the generalized KdV equation and $q_0(x)$ is similar to wave profiles in equations of gas dynamics, see for example [46] and [60].

In Figure 3.4 we again observe that better approximations are produced when we reduce the amplitudes of the wave profiles.

In summary, p_0 and q_0^+ together with $j \equiv 0$ are stationary solutions of (1.4), but this couple of functions do not solve system (2.5).

CHAPTER
FOUR

SPECTRAL STABILITY IN THE FAMILY OF M^5-STANDING WAVES

4.1

Motivating the Analysis of Stability

ECM fibres alignment has a crucial role in normal tissue development and homeostasis; since their particular orientation endows tissues their functional properties. For example, tissues in muskoloskeletal system have a highly organized structure: skeletal muscle is composed of aligned bundles of multinucleated spindle shaped myotubes formed by the fusion of myoblasts [45]. This alignment provides mechanical properties to such tissues; in tendons and ligaments, collagen fibers align in parallel bundles along the direction of greatest tension [3]. Similarly, the myocardium is a highly organized tissue comprised of cardiomyocytes and fibroblasts, which facilitate the coordinated electrical and mechanical signal propagation among the cardiac muscle [38]. On the other hand, neurite outgrowth extends directionally parallel to uniaxially aligned ECM pathways [36].

Whether due to traumatic injury, muscular dystrophy or aging, damaged tissue often can neither be repaired nor recover in a satisfactory way, as a consequence, native tissue properties are not completely regenerated and tissue mechanical quality is inferior. Focused on the development of engineered tissues capable of repairing, maintaining, or improving the function of native tissues that are defective due to pathological conditions, the growing tissue engineering applies principles and methods of engineering, material science, and cell and molecular biology. A persistent challenge in tissue regeneration is to devise adequate structural templates capable of guiding the assembly of cells and ECM into such arrangements that the physical and mechanical properties of the undamaged tissue are maintained [54]. For example, Huang *et al.* [27] report that fabricated micron scale micropatterned PDMS, with parallel microgrooves, can promote myoblast cellular alignment along the direction of the microgrooves. In contrast, non-patterned PDMS films, with arbitrary axes of alignment, were unable to promote cell alignment, as myocytes remained randomly oriented after 7 days in culture. According to Huang *et al.*, creating aligned skeletal muscle

has potential for the treatment of muscular injury or muscular dysfunction. Singh *et al.* [54] utilized a striped pattern to direct fibroblasts. The authors used NIH 3T3 fibroblasts plated on a micron scale stripe-patterned ECM/PET substrate. Singh *et al.* have observed that fibroblasts spread in alignment with the pattern. After 10 days of seeded, fibroblasts assembled fibronectin ECM fibrils parallelly aligned to the underlying patterned stripes. The authors showed that oriented neurite outgrowt is supported by such cell-assembled aligned ECM. Their system provides a template for studying the effects of alignment in nervous system repair devices. These two studies suggest that, once ECM alignment is achieved, cells will orient in line with the underlying pattern. And conversely, that it will result in an aligned ECM arrangement from aligned patterned cell cultures.

All this highlights the importance of spatial alignment in functional tissues and their potential clinical uses. Therefore, maintaining the structural integrity of the ECM is an important aspect as the orientation of the fibers influences the cell mass needed for tissue structure and function, or allows guiding invasive brain tumor cells for a complete removal (see Chapter 2).

During the previous chapters we have seen that the M^5-model suggests that cellular aggregates have no characteristic sizes and that these might depend on their wave speed. Such difference in the sizes leads to different topographic patterns. We would like to identify, according to the model, which of the paths of reoriented fibres, formed by spreading pulse-shaped aggregates, can persists over a long time. This question is associated with the concept of orbital asymptotic stability, which refers to whether a solution to (1.4) starting close to a certain standing- or traveling-wave profile will tend to some translate thereof as time increases.

Recently, in a study on stability of traveling waves in nonstrictly hyperbolic systems, Rottmann-Matthes [49] proved linear stability—the decay of the solutions of a linearized PDE-system around the wave profiles—from the spectral stability of traveling wave solutions in systems of the form

$$v_t = Bv_x + f(v). \tag{4.1}$$

Later, based on linear estimates from [49], Rottmann-Matthes showed in [50] nonlinear asymptotic stability with asymptotic phase of a traveling wave. Their results apply to systems where $f \quad C^3(\mathbb{R}^m;\mathbb{R}^m)$ and $B \quad \mathbb{R}^{m\times m}$ is a diagonal matrix with diagonal entries $b_{11} \geq \cdots \geq b_{mm}$.

In a moving frame, the linearization of (4.1) aroud a traveling wave $\underline{v}$ with wave speed $\underline{\lambda}$ writes

$$v_t = (\underline{\lambda}I + B)v_x + f_v(\underline{v})v =: (\underline{\lambda}I + B)v_x + C(x)v =: Pv. \tag{4.2}$$

Rottmann-Matthes considers the following assumptions on the linear operator P:

1. $\underline{\lambda}I + B \quad \mathbb{R}^{m\times m}$ is an invertible diagonal matrix with r positive and $m - r$ negative eigenvalues.

2. C is a matrix valued function in $C_b^1(\mathbb{R},\mathbb{R}^{m\times m})$ having the limits

$$\lim_{x \ \pm} C(x) = C_\pm \quad \text{and} \quad \lim_{x \ \pm} C_x(x) = 0.$$

3. There is $\delta > 0$ so that $s \quad s \quad \mathbb{C}$ $\det(sI - i\omega(\lambda I + B) - C_{\pm})$ for some $\omega \quad \mathbb{R}$ implies $\Re e\, s \leq -\delta$.

4. Zero is an algebraically simple eigenvalue of P and $\sigma_{\rm pt}(P) \setminus \ \Re e\, s > -\delta \ = \ 0$, with $\sigma_{\rm pt}(P)$ denoting the point spectrum of P.

The results of Rottmann-Matthes were a source of motivation to study the spectral stability of the standing and traveling wave solutions of the one-dimesional M^5-model. In this chapter, we show that the members of the family of standing waves are spectrally stable. We have found from our investigation that the results of Rottmann-Matthes [50] do not cover the standing case since several of the assumptions can not be satisfied. Up to now we have not found a way to overcome such a difficulty and the question about the asymptotic stability of the standing pulses and wave fronts remains open. The results presented in this chapter may be seen as the first step in the search of nonlinear stability of such standing wave profiles and as our contribution to the theory of spectral stability. All of the results in the chapter have recently been published in [7].

Notation. *Throughout this and the next chapter, L^2 denotes the space of all square integrable functions on $\mathbb{R}$ with norm $\|f\|_{L^2} = (\int_{\mathbb{R}} f(x)^2\,dx)^{1/2}$. We denote by H^n ($n \geq 1$) the usual Sobolev space on $\mathbb{R}$ with norm $\|f\|_{H^n} = (\sum_{i=0}^{n} \|\partial_x^i f\|_{L^2}^2)^{1/2}$.*

4.2

The Spectral Problem

This section is concerned with the formulation of the spectral stability problem for the members of the family of standing wave solutions of system (1.4), whose existence and structure has been established by the results of Theorem 2.2, Lemma 2.3 and the results derived therefrom (see Section 2.2). All members of this family consist of a function identically zero, $\bar{j} \equiv 0$, which emerges from taking $c = 0$ in formula (2.3), and a wave profile $(\bar{p}, \bar{q}^+)$ that satisfies system (2.5). For $c = 0$, the latter reads

$$\begin{aligned} \bar{p}_x &= \frac{\mu}{s}\bar{p}(2\bar{q}^+ - 1), \\ \bar{q}^+_x &= -\frac{2\kappa}{s}\bar{p}\left(1 - \bar{q}^+\right)\bar{q}^+, \end{aligned} \tag{4.3}$$

and is subject to the boundary conditions $\bar{p}(\pm \quad) = 0$, $\bar{q}^+(- \quad) = q_l^+$ and $\bar{q}^+(+ \quad) = q_r^+$, where q_l^+ and q_r^+ are given by (3.10).

To study the spectral stability, for each member $(\bar{p}(x), \bar{j}(x), \bar{q}^+(x))$ of the family of standing waves we consider a solution to system (1.4) of the form

$$(p(x,t), j(x,t), q^+(x,t)) = (\bar{p}(x), 0, \bar{q}^+(x)) + (\tilde{p}(x,t), \tilde{j}(x,t), \tilde{q}^+(x,t)), \tag{4.4}$$

where $\tilde{p}(x,t)$, $\tilde{j}(x,t)$ and $\tilde{q}^+(x,t)$ are perturbations. Perturbations initially small at time $t = 0$ may not remain so, indeed their moduli may grow in time without bound. For example, in [11], certain solutions to a class of KleinGordon-type equations with initial data arbitrarily close to traveling wave solutions blow up in finite time.

We substitute (4.4) into (1.4), getting a nonlinear system for $\tilde{p}$, $\tilde{j}$ and $\tilde{q}^+$:

$$\begin{aligned}
\tilde{p}_t &= -\tilde{j}_z, \\
\tilde{j}_t &= -s^2\tilde{p}_z - \mu\tilde{j} + \mu s\left[\left(2\bar{q}^+ - 1\right)\tilde{p} + 2\bar{p}\tilde{q}^+ + 2\tilde{p}\tilde{q}^+\right], \\
\tilde{q}^+_t &= \frac{2\kappa}{s}\left[\bar{q}^+\left(1-\bar{q}^+\right)\tilde{j} + (1-2\bar{q}^+)\tilde{j}\tilde{q}^+ - \tilde{j}(\tilde{q}^+)^2\right].
\end{aligned}$$

Then, we neglect the nonlinear terms in the perturbations in order to obtain a linearized system around the wave profiles:

$$\begin{aligned}
\tilde{p}_t &= -\tilde{j}_x, \\
\tilde{j}_t &= -s^2\tilde{p}_x - \mu\tilde{j} + \mu s\left[\left(2\bar{q}^+ - 1\right)\tilde{p} + 2\bar{p}\tilde{q}^+\right], \\
\tilde{q}^+_t &= \frac{2\kappa}{s}\bar{q}^+\left(1-\bar{q}^+\right)\tilde{j}.
\end{aligned}$$

Upon seeking for perturbations of the form $e^{\lambda t}p(x)$, $e^{\lambda t}j(x)$ and $e^{\lambda t}q^+(x)$, with $\lambda \in \mathbb{C}$, one obtains the spectral problem

$$\begin{aligned}
\lambda p &= -j_x, \\
\lambda j &= -s^2 p_x - \mu j + \mu s\left[\left(2\bar{q}^+ - 1\right)p + 2\bar{p}q^+\right], \\
\lambda q^+ &= \frac{2\kappa}{s}\bar{q}^+\left(1-\bar{q}^+\right)j.
\end{aligned} \tag{4.5}$$

We are interested in solutions of problem (4.5) in the Sobolev space $H^1(\mathbb{R};\mathbb{C}^3)$. We start our study by giving some definitions used in the stability theory [33].

Definition 4.1. Let $\mathcal{X}$ be a Banach space and let $\mathcal{L} : D(\mathcal{L}) \subset \mathcal{X} \to \mathcal{X}$ be a linear operator with dense domain $D(\mathcal{L}) \subset \mathcal{X}$. The *resolvent set* of $\mathcal{L}$ is the set of all numbers $\lambda \in \mathbb{C}$ such that the operator $\mathcal{L} - \lambda\mathcal{I}$ has a bounded inverse. The complement of the resolvent is called the *spectrum* $\sigma(\mathcal{L})$. We say that $\lambda \in \sigma(\mathcal{L})$ is an *eigenvalue* of $\mathcal{L}$ if $\mathcal{L} - \lambda\mathcal{I}$ has a nontrivial kernel.

Definition 4.2. Let $\mathcal{L} : D(\mathcal{L}) \subset \mathcal{X} \to \mathcal{X}$ be a linear, closed, densely defined operator. Its spectrum is divided into the *point spectrum* $\sigma_{\rm pt}(\mathcal{L})$, which is composed of those eigenvalues λ such that $\mathcal{L} - \lambda\mathcal{I}$ is Fredholm with index zero, and the *essential spectrum* $\sigma_{\rm ess}(\mathcal{L})$ which is the complementary part; $\sigma_{\rm ess}(\mathcal{L}) = \sigma(\mathcal{L}) \setminus \sigma_{\rm pt}(\mathcal{L})$.

Recall that a linear operator $\mathcal{L} : \mathcal{X} \to \mathcal{Y}$ is said to be a *Fredholm* operator whenever its range $\mathrm{R}(\mathcal{L})$ is closed, and $\dim[\mathrm{N}(\mathcal{L})]$ and $\mathrm{codim}[\mathrm{R}(\mathcal{L})]$ are both finite.

Remark 1. In general, the point spectrum does not represent the entire set of eigenvalues since some eigenvalues may belong to the essential spectrum. Indeed, we show in Lemma 4.4 immediately below that $\lambda = 0$ is an eigenvalue, but nevertheless it does not lie in the point spectrum; it belongs to the essential spectrum instead because the operator fails to be Fredholm. The same situation occurs in combustion fronts [20], KdV solitons [46] and fronts in isothermal autocatalytic chemical reactions [58], just to mention a few.

The spectral problem (4.5) can be written in operator notation as

$$\mathcal{L} \begin{matrix} p \\ j \\ q^+ \end{matrix} = \lambda \begin{matrix} p \\ j \\ q^+ \end{matrix}, \qquad \begin{matrix} p \\ j \\ q^+ \end{matrix} \quad H^1(\mathbb{R};\mathbb{C}^3),$$

where the operator $\mathcal{L} : H^1(\mathbb{R};\mathbb{C}^3) \quad L^2(\mathbb{R};\mathbb{C}^3)$ is defined by

$$\mathcal{L} = \begin{matrix} 0 & -\partial_x & 0 \\ -s^2\partial_x + \mu s(2\bar{q}^+ - 1) & -\mu & 2\mu s\bar{p} \\ 0 & \frac{2\kappa}{s}\bar{q}^+(1-\bar{q}^+) & 0 \end{matrix} .$$

Definition 4.3. Let $(\bar{p}(x), \bar{q}^+(x))$ be a wave solution given by system (4.3), and let $\bar{j}(x)$ be an identically zero function. We say that the triad $(\bar{p}(x), \bar{j}(x), \bar{q}^+(x))$ is *spectrally stable* if no element of the spectrum of $\mathcal{L}$ has strictly positive real part; that is

$$\sigma(\mathcal{L}) \setminus \quad \lambda \quad \mathbb{C} \quad \Re e\,\lambda \geq 0 \quad = \quad 0 \quad .$$

Otherwise, the triad is *spectrally unstable*.

Lemma 4.4. *$\lambda = 0$ is an eigenvalue of $\mathcal{L}$ embedded in the essential spectrum with an infinite dimensional eigenspace.*

Proof. Take $\lambda = 0$ in the spectral system (4.5); since j must belong to $H^1(\mathbb{R};\mathbb{C})$, from the first equation in (4.5) it immediately follows that $j \equiv 0$. Therefore, it all comes down to solve the differential equation

$$-s^2 p_x + \mu s\left[\left(2\bar{q}^+ - 1\right)p + 2\bar{p}q^+\right] = 0. \tag{4.6}$$

The problem consists of finding nontrivial solutions (p, q^+) in the space $H^1(\mathbb{R};\mathbb{C}^2)$.

The existence of one of the desired solutions follows from the first equation in (4.3). If we differentiate the first equation in (4.3), multiply by s^2, and move all terms to the right-hand side, we can infer that $(\bar{p}_x, \bar{q}_x^+)$ satisfies (4.6). In fact, it turns out that for $q^+ = \bar{q}_x^+$ equation (4.6) has an infinite number of linearly independent solutions p belonging to $H^1(\mathbb{R};\mathbb{C})$. In other words, $(p, \bar{q}_x^+)$ is an infinite collection of linearly independent solutions in the prescribed space $H^1(\mathbb{R};\mathbb{C}^2)$ provided p is a solution of (4.6). In order to obtain such solutions, we first show that $\bar{q}_x^+ \quad H^1(\mathbb{R};\mathbb{C})$. Thereafter we solve (4.6) and verify that the solutions p belong to $H^1(\mathbb{R};\mathbb{C})$ for given $q^+ = \bar{q}_x^+$.

Since $\bar{q}_x^+$ is continuous and decays exponentially to zero as $x \quad +$ according to Lemma 2.7, then $\bar{q}_x^+ \quad L^2(\mathbb{R};\mathbb{C})$.

Now, differentiating the second equation in (4.3), we find

$$\bar{q}_{xx}^+ = -\frac{2\kappa}{s}\left(\bar{p}_x(1-\bar{q}^+)\bar{q}^+ + \bar{p}(1-2\bar{q}^+)\bar{q}_x^+\right).$$

We apply the triangle inequality to the right-hand side and take squares. We then integrate over $\mathbb{R}$ to obtain

$$\left\|\bar{q}_{xx}^+\right\|_{L^2}^2 \leq \frac{4\kappa^2}{s^2} \quad _{\mathbb{R}}\Big(\bar{p}_x \,^2 \left|\bar{q}^+(1-\bar{q}^+)\right|^2 + 2\ \bar{p}_x \ \left|\bar{q}_x^+\right| \left|\bar{p}\bar{q}^+(1-\bar{q}^+)(1-2\bar{q}^+)\right| + \left|\bar{p}(1-2\bar{q}^+)\right|^2 \left|\bar{q}_x^+\right|^2\Big)\, dx. \tag{4.7}$$

We want to prove that the right-hand side of this inequality is uniformly bounded.

From (3.10) and given that $q_r^+ \leq \bar{q}^+ \leq q_l^+$, we get

$$\left|\bar{q}^+(1-\bar{q}^+)\right| \leq \left(\frac{1}{2}+\frac{\varepsilon}{2}\right)^2 \quad \text{and} \quad \left|\bar{p}(1-2\bar{q}^+)\right| \leq \varepsilon\bar{p}_{\max}. \tag{4.8}$$

Upon applying Hölder's inequality to (4.7) and upon using (4.8), we obtain

$$\left\|\bar{q}_{xx}^+\right\|_{L^2}^2 \leq \frac{4\kappa^2}{s^2} \quad \left(\frac{1}{2}+\frac{\varepsilon}{2}\right)^4 \ \bar{p}_x \ _{L^2}^2 + 2\bar{p}_{\max}\varepsilon\left(\frac{1}{2}+\frac{\varepsilon}{2}\right)^2 \ \bar{p}_x \ _{L^2} \left\|\bar{q}_x^+\right\|_{L^2} + \varepsilon^2(\bar{p}_{\max})^2 \left\|\bar{q}_x^+\right\|_{L^2}^2 \quad .$$

We can conclude that $\bar{q}_{xx}^+ \quad L^2(\mathbb{R};\mathbb{C})$ because of continuity of $\bar{p}_x$ and its exponentially decaying at $\pm \quad$ provided by Lemma 2.7. It is thus proven that $\bar{q}_x^+ \quad H^1(\mathbb{R};\mathbb{C})$.

Next we solve equation (4.6) for the variable p. The approach is the following. From the equation for $\bar{p}$ in (4.3) we have

$$\frac{\bar{p}_x}{\bar{p}} = \frac{\mu}{s}\left(2\bar{q}^+ - 1\right). \tag{4.9}$$

Taking $q^+ = \bar{q}_x^+$ in (4.6), after the substitution of (4.9), we get

$$p_x - \frac{\bar{p}_x}{\bar{p}}p = \frac{2\mu}{s}\bar{p}\bar{q}_x^+. \tag{4.10}$$

Upon solving (4.10) for p, we get

$$p(x) = \bar{p}(x)\left(C + \frac{2\mu}{s}\left(\bar{q}^+(x) - q_l^+\right)\right), \quad C \quad \mathbb{C}. \tag{4.11}$$

Note that for $C = \frac{\mu}{s}(2q_l^+ - 1)$ we recover the solution $p = \bar{p}_x$, which is detemined by the equation for $\bar{p}$ in (4.3).

We then show that p is an element of $H^1(\mathbb{R};\mathbb{C})$. To this end we make estimates for p and p_x. Thus

$$\|p\|_{L^2}^2 = \int_{\mathbb{R}} \bar{p}^2(x) \left| C + \frac{2\mu}{s}\left(\bar{q}^+(x) - q_l^+\right)\right|^2 dx,$$

hence the right-hand side of the above equation is bounded above by

$$\left(C + \frac{2\mu}{s}\varepsilon\right)^2 \|\bar{p}\|_{L^2}^2 .$$

That $\bar{p} \in L^2(\mathbb{R};\mathbb{C})$ is a consequence of Lemma 2.7. Therefore, the above estimate implies that $p \in L^2(\mathbb{R};\mathbb{C})$.

Now, from (4.10) and the triangle inequality we have that

$$\|p_x\|_{L^2}^2 \leq \int_{\mathbb{R}} \left(\frac{\bar{p}_x}{\bar{p}}\right)^2 |p|^2 + \frac{4\mu}{s}|\bar{p}_x|\left|p\bar{q}_x^+\right| + \frac{4\mu^2}{s^2}\bar{p}^2\left|\bar{q}_x^+\right|^2 \, dx. \tag{4.12}$$

Hölder's inequality applied to (4.12) and the absolute value of (4.9) combined with (4.8) give

$$\|p_x\|_{L^2}^2 \leq \left(\frac{\mu\varepsilon}{s}\right)^2 \|p\|_{L^2}^2 + \frac{4\mu^2\varepsilon}{s^2}\bar{p}_{\max}\|p\|_{L^2}\left\|\bar{q}_x^+\right\|_{L^2} + \frac{4\mu^2}{s^2}(\bar{p}_{\max})^2\left\|\bar{q}_x^+\right\|_{L^2}^2 .$$

This shows that $p \in H^1(\mathbb{R};\mathbb{C})$.

The infinite dimension of the eigenspace is a direct consequence of the linear independence of the solutions given by formula (4.11): let p_1 and p_2 be two solutions corresponding to two different values of C, say C_1 and C_2; it is not difficult to check that the Wronskian of these solutions is $W(p_1,p_2)(x) = \frac{2\mu}{s}\bar{p}^2\bar{q}_x^+(C_1 - C_2)$. Since $\bar{p} > 0$ and $0 < \bar{q}^+ < 1$ on the whole real line, we see from the equation for $\bar{q}^+$ in (4.3) that $\bar{q}_x^+ < 0$ for all $x \in \mathbb{R}$. Then it holds that $W(p_1,p_2)(x) = 0$ for all $x \in \mathbb{R}$. Therefore, the equation (4.6) has infinitely many linearly independent solutions. Since $(p, 0, \bar{q}_x^+)$, with p given by (4.11), is part of the set of eigenfuntions associated to $\lambda = 0$, the latter implies that the eigenspace associated to $\lambda = 0$ is infinite-dimensional.

According to the definition of Fredholm operator, the last statement above means that the operator $\mathcal{L}$ is not Fredholm. Thus, it follows that $\lambda = 0$ is an eigenvalue that belongs to the essential spectrum; see Definition 4.2. This completes the proof. □

4.3

The Quadratic Eigenvalue Problem

With the purpose of characterizing the whole spectrum we assume $\lambda = 0$ in (4.5). We then multiply by λ the second equation in (4.5) to obtain

$$\lambda^2 j = -s^2\lambda p_x - \mu\lambda j + \mu s[(2\bar{q}^+ - 1)\lambda p + 2\bar{p}\lambda q^+],$$

from the first and third equations in (4.5), we have

$$\lambda^2 j = s^2 j_{xx} - \mu\lambda j - \mu s\left[(2\bar{q}^+ - 1)j_x - 2\bar{p}\left(\frac{2\kappa}{s}\bar{q}^+(1-\bar{q}^+)\right)j\right], \tag{4.13}$$

by substituting the equation for $\bar{q}^+$ in (4.3) into (4.13), we get the quadratic eigenvalue problem (also known as a quadratic pencil)

$$s^2 j_{xx} - \mu s[(2\bar{q}^+ - 1)j_x + 2\bar{q}^+_x j] - (\lambda^2 + \mu\lambda)j = 0, \quad \lambda = 0, \quad j \quad H^2(\mathbb{R};\mathbb{C}). \tag{4.14}$$

The reformulation (4.14) of the eigenvalue problem led us to the following result:

Lemma 4.5. *$-\mu$ is an eigenvalue of $\mathcal{L}$ embedded in the essential spectrum associated with the one-dimensional eigenspace spanned by $(\bar{p}_x/\mu, \bar{p}, \bar{q}^+_x/\mu)$.*

Proof. We begin by noting that (4.14) can be written in the form

$$s^2 j_{xx} - \mu s\frac{d}{dx}\left[\left(2\bar{q}^+ - 1\right)j\right] = (\lambda^2 + \mu\lambda)j. \tag{4.15}$$

Using (4.9) to substitute $2\overline{q}^+ - 1 = s\bar{p}_x/\mu\bar{p}$ into (4.15) gives us

$$s^2\frac{d}{dx}\left(j_x - \frac{\bar{p}_x}{\bar{p}}j\right) = (\lambda^2 + \mu\lambda)j.$$

Letting $\lambda = -\mu$, leads us to the equation

$$\frac{d}{dx}\left(j_x - \frac{\bar{p}_x}{\bar{p}}j\right) = 0.$$

By intregrating this equation, we have

$$j_x - \frac{\bar{p}_x}{\bar{p}}j = C, \tag{4.16}$$

for an arbitrary constant C.

Recalling (3.10), we deduce from (4.9) that $\bar{p}_x/\bar{p}$ $\mp\varepsilon\mu/s$ as x $\pm$. From this, and the requirement j, j_x 0 as x $\pm$, we infer that the left-hand side of (4.16) tends to 0 as x $\pm$, which implies that $C = 0$.
We multiply (4.16) by $1/\bar{p}$ to obtain

$$\frac{d}{dx}\left(\frac{j}{\bar{p}}\right) = 0.$$

Thus, the solution is $j = C_0\bar{p}$, for some constant C_0.

Now, substituting $\lambda = -\mu$ and $j = \bar{p}$ into the first and third equation in (4.5) we obtain that $p = \bar{p}_x/\mu$ and $q^+ = \bar{q}^+_x/\mu$. To obtain q^+ it is necessary to use the second equation of (4.3). We conclude therefore that $-\mu$ is an eigenvalue of $\mathcal{L}$ associated with the eigenspace spanned by $(\bar{p}_x/\mu, \bar{p}, \bar{q}^+_x/\mu)$.

The fact the $-\mu$ is an element of the essential spectrum is because the differential operator defined by (4.14) is not Fredholm when $\lambda = -\mu$. For convenience, we provide this result at the end of Section 4.5 below. □

4.4

The Spectrum

To treat problem (4.14) it is useful to introduce the parameter $\tilde{\lambda} := \lambda^2 + \mu\lambda$. Thus, the eigenvalue problem now reads

$$s^2 j_{xx} - \mu s \left[(2\bar{q}^+ - 1)j_x + 2\bar{q}_x^+ j\right] =: Lj = \tilde{\lambda} j, , \quad j \quad H^2(\mathbb{R};\mathbb{C}). \tag{4.17}$$

so that the eigenvalues of (4.14) and consequently those of (4.5) are given by solutions of the equation

$$\lambda^2 + \mu\lambda - \tilde{\lambda} = 0.$$

Remark 2. From the proof of Lemma 4.5, $\tilde{\lambda} = 0$ is an eigenvalue of L associated to the eigenfunction $\bar{p}$.

4.4.1

The essential spectrum

In order to analyze the spectrum of L, we proceed as Alexander *et al.* [1] by rewriting (4.17) as the first-order system

$$\mathbf{Y}_x = \mathbf{A}(x, \tilde{\lambda})\mathbf{Y} \tag{4.18}$$

where $\mathbf{Y} = (j, j_x)^t$ and

$$\mathbf{A}(x, \tilde{\lambda}) = \begin{matrix} 0 & 1 \\ \frac{\tilde{\lambda}}{s^2} + \frac{2\mu}{s}\bar{q}_x^+ & \frac{\mu}{s}(2\bar{q}^+ - 1) \end{matrix} . \tag{4.19}$$

The aim of the reformulation is to use the exponential dichotomies enjoyed by (4.18). Hence, we introduce the definition of exponential dichotomy and Morse index given by Sandstede and Scheel in [53].

Definition 4.6. Consider the differential equation

$$\mathbf{u}_x = A(x, \lambda)\mathbf{u}, \quad \mathbf{u} \quad \mathbb{C}^n. \tag{4.20}$$

Let $I = \mathbb{R}^+, \mathbb{R}^-$ or $\mathbb{R}$, and fix λ_* $\mathbb{C}$. We say that (4.20), with $\lambda = \lambda_*$ fixed, has an *exponential dichotomy* on I if there exist positive constants K, k^s and k^u and a family of projections $P(x)$ defined and continuous for x I such that the following is true.

1. For any fixed $y \quad I$ and $\mathbf{u}_0 \quad \mathbb{C}^n$, there exists a solution $\varphi^s(x,y)\mathbf{u}_0$ of (4.20) with initial value $\varphi^s(y,y)\mathbf{u}_0 = P(y)\mathbf{u}_0$ for $x = y$, and

$$\varphi^s(x,y) \ \leq Ke^{-k^s\, x-y}\,, \quad \text{for all } \ x \geq y, \ \ x, y \quad I.$$

2. For any fixed $y \quad I$ and $\mathbf{u}_0 \quad \mathbb{C}^n$, there exists a solution $\varphi^u(x,y)\mathbf{u}_0$ of (4.20) with initial value $\varphi^u(y,y)\mathbf{u}_0 = (I - P(y))\mathbf{u}_0$ for $x = y$, and

$$\varphi^u(x,y) \ \leq Ke^{-k^u\, x-y}\,, \quad \text{for all } \ x \leq y, \ \ x, y \quad I.$$

3. The solutions $\varphi^s(x,y)\mathbf{u}_0$ and $\varphi^u(x,y)\mathbf{u}_0$ satisfy

$$\begin{aligned} \varphi^s(x,y)\mathbf{u}_0 \quad & \mathrm{R}(P(x)) \ \text{ for all } \ x \geq y, \ \ x, y \quad I, \\ \varphi^u(x,y)\mathbf{u}_0 \quad & \mathrm{N}(P(x)) \ \text{ for all } \ x \leq y, \ \ x, y \quad I. \end{aligned}$$

The x-independent dimension of $\mathrm{N}(P(x))$ is referred to as the *Morse index* $i(\lambda_*)$ of the exponential dichotomy on I. If (4.20) has exponential dichotomies on $\mathbb{R}^+$ and on $\mathbb{R}^-$, the associated Morse indices are denoted by $i_+(\lambda_*)$ and $i_-(\lambda_*)$, respectively.

Following the ideas of Flores and Plaza [13], and Sandstede [52], we consider the family of operators

$$\mathcal{T}(\tilde{\lambda}) : H^1(\mathbb{R};\mathbb{C}^2) \quad L^2(\mathbb{R};\mathbb{C}^2), \qquad \mathbf{Y} \quad \mathbf{Y}_x - \mathbf{A}(x,\tilde{\lambda})\mathbf{Y}, \tag{4.21}$$

for $\tilde{\lambda} \quad \mathbb{C}$.

By Lemma 2.7, $\mathbf{A}(x,\tilde{\lambda}) \quad \mathbf{A}_\pm(\tilde{\lambda})$ exponentially fast as $x \quad \pm \quad$, with

$$\mathbf{A}_\pm(\tilde{\lambda}) = \begin{matrix} 0 & 1 \\ \frac{\tilde{\lambda}}{s^2} & \mp\frac{\mu}{s}\varepsilon \end{matrix} \quad . \tag{4.22}$$

The operators $L - \tilde{\lambda}$ and $\mathcal{T}(\tilde{\lambda})$ are linked by their Fredholm properties. In this sense, if one operator is Fredholm so is the other, in addition to having the same Fredholm index (see [52] and the references therein). In turn, $\mathcal{T}(\tilde{\lambda})$ is Fredholm if and only if (4.18) has an exponential dichotomy on both half-lines $\mathbb{R}^+ = [0, \quad)$ and $\mathbb{R}^- = (- \quad , 0]$, [43, 44]. In such case the Fredholm index is computed by

$$\operatorname{ind}\mathcal{T}(\tilde{\lambda}) = i_-(\tilde{\lambda}) - i_+(\tilde{\lambda}).$$

Here is where the asymptotic matrices $\mathbf{A}_\pm(\tilde{\lambda})$ come into play. An exponential dichotomy on $\mathbb{R}^+$ exists if and only if $\mathbf{A}_+(\tilde{\lambda})$ is hyperbolic, in which case, the Morse index $i_+(\tilde{\lambda})$ is equal to the dimension of the unstable eigenspace of $\mathbf{A}_+(\tilde{\lambda})$. Likewise, the hyperbolicity of $\mathbf{A}_-(\tilde{\lambda})$ determines the existence of an exponential dichotomy on $\mathbb{R}^-$ and $i_-(\tilde{\lambda})$ is given by the dimension of the unstable eigenspace of $\mathbf{A}_+(\tilde{\lambda})$ (cf. [52]).

In the light of all this, the essential spectrum of L comprises all $\tilde{\lambda}$ for which (4.18) has exponential dichotomies on both $\mathbb{R}^+$ and $\mathbb{R}^-$ with distinct Morse indices, that is

$\operatorname{ind}\mathcal{T}(\tilde{\lambda}) = 0$, and those $\tilde{\lambda}$ such that (4.18) has no an exponential dichotomy on at least one half-line.

Regarding the point spectrum of L, this encompasses the values $\tilde{\lambda}$ for which $\mathcal{T}(\tilde{\lambda})$ has a nontrivial kernel (and thus (4.17) has a nonzero solution j) and (4.18) has exponential dichotomies on $\mathbb{R}^+$ and on $\mathbb{R}^-$ with the same Morse index .

We begin by identifying the set of $\tilde{\lambda}$ where the asymptotic matrices $\mathbf{A}_\pm(\tilde{\lambda})$ are not hyperbolic. Thus, consider the sets

$$\tilde{\lambda} \quad \mathbb{C} \quad \det(\mathbf{A}_\pm(\tilde{\lambda}) - aiI) = 0, \text{ for } a \quad \mathbb{R} \quad . \tag{4.23}$$

By straightforward calculations we obtain that the elements of (4.23) are points on the algebraic curves

$$\tilde{\lambda}_\pm(a) = -s^2a^2 \pm \mu s\varepsilon ai, \text{ for } a \quad \mathbb{R} \quad . \tag{4.24}$$

Note that the curves $\tilde{\lambda}_\pm(a)$ describe in fact one single parabola.

The parabola plays a key role in the hyperbolicity of the asymptotic matrices. Along the parabola the matrices $\mathbf{A}_\pm(\tilde{\lambda})$ have at least one purely imaginary eigenvalue, and on its lateral sides the matrices are hyperbolic.

Denote Ω to be the open set in the complex plane bounded on the left by the parabola (4.24), and let Θ denote the complemet of the closure of Ω. We further denote by $\mathbb{E}^s_\pm(\tilde{\lambda})$ and $\mathbb{E}^u_\pm(\tilde{\lambda})$ the stable and unstable eigenspaces of $\mathbf{A}_\pm(\tilde{\lambda})$, respectively.

Proposition 4.7. *The following statements are true.*

(i) For each $\tilde{\lambda} \quad \Omega$, $dim[\mathbb{E}^s_\pm(\tilde{\lambda})] = dim[\mathbb{E}^u_\pm(\tilde{\lambda})] = 1$.

(ii) For all $\tilde{\lambda} \quad \Theta$, $dim[\mathbb{E}^u_-(\tilde{\lambda})] = dim[\mathbb{E}^s_+(\tilde{\lambda})] = 2$.

Proof. The eigenvalues of $\mathbf{A}_-(\tilde{\lambda})$ and $\mathbf{A}_+(\tilde{\lambda})$ are given by

$$\eta^-_{1,2}(\tilde{\lambda}) = \frac{1}{2s}\left(\mu\varepsilon \pm \quad \overline{\mu^2\varepsilon^2 + 4\tilde{\lambda}}\right) \text{ and } \eta^+_{1,2}(\tilde{\lambda}) = \frac{1}{2s}\left(-\mu\varepsilon \pm \quad \overline{\mu^2\varepsilon^2 + 4\tilde{\lambda}}\right). \tag{4.25}$$

Clearly $\mathfrak{Re}\eta^-_1(\tilde{\lambda}) > 0$ and $\mathfrak{Re}\eta^+_2(\tilde{\lambda}) < 0$ for all $\tilde{\lambda} \quad \Omega$. Since $\eta^-_2(\tilde{\lambda}) = -\eta^+_1(\tilde{\lambda})$, the first statement of the proposition will be proved as soon as we have shown that $\mathfrak{Re}\eta^-_2(\tilde{\lambda}) < 0$ for all $\tilde{\lambda} \quad \Omega$.

Taking the real part of $\eta^-_2(\tilde{\lambda})$, we have

$$\mathfrak{Re}\eta^-_2(\tilde{\lambda}) = \frac{1}{2s}\left(\mu\varepsilon - \mathfrak{Re} \quad \overline{\mu^2\varepsilon^2 + 4\tilde{\lambda}}\right),$$

from this expression we see that $\mathfrak{Re}\eta^-_2(\tilde{\lambda}) < 0$ if and only if

$$\left(\mathfrak{Re} \quad \overline{\mu^2\varepsilon^2 + 4\tilde{\lambda}}\right)^2 > \mu^2\varepsilon^2. \tag{4.26}$$

Computing the left-hand side of the above inequality gives

$$\frac{1}{2}\quad \mu^2\varepsilon^2 + 4\Re e\,\tilde{\lambda} + \quad \overline{\left(\mu^2\varepsilon^2 + 4\Re e\,\tilde{\lambda}\right)^2 + 16(\Im m\,\tilde{\lambda})^2}\quad > \mu^2\varepsilon^2.$$

After some calculations we get that the inequality (4.26) is satisfied if and only if

$$(\Im m\,\tilde{\lambda})^2 > -\mu^2\varepsilon^2\Re e\,\tilde{\lambda}. \tag{4.27}$$

Consider $\tilde{\lambda}$ $\mathbb{C}$ with negative real part, we have that $\Re e\,\tilde{\lambda} = \Re e\,\tilde{\lambda}_{\pm}(a) = -a^2s^2$ for some a $\mathbb{R}$, thus, if $\tilde{\lambda}$ Ω it happens that $(\Im m\,\tilde{\lambda})^2 > (\Im m\,\tilde{\lambda}_{\pm}(a))^2 = a^2s^2\mu^2\varepsilon^2$, that is to say, $(\Im m\,\tilde{\lambda})^2 > -\mu^2\varepsilon^2\Re e\,\tilde{\lambda}$, hence the inequality (4.26) holds and consequently $\Re e\,\eta_2^-(\tilde{\lambda}) < 0$. By connectedness of the set Ω and continuity of $\eta_2^-(\tilde{\lambda})$ in $\tilde{\lambda}$, the sign of $\Re e\,\eta_2^-(\tilde{\lambda})$ must remain constant on that region. Therefore, we conclude that $\Re e\,\eta_2^-(\tilde{\lambda}) < 0$ for all $\tilde{\lambda}$ Ω.

We turn to the second statement of the Proposition. We have that every $\tilde{\lambda}$ Θ has real part $\Re e\,\tilde{\lambda} = \Re e\,\tilde{\lambda}_{\pm}(a) = -a^2s^2$ with a $\mathbb{R}$ 0 , then, because $(\Im m\,\tilde{\lambda})^2 < (\Im m\,\tilde{\lambda}_{\pm}(a))^2$ for all $\tilde{\lambda}$ Θ and all a $\mathbb{R}$ 0 , it follows that

$$(\Im m\,\tilde{\lambda})^2 < (\Im m\,\tilde{\lambda}_{\pm}(a))^2 = a^2s^2\mu^2\varepsilon^2 = -\mu^2\varepsilon^2\Re e\,\tilde{\lambda}, \qquad \tilde{\lambda} \quad \Theta, \qquad a \quad \mathbb{R} \quad 0\ .$$

By virtue of this result, inequality (4.26) is not satisfied, thus $\Re e\,\eta_2^-(\tilde{\lambda}) > 0$ and $\Re e\,\eta_1^+(\tilde{\lambda}) < 0$ for all $\tilde{\lambda}$ Θ. This proves the second statement of the proposition, since $\Re e\,\eta_1^-(\tilde{\lambda}) > 0$ and $\Re e\,\eta_2^+(\tilde{\lambda}) < 0$ are also true inside Θ. □

Lemma 4.8. *The essential spectrum of L is the whole region to the left of the parabola described by (4.24), including the parabola.*

Proof. Suppose that the matrices $\mathbf{A}_{\pm}(\tilde{\lambda})$ are hyperbolic. By Theorem 3.3 in [52], this leads to the existence of exponential dichotomies for the equation (4.18) on $\mathbb{R}^+$ and $\mathbb{R}^-$. Additionally, Theorem 3.3 tells us that the Morse indices $i_{\pm}(\tilde{\lambda})$ are equal to $\dim[\mathbb{E}^u_{\pm}(\tilde{\lambda})]$. According to Lemma 4.2 of [43], this means that $\mathcal{T}(\tilde{\lambda})$ is Fredholm with index

$$\operatorname{ind}\mathcal{T}(\tilde{\lambda}) = i_-(\tilde{\lambda}) - i_+(\tilde{\lambda}).$$

Statement (i) of Proposition 4.7 yields that $\operatorname{ind}\mathcal{T}(\tilde{\lambda}) = 0$ for all $\tilde{\lambda}$ Ω, which implies that $\sigma_{\text{ess}}(L) \subset \mathbb{C}$ Ω. To show that $\sigma_{\text{ess}}(L)$ covers $\mathbb{C}$ Ω we argue as follows. From statement (ii) of Proposition 4.7 we obtain that $\operatorname{ind}\mathcal{T}(\tilde{\lambda}) = 2$ for all $\tilde{\lambda}$ Θ, therefore $\Theta \subset \sigma_{\text{ess}}(L)$. In accordance with Theorem 3.3, the lack of hyperbolicity $\mathbf{A}_{\pm}(\tilde{\lambda})$ on the set (4.24) results in the absence of exponential dichotomies of (4.18). By Palmer's Theorem in [44], this entails that $\mathcal{T}(\tilde{\lambda})$ is not Fredholm, thereby the parabola described by (4.24) is a subset of $\sigma_{\text{ess}}(L)$. Since

$$\mathbb{C} \quad \Omega = \Theta \qquad \tilde{\lambda}_{\pm}(a) = -s^2a^2 \pm \mu s\varepsilon ai, \text{ for } a \quad \mathbb{R} \quad ,$$

we deduce that $\mathbb{C}$ $\Omega \subset \sigma_{\text{ess}}(L)$, and hence that $\sigma_{\text{ess}}(L) = \mathbb{C}$ Ω. □

From the above lemma we observe that the point spectrum of L must only contain complex numbers that belong to the region Ω. Accordingly, $\tilde{\lambda} = 0$ is an eigenvalue that does not belong to the point spectrum, $\sigma_{\rm pt}(L)$.

We show below that for all $\tilde{\lambda}$ $\sigma_{\rm pt}(L)$ any nontrivial function in the kernel of the operator $\mathcal{T}(\tilde{\lambda})$ must have exponential decay. To this end, as in [33, 46], we rewrite equation (4.18) in the following form

$$\mathbf{Y}_x = [\mathbf{A}_-(\tilde{\lambda}) + \mathbf{R}(x,\tilde{\lambda})]\mathbf{Y} \ \text{ for } \ x < 0 \ \text{ and } \ \mathbf{Y}_x = [\mathbf{A}_+(\tilde{\lambda}) + \mathbf{R}(x,\tilde{\lambda})]\mathbf{Y} \ \text{ for } \ x \geq 0,$$

where

$$\mathbf{R}(x,\tilde{\lambda}) = \begin{cases} \mathbf{A}(x,\tilde{\lambda}) - \mathbf{A}_-(\tilde{\lambda}), & x < 0, \\ \mathbf{A}(x,\tilde{\lambda}) - \mathbf{A}_+(\tilde{\lambda}), & x \geq 0. \end{cases}$$

We have by Lemma 2.7 that

$$\mathbf{R}(x,\tilde{\lambda}) \ = \ \mathbf{A}(x,\tilde{\lambda}) - \mathbf{A}_\pm(\tilde{\lambda}) \ \leq \tilde{C} e^{-\frac{\varepsilon\mu}{s}\,x} \quad \text{as} \quad x \qquad , \tag{4.28}$$

for all $\tilde{\lambda}$ $\sigma_{\rm pt}(L)$.

According to the Gap Lemma [61], if $V_j^{\pm}(\tilde{\lambda})$ are eigenvectors of $\mathbf{A}_\pm(\tilde{\lambda})$ associated with the eigenvalues $\eta_j^{\pm}(\tilde{\lambda})$, $j = 1, 2$, the decay estimate (4.28) implies that for all $\alpha < \frac{\mu\varepsilon}{s}$, the system (4.18) has a set of solutions $\mathbf{Y}_j^{\pm}(x,\tilde{\lambda})$, $j = 1, 2$, that satisfy

$$\begin{aligned} \mathbf{Y}_j^-(x,\tilde{\lambda}) &= \left(V_j^-(\tilde{\lambda}) + O\left(e^{-\alpha\,x}\,\left|V_j^-(\lambda)\right|\right)\right) e^{\eta_j^-(\tilde{\lambda})x}, \quad (j = 1,2) \quad x < 0, \\ \mathbf{Y}_j^+(x,\tilde{\lambda}) &= \left(V_j^+(\tilde{\lambda}) + O\left(e^{-\alpha\,x}\,\left|V_j^+(\lambda)\right|\right)\right) e^{\eta_j^+(\tilde{\lambda})x}, \quad (j = 1,2) \quad x > 0, \end{aligned} \tag{4.29}$$

for any $\tilde{\lambda}$ $\sigma_{\rm pt}(L)$. The importance of these relations stems from the fact that they allow us to characterize the asymptotic behaviour of the elements of the kernel of $\mathcal{T}(\tilde{\lambda})$. Indeed, we have found previously that $\Re e\,\eta_1^{\pm}(\tilde{\lambda}) > 0$ and $\Re e\,\eta_2^{\pm}(\tilde{\lambda}) < 0$ provided that $\tilde{\lambda}$ Ω, since we are interested in solutions to (4.18) in $H^1(\mathbb{R};\mathbb{C}^2)$, we observe from (4.29) that one can construct such solutions only if they decay exponentially to zero as x $+$. Thus, a vector-valued function $\mathbf{Y}(x,\tilde{\lambda})$ $N(\mathcal{T}(\tilde{\lambda}))$ is spanned by $\mathbf{Y}_1^-(x,\tilde{\lambda})$ in $x < 0$ and by $\mathbf{Y}_2^+(x,\tilde{\lambda})$ in $x > 0$, meaning that $\mathbf{Y}(x,\tilde{\lambda}) = \alpha_0\mathbf{Y}_1^-(x,\tilde{\lambda}) = \beta_0\mathbf{Y}_2^+(x,\tilde{\lambda})$ for some nonzero α_0, β_0 $\mathbb{C}$.

Furthermore, we have the following:

Proposition 4.9. *Let $\tilde{\lambda}$ $\sigma_{pt}(L)$ and $\mathbf{Y}(x,\tilde{\lambda})$ $N(\mathcal{T}(\tilde{\lambda}))$, then there are nonzero constants α_0, β_0 $\mathbb{C}$ such that $\mathbf{Y}(x,\tilde{\lambda})$ decays exponentially fast as x $+$ satisfying*

$$\begin{aligned} \mathbf{Y}(x,\tilde{\lambda}) \quad & \alpha_0 V_1^-(\tilde{\lambda}) e^{\eta_1^-(\tilde{\lambda})x} \quad \textit{as} \quad x \quad - \ , \\ \mathbf{Y}(x,\tilde{\lambda}) \quad & \beta_0 V_2^+(\tilde{\lambda}) e^{\eta_2^+(\tilde{\lambda})x} \quad \textit{as} \quad x \quad + \ , \end{aligned}$$

where $V_1^-(\tilde{\lambda})$ and $V_2^+(\tilde{\lambda})$ are eigenvectors associated to the unstable and stable eigenvalues $\eta_1^-(\tilde{\lambda})$ and $\eta_2^+(\tilde{\lambda})$, respectively.

There is hereby established that for every $\tilde{\lambda}$ $\sigma_{\rm pt}(L)$ the associated eigenfunction j approaches exponentially to zero as x $+$.

4.4.2

Integrated equation

Suppose that $\tilde{\lambda}$ $\sigma_{\mathrm{pt}}(L)$ is an eigenvalue with a corresponding eigenfunction j $H^2(\mathbb{R};\mathbb{C})$. Let us rewrite equation (4.17) in the form

$$s^2 j_{xx} - \mu s \left((2\bar{q}^{+} - 1)j\right)_x = \tilde{\lambda} j,$$

from which we obtain

$$s^2 \frac{d}{dx}\left(j_x - \frac{\mu}{s}(2\bar{q}^{+} - 1)j\right) = \tilde{\lambda} j. \tag{4.30}$$

Applying the technique conceived by Goodman [21], we introduce the *integrated variable*

$$w(x) := \int_{-}^{x} j(y)dy. \tag{4.31}$$

We integrate (4.30) from $-$ to x and obtain

$$\tilde{\lambda} w(x) = \tilde{\lambda} \int_{-}^{x} j(y)dy = s^2 \left(j_x(x) - \frac{\mu}{s}(2\bar{q}^{+} - 1)j(x)\right), \tag{4.32}$$

then, we substitute j for w in (4.32) in order to obtain the *integrated eigenvalue equation*

$$s^2 \left(w_{xx} - \frac{\mu}{s}(2\bar{q}^{+} - 1)w_x\right) =: \mathscr{L} w = \tilde{\lambda} w. \tag{4.33}$$

The significance of the above equation arises from the fact that the point spectra of L and $\mathscr{L}$ are the same (see Proposition 4.10 below). This result will prove very useful for characterizing the point spectrum of L as the integrated eigenvalue problem (4.33) will provide the required information. The same approach has been carried out by Zumbrun [60] and Humpherys [29] in the context of viscous conservation laws.

The family of operators associated with (4.33) is given by

$$\begin{aligned} \mathcal{T}^I(\tilde{\lambda}) : H^1(\mathbb{R};\mathbb{C}^2) &\quad L^2(\mathbb{R};\mathbb{C}^2), \\ \mathbf{W} &\quad \mathbf{W}_x - \mathbf{A}^I(x,\tilde{\lambda})\mathbf{W}, \quad \tilde{\lambda} \quad \mathbb{C} \quad 0 \ , \end{aligned}$$

where $\mathbf{W} = (w, w_x)^t$ and

$$\mathbf{A}^I(x,\tilde{\lambda}) = \begin{matrix} 0 & 1 \\ \frac{\tilde{\lambda}}{s^2} & \frac{\mu}{s}(2\bar{q}^{+} - 1) \end{matrix} \ .$$

Remark 3. We point out that $\mathbf{A}^I(x,\tilde{\lambda})$ has the same asymptotic limits as $\mathbf{A}(x,\tilde{\lambda})$. Thus the essential spectrum of L and $\mathscr{L}$ coincide, and therefore the point spectrum of $\mathscr{L}$ is also contained in the set Ω. We may use arguments similar to those that led to Proposition

4.9, to conclude that for a given $\tilde{\lambda}$ $\sigma_{\rm pt}(\mathscr{L})$, there exist nonzero constants α_0, β_0 $\mathbb{C}$ such that the corresponding function $\mathbf{W}(x, \tilde{\lambda})$ $N(\mathcal{T}^I(\tilde{\lambda}))$ has the asymptotic behaviour

$$\begin{aligned} \mathbf{W}(x, \tilde{\lambda}) &\quad \alpha_0 V_1^-(\tilde{\lambda}) e^{\eta_1^-(\tilde{\lambda})x} \quad \text{as} \quad x \quad - \quad , \\ \mathbf{W}(x, \tilde{\lambda}) &\quad \beta_0 V_2^+(\tilde{\lambda}) e^{\eta_2^+(\tilde{\lambda})x} \quad \text{as} \quad x \quad + \quad . \end{aligned}$$

Proposition 4.10. *The point spectrum of L and point spectrum of $\mathscr{L}$ coincide.*

Proof. We begin by proving that $\sigma_{\rm pt}(L) \subset \sigma_{\rm pt}(\mathscr{L})$. Observe that the existence of the eigenpair $(j, \tilde{\lambda})$ of (4.17) gives rise to a solution $(w, \tilde{\lambda})$ of equation (4.33), then the problem consists in checking that w belongs to $H^2(\mathbb{R}; \mathbb{C})$. Since j $H^2(\mathbb{R}; \mathbb{C})$, it is clear that w_x, w_{xx} $L^2(\mathbb{R}; \mathbb{C})$. Thus, we only need to show that w $L^2(\mathbb{R}; \mathbb{C})$. By Plancherel's theorem, it suffices to show that $\hat{w}$ $L^2(\mathbb{R}; \mathbb{C})$. For this purpose, we differentiate (4.31) and take the Fourier transform to obtain $ik\hat{w}(k) = \hat{j}(k)$. So we have that

$$\hat{w} \ {}^2_{L^2} = \int_{\mathbb{R}} \frac{\hat{j}(k)\ ^2}{k^2}\, dk.$$

The above integral may be split into three parts

$$\int_{\mathbb{R}} \frac{\hat{j}(k)\ ^2}{k^2}\, dk = \int_{-}^{-a} \frac{\hat{j}(k)\ ^2}{k^2}\, dk + \int_{-a}^{a} \frac{\hat{j}(k)\ ^2}{k^2}\, dk + \int_{a}^{+} \frac{\hat{j}(k)\ ^2}{k^2}\, dk,$$

with $a > 1$. The first and the last integral converge because are both bounded above by $\hat{j}\ {}^2_{L^2}$. Given that $\hat{j}(k)$ is a continuous function, then to establish the convergence of the second integral we only need to show that $\hat{j}(k)/k$ tends to a finite limit as k 0. First note that

$$w(+\quad) = \int_{-}^{+} j(y)\, dy = \quad \overline{2\pi}\hat{j}(0).$$

On the other hand, since $\tilde{\lambda} = 0$ and, j and j_x decay to zero at $x = \pm$, it follows from (4.32) that w approaches zero as x $+$. Which implies that $\hat{j}(0) = 0$. Hence, using L'Hospital's rule, we get

$$\lim_{k \ 0} \frac{\hat{j}(k)}{k} = \lim_{k \ 0} \frac{d}{dk}\hat{j}(k) = \int_{\mathbb{R}} y j(y)\, dy.$$

The fact that j decays exponentially fast to zero as y ensures the convergence of the integral.

Next we show that $\sigma_{\rm pt}(\mathscr{L}) \subset \sigma_{\rm pt}(L)$. Let w $H^2(\mathbb{R}; \mathbb{C})$ be an eigenfunction of (4.33) for $\tilde{\lambda}$ $\sigma_{\rm pt}(\mathscr{L})$. Setting $j = w_x$, it is readily seen that

$$w(x) = \int_{-}^{x} j(y) dy. \tag{4.34}$$

Upon substituting $w_x = j$ and (4.34) into (4.33), and differentiating, we readily obtain

$$s^2 \frac{d}{dx}\left(j_x - \frac{\mu}{s}(2\bar{q}^+ - 1) j \right) = \tilde{\lambda} j.$$

Thus, if we show that j belongs to the desired space $H^2(\mathbb{R};\mathbb{C})$, then it would follow that $\sigma_{\rm pt}(\mathscr{L}) \subset \sigma_{\rm pt}(L)$. Clearly $j \quad H^1(\mathbb{R};\mathbb{C})$. Then it is only necessary to check that $j_{xx} \quad L^2(\mathbb{R};\mathbb{C})$. This is achieved by showing that $w_{xxx} \quad L^2(\mathbb{R};\mathbb{C})$. Hence, after differentiation of (4.33) and upon substituting w_{xx} from (4.33), we arrive at

$$s^2 w_{xxx} = (2\mu s \bar{q}_x^+ + \mu^2(2\bar{q}^+ - 1)^2 + \tilde{\lambda}) w_x + \frac{\mu}{s}\tilde{\lambda}(2\bar{q}^+ - 1) w.$$

Therefore, we use the exponential decay of w and w_x together with the boundedness of $\bar{q}^+$ and $\bar{q}_x^+$, to conclude that $w_{xxx} \quad L^2(\mathbb{R};\mathbb{C})$. □

4.4.3

Energy estimates

In what follows we use energy methods [13, 20, 28] to prove that the point spectrum of the operator $\mathscr{L}$ is the empty set.

Lemma 4.11. *The point spectrum of $\mathscr{L}$ is empty.*

Proof. We use (4.9) to substitute $2\bar{q}^+ - 1 = s\bar{p}_x/\mu\bar{p}$ into (4.33). This gives

$$s^2 \left(w_{xx} - \frac{\bar{p}_x}{\bar{p}} w_x \right) = \tilde{\lambda} w. \tag{4.35}$$

Upon multiplying (4.35) by the integrating factor $1/\bar{p}$, we obtain that w satisfies

$$s^2 \frac{d}{dx}\left(\frac{w_x}{\bar{p}} \right) = \tilde{\lambda} \frac{w}{\bar{p}}. \tag{4.36}$$

We now multiply (4.36) by the complex conjugate w^* and integrate over $\mathbb{R}$ to obtain

$$s^2 \int_{\mathbb{R}} \frac{d}{dx}\left(\frac{w_x}{\bar{p}} \right) w^* \, dx = \tilde{\lambda} \int_{\mathbb{R}} \frac{|w|^2}{\bar{p}} \, dx.$$

Claim. $w/\bar{p}, w_x/\bar{p} \quad 0$ exponentially as $x \quad +\infty$.

Indeed, from Lemma 2.7 and Remark 3 we have that

$$\bar{p}^{-\frac{1}{2}} \mathbf{W}(x,\tilde{\lambda}) \sim C_\alpha V_1^-(\tilde{\lambda}) e^{(\eta_1^-(\tilde{\lambda}) - \frac{\mu\varepsilon}{2s})x} = C_\alpha V_1^-(\tilde{\lambda}) e^{\frac{1}{2s}\overline{\mu^2 s^2 + 4\tilde{\lambda}} x} \quad \text{as} \quad x \quad -\infty,$$
$$\bar{p}^{-\frac{1}{2}} \mathbf{W}(x,\tilde{\lambda}) \sim C_\beta V_2^+(\tilde{\lambda}) e^{(\eta_2^+(\tilde{\lambda}) + \frac{\mu\varepsilon}{2s})x} = C_\beta V_2^+(\tilde{\lambda}) e^{-\frac{1}{2s}\overline{\mu^2 s^2 + 4\tilde{\lambda}} x} \quad \text{as} \quad x \quad +\infty,$$

for some nonzero $C_\alpha, C_\beta \quad \mathbb{C}$.

Recall that $\mathbf{W} = (w, w_x)^t$. Thus, upon noticing that

$$\Re e \quad \overline{\mu^2 s^2 + 4\tilde{\lambda}} = |\mu^2 s^2 + 4\tilde{\lambda}|^{\frac{1}{2}} \cos(\arg(\mu^2 s^2 + 4\tilde{\lambda})/2)$$

is positive for all $\tilde{\lambda} \quad \sigma_{\rm pt}(\mathscr{L}) \subset \Omega$, we obtain the exponential convergence to zero.

In view of the claim, we can integrate the left-hand side by parts. We infer that

$$-s^2 \quad \int_{\mathbb{R}} \frac{w_x}{\bar{p}}^2 dx = \tilde{\lambda} \quad \int_{\mathbb{R}} \frac{w}{\bar{p}}^2 dx.$$

This shows that $\tilde{\lambda} < 0$. But this contradicts $\tilde{\lambda} \quad \sigma_{\rm pt}(\mathscr{L}) \subset \Omega$, because of the fact that the negative half-real line is a subset of $\sigma_{\rm ess}(\mathscr{L}) = \mathbb{C} \ \Omega$ (see Lemma 4.8). Therefore, there is no point spectrum for $\mathscr{L}$. □

4.4.4

The point spectrum of L

The results of Proposition 4.10 and Lemma 4.11 come together in the following theorem.

Theorem 4.12. *The point spectrum of the quadratic eigenvalue problem (4.14) is the empty set.*

4.5

Spectral stability

We begin the section with our main result.

Theorem 4.13. *The family of standing waves is spectrally stable.*

In view of Theorem 4.12, the point spectrum of $\mathcal{L}$ is empty, meaning that the spectrum is made up completely of essential spectrum. This being so, we must show that the rest of the essential spectrum, namely the non-zero elements, is composed of complex numbers with negative real part. In this fashion, we finish the proof of Theorem 4.13. For this purpose, we will show that the essential spectrum of the equivalent problem (4.14) is a subset of the stable half-plane. As before, we may associate (4.14) with the family of operators

$$\mathcal{T}(\lambda^2 + \mu\lambda) = \mathbf{Y}_x - \mathbf{A}(x, \lambda^2 + \mu\lambda)\mathbf{Y}, \quad \text{for} \quad \lambda \quad \mathbb{C} \quad 0 \ .$$

Proposition 4.14. *Let* $\Omega^S = \ \lambda \quad \mathbb{C} \quad 0 \quad \Re e\,\lambda \geq 0$ *. Then, for all* $\lambda \quad \Omega^S$*, the matrices* $\mathbf{A}_\pm\left(\lambda^2 + \mu\lambda\right)$ *are hyperbolic with one-dimensional eigenspaces* $\mathbb{E}^s_\pm(\lambda^2 + \mu\lambda)$ *and* $\mathbb{E}^u_\pm(\lambda^2 + \mu\lambda)$*.*

Proof. We begin by proving that the set

$$\left\{\lambda \quad \mathbb{C} \quad 0 \quad \det(\mathbf{A}_{\pm}(\lambda^2+\mu\lambda)-aiI)=0, \text{ for } a \quad \mathbb{R}\right\} \tag{4.37}$$

contains only complex numbers with negative real part.

Computing the determinant, one may write (4.37) as

$$\left\{\lambda \quad \mathbb{C} \quad 0 \quad \lambda^2+B(a)\lambda+C(a)=0, \text{ for } a \quad \mathbb{R}\right\}, \tag{4.38}$$

where $B(a)=\mu$ and $C(a)=a^2s^2 \mp a\mu s\varepsilon i$.

Solving the characteristic polynomial, we find that (4.37) consists of the curves

$$\lambda_{1,2}(a)=\frac{-B(a)\pm \quad \overline{D(a)}}{2}, \quad a \quad \mathbb{R}, \tag{4.39}$$

where $D(a)=\mu^2-4(a^2s^2 \mp a\mu s\varepsilon i)$.

Since $B(a)<0$, then clearly $\mathfrak{Re}\,\lambda_2(a)<0$ for all $a \quad \mathbb{R}$. On the other hand, observe that $\mathfrak{Re}\,\lambda_1(a)<0$ if and only if

$$(\mathfrak{Re}\,B(a))^2>\left(\mathfrak{Re} \quad \overline{D(a)}\right)^2=\frac{1}{2}\left(\mathfrak{Re}\,D(a)+ \quad \overline{(\mathfrak{Re}\,D(a))^2+(\mathfrak{Im}\,D(a))^2}\right),$$

for all $a \quad \mathbb{R} \quad 0$. We deduce from this observation that $\mathfrak{Re}\,\lambda_1(a)$ is negative if and only if

$$(\mathfrak{Im}\,D(a))^2+4(\mathfrak{Re}\,B(a))^2\mathfrak{Re}\,D(a)-4(\mathfrak{Re}\,B(a))^4<0, \quad a \quad \mathbb{R} \quad 0 \ . \tag{4.40}$$

We have excluded $a=0$ because $\lambda(0)=0$; such value was left out of the analysis of the quadratic eigenvalue problem.

After some elementary calculations, we have

$$(\mathfrak{Im}\,D(a))^2+4(\mathfrak{Re}\,B(a))^2\mathfrak{Re}\,D(a)-4(\mathfrak{Re}\,B(a))^4=-16\mu^2a^2s^2(1-\varepsilon^2),$$

for all $a \quad \mathbb{R} \quad 0$, therefore we can conclude (4.40) since $1-\varepsilon^2>0$ as $0<\varepsilon<1$. Thus, it follows that matrices $\mathbf{A}_{\pm}(\lambda^2+\mu\lambda)$ are hyperbolic on Ω^S.

It remains to verify that the stable and unstable eigenspaces are one-dimensional. Consider $\lambda=\zeta \quad \mathbb{R}^+ \subset \Omega^S$, it is clear that $\zeta^2+\mu\zeta \quad \Omega$, then by Proposition 4.7, $\dim[\mathbb{E}^s_{\pm}(\zeta^2+\mu\zeta)]=1$ and $\dim[\mathbb{E}^u_{\pm}(\zeta^2+\mu\zeta)]=1$. Therefore, from the fact that Ω^S is connected and $\eta^{\pm}_{1,2}(\cdot)$ are continuous, it follows that $\dim[\mathbb{E}^s_{\pm}(\lambda^2+\mu\lambda)]=1$ and $\dim[\mathbb{E}^u_{\pm}(\lambda^2+\mu\lambda)]=1$ for all $\lambda \quad \Omega^S$. □

Lemma 4.15. *The rest of the essential spectrum of $\mathcal{L}$ is a subset of the open left-half complex plane.*

Proof. By similar arguments as used in the proof of Lemma 4.8, one can show that

$$\sigma_{\text{ess}}(\mathcal{L}) \quad 0 \ \subset \ \lambda \quad \mathbb{C} \ \ \mathfrak{Re}\,\lambda<0 \ .$$

□

4.5.1

End of the proof of Lemma 4.5.

Observe that $(\lambda, a) = (-\mu, 0)$ is a solution of the characteristic polynomial in (4.38), which means that 0 is an eigenvalue of the asymptotic matrices $\mathbf{A}_{\pm}(0)$. In other words, $\mathbf{A}_{\pm}(0)$ are nonhyperbolic. As consequence of the Theorem 3.3 of [52] and Palmer's Theorem in [44], the operator $\mathcal{T}(0)$ is not Freholm, therefore $-\mu$ belongs to the essential spectrum of $\mathcal{L}$.

CHAPTER

FIVE

THE UNSTABLE SPECTRUM IN THE FAMILY OF M^5-TRAVELING WAVES

In this chapter we collect the results that we have obtained so far on the spectral stability of the M^5-traveling waves. We show that they are spectrally unstable in $H^1(\mathbb{R};\mathbb{C}^3)$ as the essential spectrum includes the imaginary axis. To remedy this we have built a weighted Sobolev space where the essential spectrum lies on the open left-half complex plane, away from the imaginary axis. The results in the current chapter look promising since among the conditions considered by Rottmann-Matthes [50] it only remains to ensure that the nonzero elements of the point spectrum belong to the open left-half complex plane, although up until now this has represented a great research challenge.

5.1

The Spectral Problem the for M^5-Traveling Waves

In the moving coordinate frame $(z,t) = (x - ct, t)$, where $0 < c < s$, traveling waves $\bar{p}$, $\bar{j}$ and $\bar{q}^+$ are time-independent solutions of the system

$$\begin{aligned} p_t &= cp_z - j_z, \\ j_t &= -s^2 p_z + cj_z - \mu j + \mu s\left(2q^+ - 1\right)p, \\ q_t^+ &= cq_z^+ + \frac{2\kappa}{s} jq^+\left(1 - q^+\right), \end{aligned} \tag{5.1}$$

which is why their spectral stability is determined by linearizing (5.1) around them:

$$\begin{aligned} p_t &= cp_z - j_z, \\ j_t &= -s^2 p_z + cj_z - \mu j + \mu s\left[\left(2\bar{q}^+ - 1\right)p + 2\bar{p}q^+\right], \\ q_t^+ &= cq_z^+ + \frac{2\kappa}{s}\left[\bar{q}^+\left(1 - \bar{q}^+\right)j + \bar{j}\left(1 - 2\bar{q}^+\right)q^+\right]. \end{aligned}$$

Then, considering pertubations of the form $e^{\lambda t}p(z)$, $e^{\lambda t}j(z)$ and $e^{\lambda t}q^+(z)$, with $\lambda \quad \mathbb{C}$, we have the spectral problem

$$\begin{aligned} \lambda p &= cp_z - j_z, \\ \lambda j &= -s^2 p_z + cj_z - \mu j + \mu s\left(\left(2\bar{q}^+ - 1\right)p + 2\bar{p}q^+\right), \\ \lambda q^+ &= cq_z^+ + \frac{2\kappa}{s}\left(\bar{q}^+\left(1-\bar{q}^+\right)j + \bar{j}\left(1-2\bar{q}^+\right)q^+\right), \end{aligned} \tag{5.2}$$

which can be formulated as the spectral system

$$\mathcal{L}^c \begin{matrix} p \\ j \\ q^+ \end{matrix} = \lambda \begin{matrix} p \\ j \\ q^+ \end{matrix}, \qquad \begin{matrix} p \\ j \\ q^+ \end{matrix} \quad H^1(\mathbb{R};\mathbb{C}^3), \tag{5.3}$$

where the operator $\mathcal{L}^c : H^1(\mathbb{R};\mathbb{C}^3) \quad L^2(\mathbb{R};\mathbb{C}^3)$ is defined by

$$\mathcal{L}^c = \begin{matrix} c\partial_z & -\partial_z & 0 \\ -s^2\partial_z + \mu s(2\bar{q}^+ - 1) & c\partial_z - \mu & 2\mu s\bar{p} \\ 0 & \frac{2\kappa}{s}\bar{q}^+(1-\bar{q}^+) & c\partial_z + \frac{2\kappa}{s}\bar{j}\,(1-2\bar{q}^+) \end{matrix}, \quad 0 < c < s.$$

5.2

The Eigenvalue $\lambda = 0$

In this section we show that unlike the standing case, for all wave speed $c \quad (0, s)$, zero is an eigenvalue whose eigenspace has dimension one.

Lemma 5.1. *For each wave speed $0 < c < s$, $\lambda = 0$ is an eigenvalue of $\mathcal{L}^c$ with a 1-dimensional eigenspace generated by $(\bar{p}_z, \bar{j}_z, \bar{q}_z^+)$.*

Proof. Set $\lambda = 0$ in (5.3), integration in $(- \quad, z)$ of the first equation there, together with the condition $(p, j, q^+) \quad H^1(\mathbb{R};\mathbb{C}^3)$, yields

$$j = cp. \tag{5.4}$$

By substitution of (5.4) into (5.3), and considering $\lambda = 0$, problem (5.3) reduces to the system

$$\begin{aligned} p_z &= \frac{\mu}{s^2 - c^2}\left(\left(2s\bar{q}^+ - (c+s)\right)p + 2s\bar{p}q^+\right), \\ q_z^+ &= -\frac{2\kappa}{s}(\bar{q}^+\left(1-\bar{q}^+\right)p + \bar{p}\left(1-2\bar{q}^+\right)q^+); \end{aligned} \tag{5.5}$$

in the equation for q^+ we have used the invariant of motion $\bar{j} = c\bar{p}$. As a result of this reduction, the spectral problem (5.3) may have at most two linearly independent eigenfunctions associated to $\lambda = 0$. Thus, in order to find the solutions of (5.3) for such λ, all we need is to solve the system (5.5). Next we show that $(\bar{p}_z, \bar{q}_z^+)$ and $(\bar{p}_{q_l^+}, \bar{q}_{q_l^+}^+)$ are linearly independent solutions of (5.5).

We differentiate (2.5) with respect to z and rearrange the terms to obtain that $(\bar{p}_z, \bar{q}_z^+)$ is a solution of (5.5), that is,

$$\begin{aligned} \bar{p}_{zz} &= \frac{\mu}{s^2 - c^2}\left((2s\bar{q}^+ - (c+s))\bar{p}_z + 2s\bar{p}\bar{q}_z^+\right), \\ \bar{q}_{zz}^+ &= -\frac{2\kappa}{s}(\bar{q}^+\left(1 - \bar{q}^+\right)\bar{p}_z + \bar{p}\left(1 - 2\bar{q}^+\right)\bar{q}_z^+). \end{aligned} \tag{5.6}$$

Similarly, differentiating (2.5) partially with respect to the left state q_l^+, we find that $(\bar{p}_{q_l^+}, \bar{q}_{q_l^+}^+)$ is a solution to system (5.5). Hence

$$\begin{aligned} \bar{p}_{q_l^+ z} &= \frac{\mu}{s^2 - c^2}\left((2s\bar{q}^+ - (c+s))\bar{p}_{q_l^+,} + 2s\bar{p}\bar{q}_{q_l^+}^+\right), \\ \bar{q}_{q_l^+ z}^+ &= -\frac{2\kappa}{s}(\bar{q}^+\left(1 - \bar{q}^+\right)\bar{p}_{q_l^+} + \bar{p}\left(1 - 2\bar{q}^+\right)\bar{q}_{q_l^+}^+). \end{aligned}$$

To be sure that $(\bar{p}_z, \bar{q}_z^+)$ and $(\bar{p}_{q_l^+}, \bar{q}_{q_l^+}^+)$ are linearly independent we have to check that their Wronskian is different from zero at least at one point.

We thus proceed as follows. Wang *et al.* [56] observed that for all left state $\theta^* < q_l^+ < 1$, the pulse $\bar{p}$ attains its maximum when $\bar{q}^+ = \theta^*$ (recall $\theta^* = \frac{c+s}{2s}$); due to the translation invariance of the traveling waves we can assume that such values of $\bar{p}$ and $\bar{q}^+$ are reached at $z = 0$. We then have that $\bar{p}_z(0) = 0$ and $\bar{q}_{q_l^+}^+(0) = \partial_{q_l^+}\theta^* = 0$. On the other hand, Wang and coworkers further noted that the maximum of $\bar{p}$ is a increasing function with respect to q_l^+, this means that $\bar{p}_{q_l^+}(0) = \partial_{q_l^+}\bar{p}_{\max} > 0$. Hence, from all these results and the fact that $\bar{q}_z^+ < 0$ for all $z \quad \mathbb{R}$, we have that the Wronskian at $z = 0$ is positive:

$$w(0) = \left[\bar{p}_z\bar{q}_{q_l^+}^+ - \bar{p}_{q_l^+}\bar{q}_z^+\right]_{z=0} = -\bar{p}_{q_l^+}(0)\bar{q}_z^+(0) > 0.$$

Actually, $(\bar{p}_{q_r^+}, \bar{q}_{q_r^+}^+)$ is also a solution of (5.5), but in view of Proposition 2.4 we can write

$$\frac{\partial\bar{p}}{\partial q_l^+} = \frac{\partial\bar{p}}{\partial q_r^+}\frac{\partial q_r^+}{\partial q_l^+} \quad \text{and} \quad \frac{\partial\bar{q}^+}{\partial q_l^+} = \frac{\partial\bar{q}^+}{\partial q_r^+}\frac{\partial q_r^+}{\partial q_l^+},$$

which we use to compute the Wroskian of $(\bar{p}_{q_l^+}, \bar{q}_{q_l^+}^+), (\bar{p}_{q_r^+}, \bar{q}_{q_r^+}^+)$, obtaining that it is zero and consequently that this pair of solutions is linearly dependent.

Below we deduce that the associated eigenspace has dimension equal to one. From (5.6) and the results of Lemma 2.7 on the exponential decay of $\bar{p}_z$ and $\bar{q}_z^+$, we have that

$$(\bar{p}_z, \bar{j}_z, \bar{q}_z^+) = (\bar{p}_z, c\bar{p}_z, \bar{q}_z^+) \quad H^1(\mathbb{R}; \mathbb{C}^3).$$

Therefore, $\lambda = 0$ is an eigenvalue and $(\bar{p}_z, \bar{j}_z, \bar{q}_z^+)$ is an associated eigenfunction. To prove that this is the only eigenfunction we will show that $(\bar{p}_{q_l^+}, \bar{q}^+_{q_l^+})$ tends to a nonzero limit as $z \quad \pm \quad$, which automatically leaves the function $(\bar{p}_{q_l^+}, \bar{j}_{q_l^+}, \bar{q}^+_{q_l^+}) = (\bar{p}_{q_l^+}, c\bar{p}_{q_l^+}, \bar{q}^+_{q_l^+})$ out of $L^2(\mathbb{R};\mathbb{C}^3)$ and therefore out of $H^1(\mathbb{R};\mathbb{C}^3)$.

Let us write (5.5) in the vector form

$$\mathbf{W}_z = \mathbb{A}(z)\,\mathbf{W}, \tag{5.7}$$

where $\mathbf{W} = (p, q^+)^t$ and

$$\mathbb{A}(z) = \begin{matrix} \frac{(2s\bar{q}^+ - (c+s))\mu}{s^2-c^2} & \frac{2\mu s\bar{p}}{s^2-c^2} \\ -\frac{2\kappa\bar{q}^+(1-\bar{q}^+)}{s} & -\frac{2\kappa\bar{p}(1-2\bar{q}^+)}{s} \end{matrix}.$$

Define the parameters

$$\alpha_r := \lim_{z \to +} \frac{(c+s-2s\bar{q}^+)\mu}{2(s^2-c^2)} = \frac{(c+s-2sq_r^+)\mu}{2(s^2-c^2)} > 0,$$
$$\alpha_l := \lim_{z \to -} \frac{(c+s-2s\bar{q}^+)\mu}{2(s^2-c^2)} = \frac{(c+s-2sq_l^+)\mu}{2(s^2-c^2)} < 0.$$

Letting $z \quad \pm \quad$, we obtain

$$\mathbb{A}_\pm := \lim_{z \to \pm} \mathbb{A}(z) = \begin{matrix} -2\alpha_m & 0 \\ -\frac{2\kappa q_m^+(1-q_m^+)}{s} & 0 \end{matrix},$$

where $m = r, l$ at $\pm \quad$, respectively.

It happens that $\mathbb{A}(z)$ approaches exponentially to its limits $\mathbb{A}_\pm$ as $z \quad \pm \quad$, which is a direct consequence of the exponential convergence of the waves to their steady states. Well, from the results in Lemma 2.7 we are able to obtain the exponential decay estimates

$$\|\mathbb{A}(z) - \mathbb{A}_\pm\| \le Ce^{-2\alpha_m z}, \quad \text{for} \quad z \quad \pm \quad , \tag{5.8}$$

with $\alpha_m = \alpha_{r,l}$ at $\pm \quad$.

This makes it possible to use the Gap Lemma [61] to establish a relation between the solutions of (5.7) and the solutions of the constant coefficient systems

$$\mathbf{Z}_z = \mathbb{A}_\pm \mathbf{Z}. \tag{5.9}$$

The idea consists in using such relation to deduce that the limit of $\bar{q}^+_{q_l^+}$ as $z \quad \pm \quad$ must be nonzero.

The eigenvalues of $\mathbb{A}_\pm$ and their respective associated eigenvectors are

$$\nu_1^\pm = 0, \qquad \nu_2^\pm = -2\alpha_m,$$
$$v_1^\pm = \begin{pmatrix} 0 \\ 1 \end{pmatrix}, \qquad v_2^\pm = \begin{matrix} 1 \\ -\frac{2\kappa q_m^+(1-q_m^+)}{s\nu_2^\pm} \end{matrix}.$$

Then the solutions of (5.9) are given by

$$\mathbf{Z}_j^{\pm} = v_j^{\pm} e^{\nu_j^{\pm} z}, \quad j = 1, 2.$$

We now apply the Gap Lemma [61], according to which the existence of the uniform decay rates (5.8) implies that the system (5.5) has a set of solutions $\mathbf{W}_j^{\pm}(z)$, $j = 1, 2$, satisfying

$$\begin{aligned}
\mathbf{W}_j^{-}(z) &= \left(v_j^{-} + \mathcal{O}\left(e^{-\alpha\, x} \, \left| v_j^{-} \right| \right) \right) e^{\nu_j^{-} z}, \quad (j = 1, 2) \quad z < 0, \\
\mathbf{W}_j^{+}(z) &= \left(v_j^{+} + \mathcal{O}\left(e^{-\alpha\, x} \, \left| v_j^{+} \right| \right) \right) e^{\nu_j^{+} z}, \quad (j = 1, 2) \quad z > 0,
\end{aligned}$$

for all $\alpha < -2\alpha_l, 2\alpha_r$.

In other words, the Gap Lemma says that there exist solutions $\mathbf{W}_j^{\pm}(z)$, $j = 1, 2$, with the asymptotic limits

$$\lim_{z \ \pm} \ \mathbf{W}_1^{\pm}(z) = (0, 1)^t \quad \text{and} \quad \lim_{z \ \pm} \ \mathbf{W}_2^{\pm}(z) = (0, 0)^t. \tag{5.10}$$

Since $\bar{p}_z, \bar{q}_z^{+}$ 0 as z $\pm$, we can conclude that $(\bar{p}_z, \bar{q}_z^{+})^t$ in $z > 0$ is spanned by $\mathbf{W}_2^{+}(z)$ and is spanned by $\mathbf{W}_2^{-}(z)$ in $z < 0$. Thus, $(\bar{p}_z, \bar{q}_z^{+})^t = \alpha_0 \mathbf{W}_2^{+}(z) = \beta_0 \mathbf{W}_2^{-}(z)$ for some nonzero constants α_0, β_0 $\mathbb{C}$

For its part, $(\bar{p}_{q_l^{+}}, \bar{q}_{q_l^{+}}^{+})^t$ is spanned by $\left\{ \mathbf{W}_1^{+}(z), \mathbf{W}_2^{+}(z) \right\}$ in $z > 0$, meanwhile it is spanned by $\left\{ \mathbf{W}_1^{-}(z), \mathbf{W}_2^{-}(z) \right\}$ in $z < 0$. Then

$$(\bar{p}_{q_l^{+}}, \bar{q}_{q_l^{+}}^{+})^t = \begin{array}{ll} \alpha_0^{-} \mathbf{W}_1^{-}(z) + \beta_0^{-} \mathbf{W}_2^{-}(z), & \text{for } z < 0, \\ \alpha_0^{+} \mathbf{W}_1^{+}(z) + \beta_0^{+} \mathbf{W}_2^{+}(z), & \text{for } z > 0, \end{array} \tag{5.11}$$

for nonzero $\alpha_0^{\pm}$ $\mathbb{C}$ and some $\beta_0^{\pm}$ $\mathbb{C}$. From this and (5.10) we have that

$$\lim_{z \ \pm} \ (\bar{p}_{q_l^{+}}, \bar{q}_{q_l^{+}}^{+})^t = \alpha_0^{\pm} (0, 1)^t, \quad \alpha_0^{\pm} = 0.$$

Thus $(\bar{p}_{q_l^{+}}, \bar{j}_{q_l^{+}}, \bar{q}_{q_l^{+}}^{+})$ / $H^1(\mathbb{R}, \mathbb{C}^3)$ and consequently $(\bar{p}_z, \bar{j}_z, \bar{q}_z^{+})$ is the only eigenfunction associated to $\lambda = 0$. This proves Lemma 5.1. □

5.3

The Unstable Spectrum

Definition 5.2. Let c $(0, s)$ be fixed. A traveling wave solution $(\bar{p}(z), \bar{j}(z), \bar{q}^{+}(z))$ of system (1.4) is *spectrally stable* if no element of the spectrum of $\mathcal{L}^c$ has strictly positive real part; that is

$$\sigma(\mathcal{L}^c) \setminus \quad \lambda \quad \mathbb{C} \quad \Re e \lambda \geq 0 \quad = \quad 0 \quad .$$

Otherwise, we say that the traveling wave is *spectrally unstable*.

Traveling wave profiles have quite different spectral features from those of standing waves. Our assertion follow from the result in Lemma 5.1 about the dimension one of the eigenspace associated to the zero eigenvalue, and mainly from the spectral instability stated in the next theorem.

Theorem 5.3. *For each fixed c satisfying* $0 < c < s$*, the corresponding family of traveling waves is spectrally unstable, that is,* $\sigma(\mathcal{L}^c) \setminus \quad \lambda \quad \mathbb{C} \quad 0 \quad \Re e\,\lambda \geq 0 \quad = \quad .$

In order to prove the theorem we shall show that the essential spectrum touches the closed right-half complex plane.

5.3.1

The unstable essential spectrum

As we did in Chapter 4 we recast (5.3) as a first order ODE system

$$\mathbf{Y}_z = \mathbf{A}(z,\lambda)\mathbf{Y}, \tag{5.12}$$

with $\mathbf{Y} = (p, j, q^+)^t$ and

$$\mathbf{A}(z,\lambda) = \begin{matrix} \frac{1}{c^2-s^2}\left(-\mu s\left(2\bar{q}^+ - 1\right) + c\lambda\right) & \frac{1}{c^2-s^2}\left(\mu+\lambda\right) & -\frac{2\mu s\bar{p}}{c^2-s^2} \\ \frac{1}{c^2-s^2}\left(-c\mu s\left(2\bar{q}^+ - 1\right) + s^2\lambda\right) & \frac{c}{c^2-s^2}\left(\mu+\lambda\right) & -\frac{2c\mu s\bar{p}}{c^2-s^2} \\ 0 & -\frac{2\kappa\bar{q}^+\left(1-\bar{q}^+\right)}{cs} & -\frac{2\kappa\bar{j}\left(1-2\bar{q}^+\right)}{cs} + \frac{\lambda}{c} \end{matrix}, \quad 0 < c < s, \tag{5.13}$$

and consider the family of linear, closed and densely defined operators

$$\begin{matrix} \mathcal{T}^c(\lambda) : H^1(\mathbb{R};\mathbb{C}^3) & L^2(\mathbb{R};\mathbb{C}^3), \\ \mathbf{Y} & \mathbf{Y}_z - \mathbf{A}(z,\lambda)\mathbf{Y}, \quad \lambda \quad \mathbb{C}. \end{matrix}$$

As $z \quad + \quad$ in (5.12) we obtain the constant-coefficient limiting system

$$\mathbf{Y}_z = \mathbf{A}_\pm(\lambda)\mathbf{Y}, \tag{5.14}$$

where

$$\mathbf{A}_\pm(\lambda) := \lim_{z \atop \pm} \mathbf{A}(z,\lambda).$$

These asymptotic matrices are

$$\mathbf{A}_\pm(\lambda) = \begin{matrix} (-\mu s(2q_m^+ - 1) + c\lambda)/(c^2 - s^2) & (\mu+\lambda)/(c^2-s^2) & 0 \\ (-c\mu s(2q_m^+ - 1) + s^2\lambda)/(c^2-s^2) & c\,(\mu+\lambda)/(c^2-s^2) & 0 \\ 0 & -2\kappa q_m^+(1-q_m^+)/cs & \lambda/c \end{matrix},$$

with $q_m^+ = q_{r,l}^+$ at $z = \pm$, respectively.

Let $\mathbb{C}^+$ denote the open right-half complex plane $\lambda \in \mathbb{C}$ $\Re e\lambda > 0$, and let $\mathbb{E}_\pm^s(\lambda)$ and $\mathbb{E}_\pm^u(\lambda)$ denote the stable and unstable eigenspaces of $\mathbf{A}_\pm(\lambda)$, respectively. In order to determine the location of the essential spectrum we begin with the following lemma.

Lemma 5.4. *For all* $\lambda \in \mathbb{C}^+$*, the asymptotic matrices* $\mathbf{A}_\pm(\lambda)$ *are hyperbolic and* $\dim[\mathbb{E}_\pm^s(\lambda)] = 1$ *and* $\dim[\mathbb{E}_\pm^u(\lambda)] = 2$.

Proof. We start by proving that the matrices $\mathbf{A}_\pm(\lambda)$ have purely imaginary eigenvalues only if $\lambda \in \mathbb{C} \setminus \mathbb{C}^+$.

If ai, with $a \in \mathbb{R}$, is an eigenvalue of $\mathbf{A}_\pm(\lambda)$, it solves the equation

$$\det\left(\mathbf{A}_\pm(\lambda) - aiI\right) = 0.$$

It is straightforward to compute that the characteristic equation is

$$\left(\frac{\lambda}{c} - ai\right)\left(\lambda^2 + B(a)\lambda + C(b)\right) = 0, \tag{5.15}$$

where

$$B(a) = \mu - 2aci, \quad C(a) = a^2\left(s^2 - c^2\right) + a\mu\left(2sq_m^+ - (c+s)\right)i,$$

with $q_m^+ = q_{r,l}^+$ at $z = \pm$, respectively.

Equation (5.15) has three roots

$$\lambda_1(a) = aci \quad \text{and} \quad \lambda_{2,3}(a) = \frac{-B(a) \pm \sqrt{D(a)}}{2},$$

where

$$D(a) = B^2(a) - 4C(a) = \mu^2 - 4a^2s^2 - 4a\mu s(2q_m^+ - 1)i.$$

It is clear that $\Re e\lambda_1(a) = 0$ for all $a \in \mathbb{R}$. This shows that $\mathbf{A}_\pm(\lambda)$ are nonhyperbolic matrices when λ is an element of the imaginary axis.

Now, taking the real part of $\lambda_{2,3}(a)$ yields

$$\Re e\,\lambda_{2,3}(a) = \left(-\Re eB(a) \pm \Re e\sqrt{D(a)}\right)/2.$$

Since $\Re eB(a) > 0$, then clearly $\Re e\lambda_3(a) < 0$ for all $a \in \mathbb{R}$. On the other hand, we observe that $\Re e\lambda_2(a) \leq 0$ if and only if

$$(\Re eB(a))^2 \geq \left(\Re e\sqrt{D(a)}\right)^2 = \frac{1}{2}\left(\Re eD(a) + \sqrt{(\Re eD(a))^2 + (\Im mD(a))^2}\right).$$

It is not hard to see the above inequality is satisfied if and only if

$$(\Im mD(a))^2 + 4(\Re eB(a))^2\,\Re eD(a) - 4(\Re eB(a))^4 \leq 0. \tag{5.16}$$

One can get that

$$(\mathfrak{I}m\,D\,(a))^2+4\,(\mathfrak{R}e\,B\,(a))^2\,\mathfrak{R}e\,D\,(a)-4\,(\mathfrak{R}e\,B\,(a))^4$$
$$=(4a\mu s(2q_m^+-1))^2+4\mu^2\left(\mu^2-4a^2s^2\right)-4\mu^4=-64a^2\mu^2s^2q_m^+(1-q_m^+),$$

since $0<q_m^+<1$, it follows that inequality (5.16) is true for all a $\mathbb{R}$, which implies that $\mathfrak{R}e\,\lambda_2(a)\leq 0$ for all a $\mathbb{R}$. This, together with the fact that $\mathfrak{R}e\,\lambda_1(a)=0$ for all a $\mathbb{R}$, lead us to conclude that whenever the asymptotic matrices $\mathbf{A}_\pm(\lambda)$ are nonhyperbolic, it holds that λ belongs to the closed left-half complex plane. Therefore the matrices $\mathbf{A}_\pm(\lambda)$ are hyperbolic in $\mathbb{C}^+$.

The next concern is to calculate $\dim[\mathbb{E}^s_\pm(\lambda)]$ and $\dim[\mathbb{E}^u_\pm(\lambda)]$ in $\mathbb{C}^+$, for this purpose we find the eigenvalues of $\mathbf{A}_\pm(\lambda)$, which turn out to be

$$\eta_1^\pm(\lambda)=\frac{\lambda}{c},$$
$$\eta_{2,3}^\pm(\lambda)=\frac{c(\mu+2\lambda)-\mu s(2q_m^+-1)\pm\sqrt{(c(\mu+2\lambda)-\mu s(2q_m^+-1))^2+4(s^2-c^2)\lambda(\mu+\lambda)}}{2(c^2-s^2)}.$$

Clearly $\mathfrak{R}e\,\eta_1^\pm(\lambda)>0$ for all λ $\mathbb{C}^+$. Set now $\lambda=\beta$ $\mathbb{R}^+=(0,+\ )$, we have that $\eta_2^\pm(\beta)<0$ and $\eta_3^\pm(\beta)>0$, because $c<s$. Since $\eta_{2,3}^\pm(\lambda)$ are continuous functions and $\mathbb{C}^+$ is connected, their real part does not change sign on $\mathbb{C}^+$, and consequently $\mathfrak{R}e\,\eta_2^\pm(\lambda)<0$ and $\mathfrak{R}e\,\eta_3^\pm(\lambda)>0$ for all λ $\mathbb{C}^+$. Hence, $\dim[\mathbb{E}^s_\pm(\lambda)]=1$ and $\dim[\mathbb{E}^u_\pm(\lambda)]=2$ for all λ $\mathbb{C}^+$. □

Lemma 5.5. *The essential spectrum is a subset of the left-half complex plane and contains the imaginary axis.*

Proof. Let λ $\mathbb{C}^+$, from Lemma 5.4 we know that $\mathbf{A}_+(\lambda)$ and $\mathbf{A}_-(\lambda)$ are hyperbolic matrices, which, by Theorem 3.3 in [52] implies that equation (5.12) has exponential dichotomies in $\mathbb{R}^+$ and $\mathbb{R}^-$ with Morse indices $i_+(\lambda)=\dim[\mathbb{E}^u_+(\lambda)]=2$ and $i_-(\lambda)=\dim[\mathbb{E}^u_-(\lambda)]=2$, respectively. Hence, as a consequence of Lemma 4.2 in [43], this signifies that $\mathcal{T}^c(\lambda)$ is Fredholm with index zero, given by

$$\operatorname{ind}\mathcal{T}^c(\lambda)=i_-(\lambda)-i_+(\lambda)=0.$$

Therefore, according to the definition of essential spectrum we have that the essential spectrum lies outside $\mathbb{C}^+$, that is, $\sigma_{\text{ess}}(\mathcal{T}^c)\subset\mathbb{C}$ $\mathbb{C}^+$.

From the proof of Lemma 5.4 we have that $\mathbf{A}_\pm(\lambda)$ are nonhyperbolic for all λ $i\mathbb{R}$, thus, in view of Theorem 3.3 in [52], the equation (5.12) has no exponetial dichotomies nethier on $\mathbb{R}^+$ nor $\mathbb{R}^-$. Thus, due to Palmer's Theorem [44], $\mathcal{T}^c(\lambda)$ is not Fredholm, which lead us to conclude that $i\mathbb{R}\subset\sigma_{\text{ess}}(\mathcal{T}^c)$. □

Corollary 5.6. *The eigenvalue $\lambda=0$ is embedded in the essential spectrum.*

Despite the result in Theorem 5.3, there is still the possibility of achieving spectral stability; our hope is to find a suitable weighted space in which the essential spectrum can be shifted to the left, so that none of the elements of the imaginary axis belongs to the essential spectrum. It should be emphasized, however, that the existence of such space does not assure spectral stability because we do not know the location of the point spectrum.

5.4

The Impossible Weighted Space

To stabilize the essential spectrum it seems natural to work on the weighted Sobolev space

$$H^1_w(\mathbb{R};\mathbb{C}^3) = \left\{(p,j,q^+) \;\; w(\partial_z^i p, \partial_z^i j, \partial_z^i q^+) \quad L^2(\mathbb{R};\mathbb{C}^3) \text{ for } i=0,1\right\}, \tag{5.17}$$

where the weight function w satisfies

$$\frac{w_z}{w}(+\quad) = w_+ \quad \text{and} \quad \frac{w_z}{w}(-\quad) = w_-, \quad w_\pm \quad \mathbb{R}.$$

The technique consists of choosing a suitable positive weight function w so that the essential spectrum can be shifted to the left. Unfortunately, in regard to our problem, this is not possible. It will be shown below that the existence of such function is impossible. However, the possibilities do not end here, in the subsequent section, Section 5.5, we reach the desired stabilization when perturbations are constrained to belong to a weighted space $H^1_{w_\alpha}(\mathbb{R};\mathbb{C}^2) \times H^1_{w_\varepsilon}(\mathbb{R};\mathbb{C})$, for suitable choices of w_α and w_ε.

To prove the impossibility of existence of the space (5.17) we proceed as follows. Suppose that $(p,j,q^+) \quad H^1_w(\mathbb{R};\mathbb{C}^3)$ for some weight function w, then there exists a vector function $(\tilde{p},\tilde{j},\tilde{q}^+) \quad H^1(\mathbb{R};\mathbb{C}^3)$ such that $(p,j,q^+) = w^{-1}(\tilde{p},\tilde{j},\tilde{q}^+)$ (see the Appendix). Upon substituting the latter into (5.3), we reach the eigenvalue problem

$$\begin{aligned}
\lambda\tilde{p} &= \tilde{p}_z - c\tilde{p}\frac{w_z}{w} - \tilde{j}_z + \tilde{j}\frac{w_z}{w},\\
\lambda\tilde{j} &= -s^2\tilde{p}_z + s^2\tilde{p}\frac{w_z}{w} + c\tilde{j}_z - c\tilde{j}\frac{w_z}{w} - \mu\tilde{j} + \mu s\left[\left(2\bar{q}^+ - 1\right)\tilde{p} + 2\bar{p}\tilde{q}^+\right],\\
\lambda\tilde{q}^+ &= c\tilde{q}^+_z - c\tilde{q}^+\frac{w_z}{w} + \frac{2\kappa}{s}\left[\bar{q}^+\left(1-\bar{q}^+\right)\tilde{j} + \bar{j}\left(1-2\bar{q}^+\right)\tilde{q}^+\right].
\end{aligned} \tag{5.18}$$

For notational convenience, the superscript tilde notation will be omitted on $\tilde{p}$, $\tilde{j}$ and $\tilde{q}^+$.

We recast (5.18) as the first order system

$$\mathbf{Y}_z = \mathbf{A}^w(z,\lambda)\mathbf{Y},$$

where $\mathbf{Y} = (p,j,q^+)^t$ and

$$\mathbf{A}^w(z,\lambda) = \begin{pmatrix}
\frac{w_z}{w} + \frac{1}{c^2-s^2}\left(-\mu s\left(2\bar{q}^+ - 1\right) + c\lambda\right) & \frac{1}{c^2-s^2}\left(\mu+\lambda\right) & -\frac{2\mu s\bar{p}}{c^2-s^2}\\
\frac{1}{c^2-s^2}\left(-c\mu s\left(2\bar{q}^+ - 1\right) + s^2\lambda\right) & \frac{w_z}{w} + \frac{c}{c^2-s^2}\left(\mu+\lambda\right) & -\frac{2c\mu s\bar{p}}{c^2-s^2}\\
0 & -\frac{2\kappa\bar{q}^+\left(1-\bar{q}^+\right)}{cs} & \frac{w_z}{w} - \frac{2\kappa\bar{j}\left(1-2\bar{q}^+\right)}{cs} + \frac{\lambda}{c}
\end{pmatrix}.$$

The asymptotic matrices are given by

$$\mathbf{A}_{\pm}^{w}(\lambda) = \begin{matrix} w_{\pm} + \frac{1}{c^2-s^2}\left(-\mu s\left(2q_m^+ - 1\right) + c\lambda\right) & \frac{1}{c^2-s^2}\left(\mu + \lambda\right) & 0 \\ \frac{1}{c^2-s^2}\left(-c\mu s\left(2q_m^+ - 1\right) + s^2\lambda\right) & w_{\pm} + \frac{c}{c^2-s^2}\left(\mu + \lambda\right) & 0 \\ 0 & -\frac{2\kappa q_m^+\left(1-q_m^+\right)}{cs} & w_{\pm} + \frac{\lambda}{c} \end{matrix},$$

with $q_m^+ = q_{r,l}^+$ at $\pm$, respectively.

We find that λ is a root of the characteristic polynomial

$$\det\left(\mathbf{A}_{\pm}^{w}(\lambda) - aiI\right), \quad a \quad \mathbb{R},$$

if and only if

$$\left(\frac{\lambda}{c} + w_{\pm} - ai\right)\left(\lambda^2 + B(a)\lambda + C(a)\right) = 0,$$

where

$$B(a) = \mu + 2c(w_{\pm} - ai)$$

and

$$C(a) = -w_{\pm}\mu(2sq_m^+ - (s+c)) + (c^2-s^2)(w_{\pm}^2 - a^2) + (\mu(2sq_m^+ - (s+c)) - 2w_{\pm}(c^2-s^2))ai.$$

As before, the characteristic equation has three roots

$$\lambda_1(a) = -w_{\pm}c + aci \quad \text{and} \quad \lambda_{2,3}(a) = \frac{-B(a) \pm \quad \overline{D(a)}}{2},$$

where $D(a) = B^2(a) - 4C(a)$.

Notice that, in order to shift the essential spectrum to the left, it is necessary that $w_{\pm} > 0$ and $\Re e\lambda_{2,3}(a) < 0$ for all $a \quad \mathbb{R}$. Upon assuming the former, we have that $\Re e\lambda_{2,3}(a) < 0$ if and only if

$$\left(\Im m D(a)\right)^2 + 4\left(\Re e B(a)\right)^2 \Re e D(a) - 4\left(\Re e B(a)\right)^4 < 0, \qquad a \quad \mathbb{R}. \tag{5.19}$$

One can derive that $\Im m D(a) = -4as(\mu(2q_m^+ - 1) + 2sw_{\pm})$. By plugging this, together with $\Re e D(a) = \left(\Re e B(a)\right)^2 - \left(\Im m B(a)\right)^2 - 4\Re e C(a)$, into (5.19), we find that

$$\begin{aligned} &\left(\Im m D(a)\right)^2 - 4\left(\Re e B(a)\right)^2\left(\left(\Im m B(a)\right)^2 + 4\Re e C(a)\right) \\ &\qquad = 16a^2s^2(\mu(2q_m^+ - 1) + 2sw_{\pm})^2 \\ &\qquad - 4(\mu + 2cw_{\pm})^2(4a^2c^2 + 4(-w_{\pm}\mu(2sq_m^+ - (s+c)) + (c^2-s^2)(w_{\pm}^2 - a^2))) \\ &\qquad = 16a^2s^2((\mu(2q_m^+ - 1) + 2sw_{\pm})^2 - (\mu + 2cw_{\pm})^2) \\ &\qquad\qquad + 16w_{\pm}(\mu + 2cw_{\pm})^2(\mu(2sq_m^+ - (s+c)) + w_{\pm}(s^2 - c^2)). \end{aligned}$$

We observe that this quantity is negative for all $a \quad \mathbb{R}$ if and only if

$$(\mu(2q_m^+ - 1) + 2sw_{\pm})^2 - (\mu + 2cw_{\pm})^2 < 0 \quad \text{and} \quad \mu(2sq_m^+ - (s+c)) + w_{\pm}(s^2 - c^2) < 0. \tag{5.20}$$

Now, see that the second inequality in (5.20) follows if and only if

$$w_{\pm}(s^2 - c^2) < -\mu(2sq_m^+ - (s+c)).$$

In the case $q_m^+ = q_l^+$ we have that $2sq_l^+ - (s+c) > 0$, since from Theorem 2.2 one has that $q_l^+ > (c+s)/2s$. Thus, it is impossible to satisfy the latter inequality since $w_-(s^2 - c^2)$ is positive and $-\mu(2sq_l^+ - (s+c))$ is negative. The previous analysis shows that the existence of the weighted space of the type of (5.17) is impossible.

5.5

An Appropriate Weighted Space

In this section we move the essential spectrum to the left of the imaginary axis. To resolve the issue that the essential spectrum reaches the imaginary axis, rather than taking perturbations in $H^1(\mathbb{R};\mathbb{C}^3)$ we restrict to perturbations that belong to the weighted space

$$\begin{aligned} &H^1_{w_\alpha}(\mathbb{R};\mathbb{C}^2) \times H^1_{w_\varepsilon}(\mathbb{R};\mathbb{C}) \\ &\qquad = \left\{(p,j,q^+) \;\; w_\alpha(\partial_z^i p, \partial_z^i j) \quad L^2(\mathbb{R};\mathbb{C}^2) \text{ and } w_\varepsilon \partial_z^i q^+ \quad L^2(\mathbb{R};\mathbb{C}) \text{ for } i = 0,1\right\}; \end{aligned}$$

where the weight functions are $w_\alpha(z) = e^{\alpha_l z} + e^{\alpha_r z}$ and $w_\varepsilon(z) = e^{-\alpha_l \varepsilon z}$, with $\varepsilon > 0$ small.

Recall that

$$\alpha_l = \frac{(c+s-2sq_l^+)\mu}{2(s^2-c^2)} < 0 \quad \text{and} \quad \alpha_r = \frac{(c+s-2sq_r^+)\mu}{2(s^2-c^2)} > 0.$$

Let $(p,j,q^+) \quad H^1_{w_\alpha}(\mathbb{R};\mathbb{C}^2) \times H^1_{w_\varepsilon}(\mathbb{R};\mathbb{C})$, since w_α/w_α and $w_\varepsilon/w_\varepsilon$ tend to a finite limit as $z \quad \pm \quad$, it turns out that $(p,j,q^+) = (w_\alpha^{-1}\tilde{p}, w_\alpha^{-1}\tilde{j}, w_\varepsilon^{-1}\tilde{q}^+)$ for $(\tilde{p},\tilde{j},\tilde{q}^+) \quad H^1(\mathbb{R};\mathbb{C}^3)$ (see the Appendix).

In the variables $\tilde{p}$, $\tilde{j}$ and $\tilde{q}^+$, the spectral problem (5.3) becomes

$$\begin{aligned} \lambda\tilde{p} &= c\tilde{p}_z - c\tilde{p}\frac{w_\alpha}{w_\alpha} - \tilde{j}_z + \tilde{j}\frac{w_\alpha}{w_\alpha}, \\ \lambda\tilde{j} &= -s^2\tilde{p}_z + s^2\tilde{p}\frac{w_\alpha}{w_\alpha} + c\tilde{j}_z - c\tilde{j}\frac{w_\alpha}{w_\alpha} - \mu\tilde{j} + \mu s\left[\left(2\bar{q}^+ - 1\right)\tilde{p} + 2\bar{p}\tilde{q}^+\frac{w_\alpha}{w_\varepsilon}\right], \\ \lambda\tilde{q}^+ &= c\tilde{q}_z^+ + c\alpha_l\varepsilon\tilde{q}^+ + \frac{2\kappa}{s}\left[\bar{q}^+\left(1-\bar{q}^+\right)\tilde{j}\frac{w_\varepsilon}{w_\alpha} + \bar{j}\left(1-2\bar{q}^+\right)\tilde{q}^+\right]. \end{aligned} \tag{5.21}$$

We drop the tilde notation and rewrite system (5.21) as

$$\mathbf{Y}_z = \mathbf{A}^{\alpha,\varepsilon}(z,\lambda)\mathbf{Y},$$

where $\mathbf{Y} = (p, j, q^+)^t$ and

$$\mathbf{A}^{\alpha,\varepsilon}(z,\lambda) = \begin{matrix} \frac{w_\alpha}{w_\alpha} + \frac{1}{c^2-s^2}\left(-\mu s\left(2\bar{q}^+ - 1\right) + c\lambda\right) & \frac{1}{c^2-s^2}\left(\mu + \lambda\right) & -\frac{2\mu s\bar{p} w_\alpha}{(c^2-s^2)w_\varepsilon} \\ \frac{1}{c^2-s^2}\left(-c\mu s\left(2\bar{q}^+ - 1\right) + s^2\lambda\right) & \frac{w_\alpha}{w_\alpha} + \frac{c}{c^2-s^2}\left(\mu + \lambda\right) & -\frac{2c\mu s\bar{p} w_\alpha}{(c^2-s^2)w_\varepsilon} \\ 0 & -\frac{2\kappa\bar{q}^+\left(1-\bar{q}^+\right)w_\varepsilon}{csw_\alpha} & \frac{w_\varepsilon}{w_\varepsilon} - \frac{2\kappa\bar{j}\left(1-2\bar{q}^+\right)}{cs} + \frac{\lambda}{c} \end{matrix}.$$

To calculate the limit of $\mathbf{A}^{\alpha,\varepsilon}(z,\lambda)$ as $z \quad \pm \quad$, we will first show that

$$\lim_{z \ \pm} \frac{w_\alpha}{w_\varepsilon}\bar{p} = 0 \quad \text{and} \quad \lim_{z \ \pm} \frac{w_\varepsilon}{w_\alpha} = 0. \tag{5.22}$$

In fact, by Lemma 2.7 we have that

$$\bar{p} = \mathcal{O}(e^{-2\alpha_l z}), \quad z < 0, \quad \text{and} \quad \bar{p} = \mathcal{O}(e^{-2\alpha_r z}), \quad z > 0.$$

We therefore obtain

$$\frac{w_\alpha}{w_\varepsilon}\bar{p} = \begin{matrix} \mathcal{O}(e^{-\alpha_l(1-\varepsilon)z} + e^{(-2\alpha_l(1-\varepsilon/2)+\alpha_r)z}), & z < 0, \\ \mathcal{O}(e^{(\alpha_l(1+\varepsilon)-2\alpha_r)z} + e^{(\alpha_l\varepsilon-\alpha_r)z}), & z > 0. \end{matrix}$$

Hence, the first limit in (5.22) is true, because $-\alpha_l > 0$, $-\alpha_r < 0$ and ε is a small positive number.

Finally, through a direct computation we have

$$\frac{w_\varepsilon}{w_\alpha} = \frac{1}{e^{\alpha_l(1+\varepsilon)z} + e^{(\alpha_r+\alpha_l\varepsilon)z}}.$$

The second limit in (5.22) holds since $\alpha_r + \alpha_l\varepsilon > 0$ if ε is chosen small enough.

In view of (5.22), when $z \quad \pm \quad$, $\mathbf{A}^{\alpha,\varepsilon}(z,\lambda)$ approaches to

$$\mathbf{A}^{\alpha,\varepsilon}_{\pm}(\lambda) = \begin{matrix} \alpha_m + \frac{1}{c^2-s^2}\left(-\mu s\left(2q^+_m - 1\right) + c\lambda\right) & \frac{1}{c^2-s^2}\left(\mu + \lambda\right) & 0 \\ \frac{1}{c^2-s^2}\left(-c\mu s\left(2q^+_m - 1\right) + s^2\lambda\right) & \alpha_m + \frac{c}{c^2-s^2}\left(\mu + \lambda\right) & 0 \\ 0 & 0 & -\alpha_l\varepsilon + \frac{\lambda}{c} \end{matrix},$$

where $\alpha_m = \alpha_{r,l}$ at $\pm \quad$, respectively.

The λ-roots of the characteristic polynomial

$$\det\left(\mathbf{A}^{\alpha,\varepsilon}_{\pm}(\lambda) - aiI\right), \quad a \quad \mathbb{R}, \tag{5.23}$$

satisfy

$$\left(\frac{\lambda}{c} - \alpha_l\varepsilon - ai\right)\left(\lambda^2 + B(a)\lambda + C(a)\right) = 0,$$

where $B(a) = \mu + 2c\alpha_m - 2aci$ and $C(a) = (s^2 - c^2)(\alpha_m^2 + a^2)$.

Such roots are

$$\lambda_1(a) = \alpha_l \varepsilon c + aci \quad \text{and} \quad \lambda_{2,3}(a) = \frac{-B\,(a) \pm \quad \overline{D\,(a)}}{2},$$

where

$$D(a) = B^2\,(a) - 4C\,(a) = (\mu + 2c\alpha_m)^2 - 4\alpha_m^2(s^2 - c^2) - 4a^2s^2 - 4ac(\mu + 2c\alpha_m)i.$$

Notice that $\Re e\,\lambda_1(a)$ is negative for all $a \quad \mathbb{R}$. Our concern is now to ensure that, for all $a \quad \mathbb{R}$, $\Re e\,\lambda_{2,3}(a)$ is negative as well. To this end, we begin by asserting that $\Re e B(a) = \mu + 2c\alpha_m$ is positive. For $\alpha_m = \alpha_r$ this is obvious, since $\alpha_r > 0$. Regarding $\alpha_m = \alpha_l$, from the facts that $c < s$ and $q_l^+ < 1$, there holds

$$\mu + 2c\alpha_l = \mu + \frac{c(c + s - 2sq_l^+)\mu}{s^2 - c^2} > \mu + \frac{c(c + s - 2s)\mu}{s^2 - c^2} = \mu - \frac{c\mu}{s + c} > \mu - \frac{c\mu}{2c} = \frac{\mu}{2} > 0.$$

Thanks to the positivity of $\Re e B(a)$ we have that

$$\Re e\,\lambda_3(a) \leq \Re e\,\lambda_2(a), \qquad a \quad \mathbb{R}.$$

Thus, it all reduces to show that $\Re e\,\lambda_2(a) < 0$ for all $a \quad \mathbb{R}$. The real part of $\lambda_2(a)$ is determined by

$$\Re e\,\lambda_2(a) = \frac{1}{2} \quad -\Re e B(a) + \frac{1}{\overline{2}} \quad \overline{\Re e D(a) + \quad \overline{(\Re e D(a))^2 + (\Im m D(a))^2}} \quad . \tag{5.24}$$

In what follows, we first prove that the quantity $\Re e D(a) + 4a^2s^2 = (\mu + 2c\mu\alpha_m)^2 - 4\alpha_m^2(s^2 - c^2)$ is positive. Secondly, from this fact we check that the inequality

$$\overline{(\Re e D(a))^2 + (\Im m D(a))^2} \leq \Re e D(a) + 8a^2s^2, \qquad a \quad \mathbb{R}, \tag{5.25}$$

holds true.

To show that $(\mu + 2c\alpha_m)^2 - 4\alpha_m^2(s^2 - c^2)$ is positive, we write

$$(\mu + 2c\alpha_m)^2 - 4\alpha_m^2(s^2 - c^2) = \left(\mu + 2c\alpha_m - 2\alpha_m \quad \overline{s^2 - c^2}\right)\left(\mu + 2c\alpha_m + 2\alpha_m \quad \overline{s^2 - c^2}\right).$$

In turns out that the factors are both positive. Certainly, in the case $\alpha_m = \alpha_l$, the first factor is posivitive because $\mu + 2c\alpha_l > 0$ and $-\alpha_l > 0$. Concerning the second factor, it can be seen that

$$\begin{aligned} \mu + 2c\alpha_l + 2\alpha_l \quad \overline{s^2 - c^2} &> \mu + 2c\alpha_l + 2\alpha_l s \\ &= \mu + 2\alpha_l(s + c) = \mu + \frac{(c + s - 2sq_l^+)\mu}{s - c} \\ &> \mu + \frac{(c + s - 2s)\mu}{s - c} = \mu - \frac{(s - c)\mu}{s - c} = 0. \end{aligned} \tag{5.26}$$

When $\alpha_m = \alpha_r$, the second factor is the sum of positive numbers. As regards the first factor, we derive

$$\begin{aligned}\mu + 2c\alpha_r - 2\alpha_r \quad \overline{s^2 - c^2} &> \mu + 2c\alpha_r - 2\alpha_r s \\ &= \mu - 2\alpha_r(s-c) = \mu - \frac{(c + s - 2sq_r^+)\mu}{s+c} \\ &> \mu + \frac{2s\mu q_r^+}{s+c} - \mu = \frac{2s\mu q_r^+}{s+c} > 0.\end{aligned} \tag{5.27}$$

We now proceed to verify (5.25). The inequality is true if and only if

$$\begin{aligned}(\Re e\, D(a))^2 + (\Im m\, D(a))^2 \le \left(\Re e\, D(a) + 8a^2 s^2\right)^2, \\ (\Im m\, D(a))^2 - 16a^2 s^2 \Re e\, D(a) - 64 a^4 s^4 \le 0, \qquad a \quad \mathbb{R}.\end{aligned} \tag{5.28}$$

Substitution of $\Re e\, D(a)$ and $\Im m\, D(a)$ yields, after a straightforward calculation,

$$(\Im m\, D(a))^2 - 16a^2 s^2 \Re e\, D(a) - 64 a^4 s^4 = -16a^2(s^2 - c^2)\left((\mu + 2c\alpha_m)^2 - 4s^2\alpha_m^2\right).$$

Inequality (5.28) will follow as soon as we establish that $(\mu + 2c\alpha_m)^2 - 4s^2\alpha_m^2 > 0$. This can be factored as

$$(\mu + 2\alpha_m(s+c))(\mu - 2\alpha_m(s-c)).$$

For $\alpha_m = \alpha_r$ the first factor is positive, and for $\alpha_m = \alpha_l$ the second factor is positive too. That $\mu + 2\alpha_l(s+c)$ and $\mu - 2\alpha_r(s-c)$ are positive has already been proved in (5.26) and (5.27), respectively. Then inequality (5.28) is true, therefore so is inequality (5.25).

We will use (5.25) in order to find a negative upper bound for $\Re e\, \lambda_2(a)$. Applying this inequality in (5.24) we get

$$\begin{aligned}\Re e\, \lambda_2(a) &< \frac{1}{2}\left(-\Re e\, B(a) + \quad \overline{\Re e\, D(a) + 4a^2 s^2}\ \right) \\ &= \frac{1}{2}\left(-(\mu + 2c\mu\alpha_m) + \quad \overline{(\mu + 2c\mu\alpha_m)^2 - 4\alpha_m^2(s^2 - c^2)}\ \right), \qquad a \quad \mathbb{R}.\end{aligned}$$

The resulting bound is negative because $(\mu + 2c\mu\alpha_m)^2 - 4\alpha_m^2(s^2 - c^2) > 0$ is lower that $\mu + 2c\mu\alpha_m > 0$ for $\alpha_m = \alpha_{r,l}$. So we have that $\Re e\, \lambda_3(a) < \Re e\, \lambda_2(a) < 0$ for all $a \quad \mathbb{R}$. Finally, we can choose ε sufficiently small in such a way that $\alpha_l \varepsilon c$, the real part of $\lambda_1(a)$, is larger than

$$\frac{1}{2}\left(-(\mu + 2c\mu\alpha_m) + \quad \overline{(\mu + 2c\mu\alpha_m)^2 - 4\alpha_m^2(s^2 - c^2)}\ \right).$$

We denote by Ω the open connected region in $\mathbb{C}$ that is bounded on the left by $\lambda_1(a)$, namely

$$\Omega = \quad \lambda \quad \mathbb{C} \ \ \Re e\, \lambda > \alpha_l \varepsilon c \quad .$$

To summarize, we have found that the parameter λ belongs to the complement of Ω whenever the matrices $\mathbf{A}_{\pm}^{\alpha,\varepsilon}(\lambda)$ are nonhyperbolic. That shows the first statement of the following lemma.

Lemma 5.7. *Let λ be an element of Ω. Then, the asymptotic matrices $\mathbf{A}_{\pm}^{\alpha,\varepsilon}(\lambda)$ are hyperbolic. Furthermore, the stable and unstable eigenspaces $\mathbb{E}_{\pm}^{\alpha,s}(\lambda)$ and $\mathbb{E}_{\pm}^{\alpha,u}(\lambda)$ have dimension 1 and 2, respectively.*

Proof. To prove the second statement, we need to compute the eigenvalues of the matrices $\mathbf{A}_{\pm}^{\alpha,\varepsilon}(\lambda)$. A direct calculation yields

$$\eta_1^{\alpha,\pm}(\lambda) = -\alpha_l\varepsilon + \frac{\lambda}{c},$$
$$\eta_{2,3}^{\alpha,\pm}(\lambda) = -\frac{c\lambda}{s^2-c^2} \mp \sqrt{\left(\frac{c\lambda}{s^2-c^2}+\alpha_m\right)^2 + \frac{\lambda(\mu+\lambda)}{s^2-c^2}},$$

with $\alpha_m = \alpha_{r,l}$ at $\pm$.

Since $-\alpha_l > 0$, we have that $\mathfrak{Re}\eta_1^{\alpha,\pm}(\lambda) > 0$ for all λ Ω. Set now $\lambda = 0$ in (5.5), we get $\eta_{2,3}^{\alpha,-}(0) = \pm\alpha_l$ and $\eta_{2,3}^{\alpha,+}(0) = \mp\alpha_r$, thus we have that $\eta_2^{\alpha,\pm}(0) < 0$ and $\eta_3^{\alpha,\pm}(0) > 0$. Due to the fact that Ω is a connected set, this is enough to conclude that $\mathfrak{Re}\eta_2^{\alpha,\pm}(\lambda) < 0$ and $\mathfrak{Re}\eta_3^{\alpha,\pm}(\lambda) > 0$ for all λ Ω, so the proof of the lemma is complete. □

5.5.1

The stable essential spectrum

The question of finding the essential spectrum of the operator $\mathcal{L}^c$, restricted to the space $H^1_{w_\alpha}(\mathbb{R};\mathbb{C}^2)\times H^1_{w_\varepsilon}(\mathbb{R};\mathbb{C})$, corresponds to the problem of determining the essential spectrum of the operator

$$\begin{array}{lll} \mathcal{T}^c(\lambda) : H^1_{w_\alpha}(\mathbb{R};\mathbb{C}^2)\times H^1_{w_\varepsilon}(\mathbb{R};\mathbb{C}) & & L^2_{w_\alpha}(\mathbb{R};\mathbb{C}^2)\times L^2_{w_\varepsilon}(\mathbb{R};\mathbb{C}) \\ \mathbf{Y} & & \mathbf{Y}_z - \mathbf{A}(z,\lambda)\mathbf{Y}, \quad \lambda \quad \mathbb{C}. \end{array} \tag{5.29}$$

For our purpose of locating the region where the essential spectrum is contained, we consider the matrix

$$\mathbf{Q}(z) := \begin{array}{ccc} \frac{1}{w_\alpha} & 0 & 0 \\ 0 & \frac{1}{w_\alpha} & 0 \\ 0 & 0 & \frac{1}{w_\varepsilon} \end{array},$$

and define the family of operators

$$\begin{array}{lll} \mathcal{T}^\alpha(\lambda) : H^1(\mathbb{R};\mathbb{C}^3) & & L^2(\mathbb{R};\mathbb{C}^3) \\ \tilde{\mathbf{Y}} & & \tilde{\mathbf{Y}}_z - \mathbf{A}^{\alpha,\varepsilon}(z,\lambda)\tilde{\mathbf{Y}}, \quad \lambda \quad \mathbb{C}. \end{array} \tag{5.30}$$

For $\tilde{\mathbf{Y}}$ $H^1(\mathbb{R};\mathbb{C}^3)$ we substitute $\mathbf{Y} = \mathbf{Q}(z)\tilde{\mathbf{Y}}$ $H^1_{w_\alpha}(\mathbb{R};\mathbb{C}^2)\times H^1_{w_\varepsilon}(\mathbb{R};\mathbb{C})$ in (5.29) to find the relation:

$$\mathcal{T}^c(\lambda)\mathbf{Y} = \mathbf{Q}(z)\mathcal{T}^\alpha(\lambda)\tilde{\mathbf{Y}}, \qquad \tilde{\mathbf{Y}} = \mathbf{Q}^{-1}(z)\mathbf{Y} \quad H^1(\mathbb{R};\mathbb{C}^3). \tag{5.31}$$

Proposition 5.8. *The operator $\mathcal{T}^c(\lambda)$, restricted to the space $H^1_{w_\alpha}(\mathbb{R};\mathbb{C}^2)\times H^1_{w_\varepsilon}(\mathbb{R};\mathbb{C})$, is Fredholm if and only if $\mathcal{T}^\alpha(\lambda)$ is, in which case their Fredholm indices agree.*

Proof. Assume that $\mathcal{T}^c(\lambda)$ is a Fredholm operator.

1. From (5.31) we infer that

$$\begin{aligned}&\mathrm{R}(\mathcal{T}^c(\lambda)) = \quad \mathbf{Q}(z)\mathbf{f} \quad \mathbf{f} \quad \mathrm{R}(\mathcal{T}^\alpha(\lambda)) \quad =: \mathbf{Q}(z)\mathrm{R}(\mathcal{T}^\alpha(\lambda)), \quad \text{or, equivalently}\\ &\mathrm{R}(\mathcal{T}^\alpha(\lambda)) = \mathbf{Q}^{-1}(z)\mathrm{R}(\mathcal{T}^c(\lambda)).\end{aligned} \tag{5.32}$$

   This implies that $\mathrm{R}(\mathcal{T}^\alpha(\lambda))$ must be closed. Indeed, suppose by contradiction that $\mathbf{f}_n \subset \mathrm{R}(\mathcal{T}^\alpha(\lambda))$ is a sequence that converges to $\mathbf{f} \;/\; \mathrm{R}(\mathcal{T}^\alpha(\lambda))$. Because $\mathbf{f}_n = \mathbf{Q}^{-1}(z)\mathbf{g}_n$ for $\mathbf{g}_n \quad \mathrm{R}(\mathcal{T}^c(\lambda))$ for all $n \quad \mathbb{N}$, we have that for each $\epsilon > 0$ there exists $N > 0$ such that

$$\begin{aligned}\epsilon > \|\mathbf{f}_n - \mathbf{f}\|_{L^2(\mathbb{R};\mathbb{C}^3)} &= \left\|\mathbf{Q}^{-1}(z)\left(\mathbf{g}_n - \mathbf{Q}(z)\mathbf{f}\right)\right\|_{L^2(\mathbb{R};\mathbb{C}^3)}\\ &= \|\mathbf{g}_n - \mathbf{Q}(z)\mathbf{f}\|_{L^2_{w_\alpha}(\mathbb{R};\mathbb{C}^2)\times L^2_{w_\varepsilon}(\mathbb{R};\mathbb{C})}, \quad \text{whenever } n > N.\end{aligned}$$

   This means that $\mathbf{g}_n \quad \mathbf{Q}(z)\mathbf{f}$. Note that $\mathbf{Q}(z)\mathbf{f}$ belongs to $L^2_{w_\alpha}(\mathbb{R};\mathbb{C}^2)\times L^2_{w_\varepsilon}(\mathbb{R};\mathbb{C})$ but not to $\mathrm{R}(\mathcal{T}^c(\lambda))$; if it did, $\mathbf{f} = \mathbf{Q}^{-1}(z)\mathbf{Q}(z)\mathbf{f}$ would belong to $\mathrm{R}(\mathcal{T}^\alpha(\lambda))$. This leads to a contradiction, since $\mathrm{R}(\mathcal{T}^c(\lambda))$ contains all of its limit points due to fact it is closed inasmuch as $\mathcal{T}^\alpha(\lambda)$ is Fredhom; therefore we conclude that $\mathrm{R}(\mathcal{T}^\alpha(\lambda))$ is closed.

2. It also follows from (5.31) that

$$\begin{aligned}&\ker(\mathcal{T}^c(\lambda)) = \mathbf{Q}(z)\ker(\mathcal{T}^\alpha(\lambda)), \quad \text{or, equivalently}\\ &\ker(\mathcal{T}^\alpha(\lambda)) = \mathbf{Q}^{-1}(z)\ker(\mathcal{T}^c(\lambda)).\end{aligned} \tag{5.33}$$

   From the bijective relation that (5.33) represents, it results that $\dim[\ker(\mathcal{T}^\alpha(\lambda))] = \dim[\ker(\mathcal{T}^c(\lambda))] < \quad$.

   Let $\mathbf{Y}_1, \mathbf{Y}_2, \ldots, \mathbf{Y}_n$ a basis of $\ker(\mathcal{T}^c(\lambda))$ and let $\tilde{\mathbf{Y}} \quad \ker(\mathcal{T}^\alpha(\lambda))$ be arbitrary. By (5.33), $\tilde{\mathbf{Y}} = \mathbf{Q}^{-1}(z)\mathbf{Y}$ for some $\mathbf{Y} \quad \ker(\mathcal{T}^c(\lambda))$, hence

$$\begin{aligned}\tilde{\mathbf{Y}} = \mathbf{Q}^{-1}(z)\mathbf{Y} &= \mathbf{Q}^{-1}(z)(a_1\mathbf{Y}_1 + a_2\mathbf{Y}_2 + \cdots + a_n\mathbf{Y}_n)\\ &= a_1\mathbf{Q}^{-1}(z)\mathbf{Y}_1 + a_2\mathbf{Q}^{-1}(z)\mathbf{Y}_2 + \cdots + a_n\mathbf{Q}^{-1}(z)\mathbf{Y}_n,\end{aligned}$$

   for some constants $a_1, a_2, \ldots, a_n \quad \mathbb{C}$. Thus

$$\mathrm{Span}(\ker(\mathcal{T}^\alpha(\lambda))) = \mathbf{Q}^{-1}(z)\mathrm{Span}(\ker(\mathcal{T}^c(\lambda))).$$

3. Note in addition that

$$\begin{aligned}L^2_{w_\alpha}(\mathbb{R};\mathbb{C}^2)\times L^2_{w_\varepsilon}(\mathbb{R};\mathbb{C}) &= \mathbf{Q}(z)L^2(\mathbb{R};\mathbb{C}^3), \quad \text{or, equivalently}\\ L^2(\mathbb{R};\mathbb{C}^3) &= \mathbf{Q}^{-1}(z)L^2_{w_\alpha}(\mathbb{R};\mathbb{C}^2)\times L^2_{w_\varepsilon}(\mathbb{R};\mathbb{C}).\end{aligned}$$

4. Next we show that the codimension of $\mathrm{R}(\mathcal{T}^\alpha(\lambda))$ equals the codimension of $\mathrm{R}(\mathcal{T}^c(\lambda))$. To do so, we use (5.32) and (5.33) to see that

$$\begin{aligned} L^2(\mathbb{R};\mathbb{C})/\mathrm{R}(\mathcal{T}^\alpha(\lambda)) &= L^2(\mathbb{R};\mathbb{C}) + \mathrm{R}(\mathcal{T}^\alpha(\lambda)) \\ &= \mathbf{Q}^{-1}(z)\left(L^2_{w_\alpha}(\mathbb{R};\mathbb{C}^2)\times L^2_{w_\varepsilon}(\mathbb{R};\mathbb{C}) + \mathrm{R}(\mathcal{T}^c(\lambda))\right), \end{aligned}$$

   from which we get

$$\mathrm{Span}\left(L^2(\mathbb{R};\mathbb{C})/\mathrm{R}(\mathcal{T}^\alpha(\lambda)\right) = \mathbf{Q}^{-1}(z)\mathrm{Span}\left(L^2_{w_\alpha}(\mathbb{R};\mathbb{C}^2)\times L^2_{w_\varepsilon}(\mathbb{R};\mathbb{C})/\mathrm{R}(\mathcal{T}^c(\lambda))\right);$$

   the statement can be proven analogously to point 2.

   Therefore

$$\begin{aligned} \mathrm{codim}[\mathrm{R}(\mathcal{T}^\alpha(\lambda))] &= \dim\left[L^2(\mathbb{R};\mathbb{C})/\mathrm{R}(\mathcal{T}^\alpha(\lambda))\right] \\ &= \dim\left[L^2_{w_\alpha}(\mathbb{R};\mathbb{C}^2)\times L^2_{w_\varepsilon}(\mathbb{R};\mathbb{C})/\mathrm{R}(\mathcal{T}^c(\lambda))\right] \\ &= \mathrm{codim}[\mathrm{R}(\mathcal{T}^c(\lambda))] < \quad . \end{aligned}$$

5. It follows from all the previous points that $\mathcal{T}^\alpha(\lambda)$ is a Fredholm operator with index

$$\begin{aligned} \mathrm{ind}\,\mathcal{T}^\alpha(\lambda) &= \dim[\ker(\mathcal{T}^\alpha(\lambda))] - \mathrm{codim}[\mathrm{R}(\mathcal{T}^\alpha(\lambda))] \\ &= \dim[\ker(\mathcal{T}^c(\lambda))] - \mathrm{codim}[\mathrm{R}(\mathcal{T}^c(\lambda))] = \mathrm{ind}\,\mathcal{T}^c(\lambda). \end{aligned}$$

The converse implication, that if $\mathcal{T}^\alpha(\lambda)$ is Fredholm then is $\mathcal{T}^c(\lambda)$, follows analogously. □

Theorem 5.9. *The essential spectrum of $\mathcal{L}^c$ in the space $H^1_{w_\alpha}(\mathbb{R};\mathbb{C}^2)\times H^1_{w_\varepsilon}(\mathbb{R};\mathbb{C})$ is contained in the stable complex half plane.*

Proof. We know that $\sigma_{\mathrm{ess}}(\mathcal{L}^c)$ is given by $\sigma_{\mathrm{ess}}(\mathcal{T}^c)$, and in turn, from Proposition 5.8, $\sigma_{\mathrm{ess}}(\mathcal{T}^c)$ in $H^1_{w_\alpha}(\mathbb{R};\mathbb{C}^2)\times H^1_{w_\varepsilon}(\mathbb{R};\mathbb{C})$ is given by $\sigma_{\mathrm{ess}}(\mathcal{T}^\alpha)$. Therefore, the proof consists in finding the region where the essential spectrum of $\mathcal{T}^\alpha$ resides.

With the same arguments as in the proof of Lemma 5.5 we infer from Lemma 5.7 that, for all $\lambda \quad \Omega$, $\mathcal{T}^\alpha(\lambda)$ is Fredholm with index zero, which comes from

$$\mathrm{ind}\,\mathcal{T}^\alpha(\lambda) = i^\alpha_-(\lambda) - i^\alpha_+(\lambda) = 0.$$

This allows us to conclude that $\sigma_{\mathrm{ess}}(\mathcal{T}^\alpha)\subset\mathbb{C} \quad \Omega$. Proving the theorem. □

5.5.2

The multiplicity of $\lambda = 0$

Following Flores and Plaza [13], and Sandstede [52], we express the matrix (5.13) as

$$\mathbf{A}(z,\lambda) = \mathbf{A}_0(z) + \lambda\mathbf{A}_1,$$

where

$$\mathbf{A}_0(z) = \begin{matrix} \frac{-\mu s(2\bar{q}^+-1)}{c^2-s^2} & \frac{\mu}{c^2-s^2} & -\frac{2\mu s\bar{p}}{c^2-s^2} \\ \frac{-c\mu s(2\bar{q}^+-1)}{c^2-s^2} & \frac{c\mu}{c^2-s^2} & -\frac{2c\mu s\bar{p}}{c^2-s^2} \\ 0 & -\frac{2\kappa\bar{q}^+(1-\bar{q}^+)}{cs} & -\frac{2\kappa\bar{j}(1-2\bar{q}^+)}{cs} \end{matrix}$$

and

$$\mathbf{A}_1 = \begin{matrix} \frac{c}{c^2-s^2} & \frac{1}{c^2-s^2} & 0 \\ \frac{s^2}{c^2-s^2} & \frac{c}{c^2-s^2} & 0 \\ 0 & 0 & \frac{1}{c} \end{matrix} .$$

Definition 5.10. Consider $\lambda \quad \sigma_{\mathrm{pt}}(\mathcal{T}^c)$. The maximal number of linearly indepondet eigenfuntions of $\mathcal{T}^c(\lambda)$ is called the geometric multiplicity of λ. Suppose that $\ker(\mathcal{T}^c(\lambda)) = \mathrm{Span} \ \mathbf{Y}_1$, the eigenvalue λ is said to have algebraic multiplicity m if there is a solution to

$$\mathcal{T}^c(\lambda)\mathbf{Y}_j = \mathbf{A}_1\mathbf{Y}_{j-1},$$

for each $j = 2, \ldots, m$, with $\mathbf{Y}_j \quad H^1_{w_\alpha} \times H^1_{w_\varepsilon}$, but there does not exist a $H^1_{w_\alpha} \times H^1_{w_\varepsilon}$ solution to

$$\mathcal{T}^c(\lambda)\mathbf{Y} = \mathbf{A}_1\mathbf{Y}_m.$$

If $\lambda \quad \sigma_{\mathrm{pt}}(\mathcal{T}^c)$ has geometric multiplicity ℓ, that is to say, $\ker(\mathcal{T}^c(\lambda)) = \mathrm{Span} \ \mathbf{Y}_1 \ldots \mathbf{Y}_\ell$, the algebraic multiplicity is the sum of the algebraic multiplicities of a maximal set of linearly independent eigenfunctions of $\mathcal{T}^c(\lambda)$.

We say that λ is simple if the geometric and algebraic multiplicity are equal to 1.

Lemma 5.11. *In $H^1_{w_\alpha}(\mathbb{R};\mathbb{C}^2) \times H^1_{w_\varepsilon}(\mathbb{R};\mathbb{C})$, $\lambda = 0$ is an element of $\sigma_{pt}(\mathcal{L}^c)$ and it is simple.*

Proof. Lemma 5.1 establishes that in $H^1(\mathbb{R};\mathbb{C}^3)$ the eigenspace associated to $\lambda = 0$ is spanned by the eigenfunction $(\bar{p}_z, \bar{j}_z, \bar{q}^+_z)$. In addition, from Theorem 5.9, $\operatorname{ind}\mathcal{L}^c = \operatorname{ind}\mathcal{T}^\alpha(0) = 0$, thus, by proving that this function also belongs to $H^1_{w_\alpha}(\mathbb{R};\mathbb{C}^2) \times H^1_{w_\varepsilon}(\mathbb{R};\mathbb{C})$, it follows that $\lambda = 0$ is an element of $\sigma_{\mathrm{pt}}(\mathcal{L}^c)$ with geometric multiplicity 1 in this weighted space.

Verification of $(\bar{p}_z, \bar{j}_z, \bar{q}^+_z) \quad H^1_{w_\alpha}(\mathbb{R};\mathbb{C}^2) \times H^1_{w_\varepsilon}(\mathbb{R};\mathbb{C})$ requires showing that $w_\alpha\partial_z^i\bar{p}$ and $w_\varepsilon\partial_z^i\bar{q}^+$ belong to $L^2(\mathbb{R};\mathbb{C})$ for $i = 1, 2$. Since, once achieved that, we will have

$$\begin{aligned} \left\|(\bar{p}_z, \bar{j}_z, \bar{q}^+_z)\right\|^2_{H^1_{w_\alpha}(\mathbb{R};\mathbb{C}^2)\times H^1_{w_\varepsilon}(\mathbb{R};\mathbb{C})} &= \left(\ w_\alpha\bar{p}_z \ {}^2_{L^1(\mathbb{R};\mathbb{C})} + \ w_\alpha\bar{p}_{zz} \ {}^2_{L^1(\mathbb{R};\mathbb{C})} \right)(1+c^2) \\ &\quad + \left\|w_\varepsilon\bar{q}^+_z\right\|^2_{L^1(\mathbb{R};\mathbb{C})} + \left\|w_\varepsilon\bar{q}^+_{zz}\right\|^2_{L^1(\mathbb{R};\mathbb{C})} < \quad . \end{aligned}$$

According to Lemma 2.7,

$$\bar{p}_z, \bar{q}^+_z = \mathcal{O}(e^{-2\alpha_l z}), \quad z < 0, \quad \text{and} \quad \bar{p}_z, \bar{q}^+_z = \mathcal{O}(e^{-2\alpha_r z}), \quad z > 0.$$

Then we get

$$w_\alpha \bar{p}_z = \begin{array}{ll} \mathcal{O}(e^{-\alpha_l z} + e^{(\alpha_r - 2\alpha_l)z}), & z < 0, \\ \mathcal{O}(e^{(\alpha_l - 2\alpha_r)z} + e^{-\alpha_r z}), & z > 0, \end{array} \quad \text{and} \quad w_\varepsilon \bar{q}_z^+ = \begin{array}{ll} \mathcal{O}(e^{-\alpha_l(2+\varepsilon)z}), & z < 0, \\ \mathcal{O}(e^{-(2\alpha_r + \alpha_l \varepsilon)z}), & z > 0. \end{array} \tag{5.34}$$

This suffices to conclude that $w_\alpha \bar{p}_z$ and $w_\varepsilon \bar{q}_z^+$ are elements of $L^2(\mathbb{R};\mathbb{C})$, provided ε is small enough.

From (5.6), $w_\alpha \bar{p}_{zz}$ and $w_\varepsilon \bar{q}_{zz}^+$ are given by

$$\begin{aligned} w_\alpha \bar{p}_{zz} &= \frac{\mu}{s^2 - c^2} \left((2s\bar{q}^+ - (c+s)) w_\alpha \bar{p}_z + 2s w_\alpha \bar{p} \bar{q}_z^+ \right), \\ w_\varepsilon \bar{q}_{zz}^+ &= -\frac{2\kappa}{s} (\bar{q}^+ \left(1 - \bar{q}^+\right) w_\varepsilon \bar{p}_z + \bar{p} \left(1 - 2\bar{q}^+\right) w_\varepsilon \bar{q}_z^+). \end{aligned} \tag{5.35}$$

Thus, to check that both belong to $L^2(\mathbb{R};\mathbb{C})$ we only need verify that all the terms in the sums on the right-hand side of (5.35) belong to $L^2(\mathbb{R};\mathbb{C})$.

We can estimate

$$\left\| (2s\bar{q}^+ - (c+s)) w_\alpha \bar{p}_z \right\|_{L^2(\mathbb{R};\mathbb{C})} < (s+c) \quad w_\alpha \bar{p}_z \quad _{L^2(\mathbb{R};\mathbb{C})},$$

and, from the second equation in (2.5),

$$\left\| w_\alpha \bar{p} \bar{q}_z^+ \right\|_{L^2(\mathbb{R};\mathbb{C})} = \frac{2\kappa}{s} \left\| w_\alpha \bar{p}^2 (1 - \bar{q}^+) \bar{q}^+ \right\|_{L^2(\mathbb{R};\mathbb{C})} < \frac{2\kappa}{s} p_{\max} q_l^+ \quad w_\alpha \bar{p} \quad _{L^2(\mathbb{R};\mathbb{C})};$$

employing Lemma 2.7, we derive

$$w_\alpha \bar{p} = \begin{array}{ll} \mathcal{O}(e^{-\alpha_l z} + e^{(\alpha_r - 2\alpha_l)z}), & z < 0, \\ \mathcal{O}(e^{(\alpha_l - 2\alpha_r)z} + e^{-\alpha_r z}), & z > 0, \end{array}$$

which guarantees that $w_\alpha \bar{p} \quad _{L^2(\mathbb{R};\mathbb{C})}$ exists.

Similarly,

$$w_\varepsilon \bar{p}_z = \begin{array}{ll} \mathcal{O}(e^{-\alpha_l(2+\varepsilon)z}), & z < 0, \\ \mathcal{O}(e^{-(2\alpha_r + \alpha_l \varepsilon)z}), & z > 0, \end{array}$$

hence,

$$\left\| w_\varepsilon \bar{q}^+ (1 - \bar{q}^+) \bar{p}_z \right\|_{L^2(\mathbb{R};\mathbb{C})} < \quad w_\varepsilon \bar{p}_z \quad _{L^2(\mathbb{R};\mathbb{C})} < \quad .$$

Finally, we have the bound

$$\left\| w_\varepsilon \bar{p} (1 - 2\bar{q}^+) \bar{q}_z^+ \right\|_{L^2(\mathbb{R};\mathbb{C})} < \bar{p}_{\max} \left\| w_\varepsilon \bar{q}_z^+ \right\|_{L^2(\mathbb{R};\mathbb{C})}.$$

As a consequence of the asymptotic behaviour of $w_\varepsilon \bar{q}_z^+$, described in (5.34), the right-hand side converges. Hence, it is true that $w_\alpha \bar{p}_{zz}$, $w_\varepsilon \bar{q}_{zz}^+ \quad L^2(\mathbb{R};\mathbb{C})$.

Concerning the algebraic multiplicity, we take $\lambda = 0$ in (5.2) and derive with respect to c. Then,

$$\begin{aligned} c\bar{p}_{cz} - \bar{j}_{cz} &= -\bar{p}_z, \\ -s^2 \bar{p}_{cz} + c\bar{j}_{cz} - \mu \bar{j}_c + \mu s \left(\left(2\bar{q}^+ - 1\right) \bar{p}_c + 2\bar{p}\bar{q}_c^+ \right) &= -\bar{j}_z, \\ c q_{cz}^+ + \frac{2\kappa}{s} \left(\bar{q}^+ \left(1 - \bar{q}^+\right) \bar{j}_c + \bar{j} \left(1 - 2\bar{q}^+\right) \bar{q}_c^+ \right) &= -\bar{q}_z^+. \end{aligned} \tag{5.36}$$

We write (5.36) as the equivalent system

$$\mathcal{T}^c(0)\mathbf{Y}_2 = \partial_x \mathbf{Y}_2 - \mathbf{A}(z,0)\mathbf{Y}_2 = \mathbf{A}_1\mathbf{Y}_1,$$

where $\mathbf{Y}_1 = (\bar{p}_z, \bar{j}_z, \bar{q}_z^+)^t$ and $\mathbf{Y}_2 = -(\bar{p}_c, \bar{j}_c, \bar{q}_c^+)^t$.

Despite the fact that $\mathbf{Y}_2$ solves equation

$$\mathcal{T}^c(0)\mathbf{Y} = \mathbf{A}_1\mathbf{Y}_1,$$

the Jordan chain ends with algebraic multiplicity 1, the reason is that $\mathbf{Y}_2$ does not belong to $L^2(\mathbb{R};\mathbb{C}^3)$, which means that it is not a member of the space $H^1_{w_\alpha}(\mathbb{R};\mathbb{C}^2) \times H^1_{w_\varepsilon}(\mathbb{R};\mathbb{C})$.

Certainly, we compute $\bar{q}_c^+$ through

$$\frac{\partial \bar{q}^+}{\partial c} = \frac{\partial \bar{q}^+}{\partial q_l^+}\frac{\partial q_l^+}{\partial q_r^+}\frac{\partial q_r^+}{\partial c}.$$

From Propositions 2.4 and 2.6, and by (5.11), $\bar{q}_c^+$ tends to a nonzero limit whose value depends on the wave speed and the end states. This leaves $\mathbf{Y}_2$ out of $L^2(\mathbb{R};\mathbb{C}^3)$. □

CHAPTER

SIX

DISCUSSION

According to the M^5-model, an architecture of matrix fibres organized in parallel promotes the formation of cellular aggregates in the form of stationary and traveling pulses. After their run trough the extracelular matrix (ECM) such pulses leave behind tracks of proteolytically reoriented fibres. This results in the formation of decreasing wave fronts that connect zones where most matrix fibres point to the right with zones where the amount of right-oriented fibres is lower. Our findings support an association of high-amplitude wave fronts with the presence of tall pulses, which suggests a positive correlation between the height of the pulses and the amplitude of the wave fronts.

We obtained analytical approximate expressions for the standing and traveling pulses and wave fronts. We observed through graphical comparisons that the approximate standing and traveling wave profiles better approximate the solutions obtained numerically as they amplitude is reduced. A very interesting result would be to prove analytically that the error can be controlled, which is highly desirable in order to ensure the accuracy of the approximations in the cases of short pulses and flat wave fronts.

In view of the important role of patterns of cells and ECM unidirectionally aligned on performance and maintenance of specialized functions of tissues, and on their medical applications, we would like to know which of the cellular aggregates and oriented structures of ECM can persist for a long time. So, our interest has focused on the spectral stability of the standing and traveling wave profiles, which according to the results of Rottmann-Matthes [49, 50], is an important step to determine orbital asymptotic stability. We have proved that each standing pulse and its corresponding wave front are spectrally stable; nevertheless, up to now this result has not been enough to conclude orbital stability. One of the difficulties we encountered when trying to apply the results of asymptotic stability of Rottmann-Matthes is the infinite-dimensional nature of the zero eigenvalue, which is far from the assumptions considered by the author. With regard to the members of the family of traveling waves, we have made significant progress towards obtaining their spectral stability. Although in principle these traveling waves are spectrally unstable, since the linearized operator has essential spectrum up to the imaginary axis, we have constructed an appropriate Sobolev weighted space where the essential spectrum lies inside the open left-half complex plane. The location of the point spectrum is still an open question, our

work continues in this direction with a view to doing the analysis of orbital stability.

APPENDIX

In this appendix we show that for a function $u \quad H^1_w(\mathbb{R};\mathbb{C})$, with a positive weight function w satisfying

$$\frac{w_z}{w}(+\quad) = w_+ \quad \text{and} \quad \frac{w_z}{w}(-\quad) = w_-, \quad w_\pm \quad \mathbb{R}, \tag{6.1}$$

there exists a function $\tilde{u} \quad H^1(\mathbb{R};\mathbb{C})$ such that $u = w^{-1}\tilde{u}$.

Let $\tilde{u} := wu$, since clearly $\tilde{u} \quad L^2(\mathbb{R};\mathbb{C})$, we need only prove that $\tilde{u}_z \quad L^2(\mathbb{R};\mathbb{C})$. So we differentiate $\tilde{u}$ to get

$$\tilde{u}_z = w_z u + w u_z = u\frac{w_z}{w} + wu,$$

from which we have that

$$\tilde{u}_z \ \le \left| u\frac{w_z}{w} \right| + \ wu \ . \tag{6.2}$$

Squaring in (6.2) and integrating over $\mathbb{R}$,

$$\begin{aligned} \int_{\mathbb{R}} \tilde{u}_z \ ^2 dz \ &\le \int_{\mathbb{R}} \left| u\frac{w_z}{w} \right|^2 dz + 2 \int_{\mathbb{R}} \left| u\frac{w_z}{w} \right| \ wu \ dz + \int_{\mathbb{R}} wu \ ^2 dz \\ &\le 2\left(\int_{\mathbb{R}} \left| u\frac{w_z}{w} \right|^2 dz + \int_{\mathbb{R}} wu \ ^2 dz \right) = 2\left(\tilde{u} \ _{L^2(\mathbb{R};\mathbb{C})} + \int_{\mathbb{R}} \left| u\frac{w_z}{w} \right|^2 dz \right). \end{aligned}$$

By condition (6.1) for a given $\varepsilon > 0$ there exist $N > 0$ such that $\ w_z/w - w_\pm \ < \varepsilon$ for $z \ > N$, therefore

$$\begin{aligned} \int_{\mathbb{R}} \left| u\frac{w_z}{w} \right|^2 dz &= \int_{-}^{-N} \left| u\frac{w_z}{w} \right|^2 dz + \int_{-N}^{N} \left| u\frac{w_z}{w} \right|^2 dz + \int_{N} \left| u\frac{w_z}{w} \right|^2 dz \\ &\le (\ w_- \ + \varepsilon)^2 \int_{-}^{-N} u \ ^2 dz + \int_{-N}^{N} \left| u\frac{w_z}{w} \right|^2 dz + (\ w_+ \ + \varepsilon)^2 \int_{N} u \ ^2 dz \\ &\le (\ w_- \ + \varepsilon)^2 \int_{\mathbb{R}} u \ ^2 dz + \sup_{-N \le z \le N} \left\{ \left| \frac{w_z}{w} \right|^2 \right\} \int_{\mathbb{R}} u \ ^2 dz \\ &\qquad + (\ w_+ \ + \varepsilon)^2 \int_{\mathbb{R}} u \ ^2 dz < \quad . \end{aligned}$$

From this, $\tilde{u}_z \quad L^2(\mathbb{R};\mathbb{C})$ and then $\tilde{u} \quad H^1(\mathbb{R};\mathbb{C})$.

BIBLIOGRAPHY

[1] J. Alexander, R. Gardner and C. K. R. T. Jones, *A topological invariant arising in the stability analysis of travelling waves*, J. Reine Angew. Math., 410 (1990), pp. 167–212.

[2] A. C. Bellail, S. B. Hunter, D. J. Brat, C. Tan and E. G. Van Meir, *Microregional extracellular matrix heterogeneity in brain modulates glioma cell invasion*, Int. J. Biochem. Cell Biol., 36 (2004), pp. 1046–1069.

[3] D. E. Birk and P. Brückner, *Collagens, suprastructures, and collagen fibril assembly*, In The Extracellular Matrix: an Overview, Springer Science & Business Media, 2011, pp. 77–115.

[4] A. G. Clark and D. M. Vignjevic, *Modes of cancer cell invasion and the role of the microenvironment*, Current Opinion in Cell Biology, 36 (2015), pp. 13–22.

[5] A. Chauviere, T. Hillen and L. Preziosi, *Modelling cell movement in anisotropic and heterogeneous network tissues*, Netw. Heterog. Media. , 2 (2007), pp. 333–357.

[6] A. Chauvière and L. Preziosi, *Mathematical framework to model migration of cell population in extracellular matrix*, In Mathematical and computational biology series: cell mechanics from singled-based models to multiscale modeling, Taylor & Francis Group, CRC Press publisher, 2010, pp. 285–318.

[7] S. Cruz-García and C. García-Reimbert, *On the spectral stability of standing waves of the one-dimensional M^5-model*, Discrete Contin. Dyn. Sys. B., 21 (2016), pp. 1079–1099.

[8] A. D. Doyle, F. W. Wang, K. Matsumoto and K. M. Yamada, *One-dimensional topography underlies three-dimensional fibrillar cell migration.*, J. Cell Biol., 184 (2009), pp. 481–490.

[9] M. Egeblad and Z. Werb, *New functions for the matrix metalloproteinases in cancer progression*, Nat. Rev. Cancer, 2 (2002), pp. 161–174.

[10] C. Engwer, T. Hillen, M. Knappitsch and C. Surulescu, *Glioma follow white matter tracts: a multiscale DTI-based model*, J. Math. Biol., 71 (2015), pp. 551–582.

[11] H. A. Erbay, S. Erbay and A. Erkip, *Existence and stability of traveling waves for a class of nonlocal nonlinear equations*, J. Math. Anal. Appl., 425 (2015), pp. 307–336.

[12] I. J. Fidler, *Metastasis: quantitative analysis of distribution and fate of tumor emboli labeled with 125I-5-Iodo-2'-deoxyuridine*, J. Nat. Cancer Inst., 45 (1970), pp. 773–782.

[13] G. Flores and R. G. Plaza, *Stability of post-fertilization traveling waves*, J. Differential Equations, 247 (2009), pp. 1529–1590.

[14] P. Friedl, *Prespecification and plasticity: shifting mechanisms of cell migration*, Curr. Opin. Cell Biol., 16 (2004), pp. 14–23.

[15] P. Friedl and E.-B. Bröcker, *The biology of cell locomotion within three-dimensional extracellular matrix*, Cell. Mol. Life Sci., 57 (2000), pp. 41–64.

[16] P. Friedl and D. Gilmour, *Collective cell migration in morphogenesis, regeneration and cancer*, Nature Rev. Mol. Cell Biol., 10 (2009), pp. 445–457.

[17] P. Friedl, Y. Hegerfeldt and M. Tusch, *Collective cell migration in morphogenesis and cancer*, Int. J. Dev. Biol., 48 (2004), pp. 441–449.

[18] P. Friedl and K. Wolf, *Tumor cell invasion and migration: diversity and escape mechanisms*, Nat. Rev. Cancer, 3 (2003), pp. 362–374.

[19] D. Gallego-Perez, N. Higuita-Castro, L. Denning, J. DeJesus, K. Dahl, A. Sarkar and D. J. Hansford, *Microfabricated mimics of in vivo structural cues for the study of guided tumor cell migration*, Lab Chip, 12 (2012), pp. 4424-4432.

[20] A. Ghazaryan and C. K. R. T. Jones, *On the stability of high lewis number combustion fronts*, Discrete Contin. Dyn. Sys. A., 24 (2009), pp. 809–826.

[21] J. Goodman, *Nonlinear asymptotic stability of viscous shock profiles for conservation laws*, Arch. Rational Mech. Anal., 95 (1986), pp. 325–344.

[22] D. Hanahan and R. A. Weinberg, *Hallmarks of cancer: The next generation*, Cell, 144 (2011), pp. 646–674.

[23] M. A. Hayat (Ed.), *Stem Cells and Cancer Stem Cells 4: Therapeutic Applications in Disease and Injury*, Springer, 2012.

[24] T. Hillen, M^5 *mesoscopic and macroscopic models for mesenchymal motion*, J. Math Biol., 53 (2006), pp. 585–616.

[25] T. Hillen, P. Hinow and Z. A. Wang, *Mathematical analysis of a kinetic model for cell movement in network tissues*, Discrete Contin. Dyn. Sys. B., 14 (2010), pp. 1055–1080.

[26] T. Hillen and K. J. Painter, *Transport and anisotropic diffusion models for movement in oriented habitats*, In Dispersal, Individual Movement and Spatial Ecology, Springer Berlin Heidelberg, 2013, pp. 177–222.

[27] N. F. Huang and R. J. Lee and S. Li, *Engineering of aligned skeletal muscle by micropatterning* , Am. J. Transl. Res., 2 (2009), pp. 43–55.

[28] J. Humpherys, *On the shock wave spectrum for isentropic gas dynamics with capillarity*, J. Differential Equations, 246 (2009), pp. 2938–2957.

[29] J. Humpherys, *Spectral energy methods and the stability of shock waves*, Ph.D. Thesis, Indiana University, University, 2002.

[30] J. K. Itano (Ed.), *Core Curriculum for Oncology Nursing*, 5th edn., Elsevier, 2015.

[31] A. Jain, M. Betancur, G. D. Patel, C. M. Valmikinathan, V. J. Mukhatyar, A. Vakharia, S. B. Pai, B. Brahma, T. J. MacDonald and R. V. Bellamkonda, *Guiding intracortical brain tumour cells to an extracortical cytotoxic hydrogel using aligned polymeric nanofibres*, Nature materials, 13 (2014), pp. 308–316.

[32] J. Johnson, M. O. Nowicki, C. H. Lee, E. A. Chiocca, M. S. Viapiano, S. E. Lawler, and J. J. Lannutti, *Quantitative analysis of complex glioma cell migration on electrospun polycaprolactone using time-lapse microscopy*, Tissue Eng. Part C, 15 (2009), pp. 531–540.

[33] T. Kapitula and K. Promislow, *Spectral and Dynamical Stability of Nonlinear Waves*, Springer, New York, 2013.

[34] D. H. Kim, P. P. Provenzano, C. L. Smith and A. Levchenko, *Matrix nanotopography as a regulator of cell function*, J. Cell Biol., 197 (2012), pp. 351–360.

[35] S. Q. Liu, *Spectral and Dynamical Stability of Nonlinear Waves*, Wiley, 2007.

[36] L. A. Lowery and D. Van Vactor, *The trip of the tip: understanding the growth cone machinery*, Nat. Rev. Mol. Cell Biol., 10 (2009), pp. 332–343.

[37] D. Lyen, D. R. Welch and B. Psaila (Eds.), *Cancer Metastasis: Biologic Basis and Therapeutics*, Cambridge University Press, 2011.

[38] D. A. Mackenna, J. H. Omens, A. D. McCulloch and J. W. Covell, *Contribution of collagen matrix to passive left ventricular mechanics in isolated rat hearts*, Am. J. Physiol., 266 (1994), pp. 1007–1018.

[39] J. A. McDonald and R. P. Mecham (Ed.), *Receptors for Extracellular Matrix*, Academic Press, San Diego, California, 1991.

[40] H. G. Othmer, S. R. Dunbar and W. Alt, *Models of dispersal in biological systems*, J. Math. Biol., 26 (1984), pp. 263–298.

[41] K. J. Painter, *Modelling cell migration strategies in the extracellular matrix*, J. Math. Biol., 58 (2009), pp. 511–543.

[42] K. J. Painter and T. Hillen, *Mathematical modelling of glioma growth: The use of Diffusion Tensor Imagin (DIT) data to predict the anisotropic pathways of cancer invasion*, J. Math. Biol., 323 (2013), pp. 25-39.

[43] K. J. Palmer, *Exponential dichotomies and transversal homoclinic points*, J. Differential Equations, 55 (1984), pp. 225–256.

[44] K. J. Palmer, *Exponential dichotomies and Freholm operators*, Proc. Amer. Math. Soc., 104 (1988), pp. 149–156.

[45] M. Papadaki, N. Bursac, R. Langer, J. Merok, G. Vunjak-Novakovic and L. E. Freed, *Tissue engineering of functional cardiac muscle: molecular, structural, and electrophysiological studies*, Am. J. Physiol. Heart Circ. Physiol., 280 (2001), pp. 168–178.

[46] R. L. Pego and M.I. Weinstein, *Asymptotic stability of solitary waves*, Commun. Math. Phys., 164 (1994), pp. 305–349.

[47] S. V. Petrovskii and B.-L. Li, *Exactly Solvable Models of Biological Invasion*, Chapman & Hall/CRC, Boca Raton, 2005.

[48] R. G. Plaza and K. Zumbrun, *An Evans function approach to spectral stability of small-amplitude shock profiles*, Discr. and Cont. Dynam. Syst., 10 (2004), pp. 885–924.

[49] J. Rottmann-Matthes, *Linear stability of traveling waves in first-order hyperbolic PDEs*, J. Dyn. Diff. Equat., 23 (2011), pp. 365–393.

[50] J. Rottmann-Matthes, *Stability and freezing of nonlinear waves in first-order hyperbolic PDEs,*, J. Dyn. Diff. Equat., 24 (2012), pp. 341–367.

[51] F. Sánchez Garduño and P. K. Maini, *An approximation to a sharp type solution of a density-dependent reaction-diffusion equation*, Appl. Math. Lett., 7 (1994), pp. 47–51.

[52] B. Sandstede, *Stability of travelling waves*, In Handbook of Dynamical Systems, North-Holland, Amsterdam, 2002, pp. 983–1055.

[53] B. Sandstede and A. Scheel, *Absolute and convective instabilities of waves on unbounded and large bounded domains*, Physica D, 145 (2000), pp. 233–277.

[54] S. Shivani, S. B. Bandini, P. E. Donnelly, J. Schwartz and J. E. Schwarzbauer., *A cell-assembled, spatially aligned extracellular matrix to promote directed tissue development*, J. Mater. Chem. B, 2 (2014), pp. 1449–1453.

[55] J. E. Talmadge and I. J. Fidler, *AACR centennial ceries: the biology of cancer metastasis: historical perspective*, Cancer Res., 70 (2010), pp. 5649–5669.

[56] Z. A. Wang, T. Hillen and M. Li, *Mesenchymal motion models in one dimension*, SIAM J. Appl. Math., 69 (2008), pp. 375–397.

[57] K. Wolf, I. Mazo, H. Leung and K. Engelke, U. H. von Andrian, E. I. Deryugina, A. Y. Strongin, E.-B. Bröcker and P. Friedl, *Compensation mechanism in tumor cell migration: mesenchymal-amoeboid transition after blocking of pericellular proteolysis*, J. Cell Biol., 160 (2003), pp. 267–277.

[58] Y. Wu and X. Xing, *Stability of traveling waves with critical speeds for p-degree Fisher-type equations*, Discrete Contin. Dyn. Sys., 20 (2008), pp. 1123–1139.

[59] Q. Xing, C. Vogt, K. W. Leong and F. Zhao, *Highly aligned nanofibrous scaffold derived from decellularized human fibroblasts*, Adv. Funct. Mater., 24 (2014), pp. 3027–3035.

[60] K. Zumbrun, *Stability and dynamics of viscous shock waves*, in: A. Bressan et al. (Eds.), Nonlinear Conservation Laws and Applications, 2011, pp. 123–167.

[61] K. Zumbrun, *Stability of large-amplitude shock waves of compressible Navier-Stokes equations*, Handbook of Fluid Mechanics, 3 (2005), pp. 311–533.